Iowa Research Online
The University of Iowa's Institutional Repository

University of Iowa
Iowa Research Online

Theses and Dissertations

Spring 2010

The DamX cell division protein of Escherichia coli: identification of amino acid residues critical for septal localization and peptidoglycan binding

Kyle Brandon Williams
University of Iowa

Copyright 2010 Kyle Brandon Williams

This dissertation is available at Iowa Research Online: http://ir.uiowa.edu/etd/625

Recommended Citation
Williams, Kyle Brandon. "The DamX cell division protein of Escherichia coli: identification of amino acid residues critical for septal localization and peptidoglycan binding." PhD (Doctor of Philosophy) thesis, University of Iowa, 2010.
http://ir.uiowa.edu/etd/625.

Follow this and additional works at: http://ir.uiowa.edu/etd


Part of the Microbiology Commons

THE DAMX CELL DIVISION PROTEIN OF ESCHERICHIA COLI: IDENTIFICATION OF AMINO ACID RESIDUES CRITICAL FOR SEPTAL LOCALIZATION AND PEPTIDOGLYCAN BINDING

by

Kyle Brandon Williams

An Abstract

Of a thesis submitted in partial fulfillment
of the requirements for the Doctor of
Philosophy degree in Microbiology
in the Graduate College of
The University of Iowa

May 2010

Thesis Supervisor: Associate Professor David Weiss

ABSTRACT

In the bacterium *Escherichia coli*, cell division involves the concerted inward growth of all three layers of the cell envelope: the cytoplasmic membrane, the peptidoglycan (PG) cell wall, and the outer membrane. This is a complex, highly regulated process that involves over 20 proteins. Four of these proteins contain a domain of ~70 amino acids known as a SPOR domain (Pfam no. 05036). One of these SPOR domains (from a protein named FtsN) has been shown previously to bind PG. In this thesis we show that six additional SPOR domains, three from *E. coli* and three from other bacterial species, also bind PG. Thus, PG binding is a general activity of SPOR domains. We then examine the SPOR domain from DamX of *E. coli* in detail. In collaboration with Dr. Andrew Fowler of the NMR Core Facility, we determined the solution structure of the domain. The domain adopts an "RNP fold," characterized by a four-stranded anti-parallel β-sheet that is buttressed on one side by α-helixes. Several mutant forms of the DamX SPOR domain were constructed and studied both *in vivo* and *in vitro*. These studies support the following inferences: 1) The β-sheet is the PG-binding site; 2) The β-sheet contains critical information for targeting the SPOR domain to the midcell; 3) The SPOR domain probably localizes to the midcell by binding preferentially to septal PG; and 4) It follows, then, that septal PG must differ from PG elsewhere around the cell. We suggest that further studies of the SPOR:PG interaction will yield novel insights into PG biogenesis during septation.

This thesis also presents an *in vivo* characterization of several mutant forms of a cytoplasmic membrane protein named FtsW, homologs of which are found in all bacteria that contain a PG cell wall. FtsW recruits a PG synthase named FtsI to the division site and might also transport PG precursors across the cytoplasmic membrane. We systematically mutagenized each of FtsW's ten transmembrane (TM) helixes and

investigated the ability of the mutant proteins to support division, localize to the division site, and recruit FtsI. This characterization leads us to propose that TM1 is involved in targeting FtsW to the division site, TM4 is involved in the putative transport activity, and TM10 is involved in recruitment of FtsI.

Abstract Approved: _____
Thesis Supervisor

_____
Title and Department

_____
Date

THE DAMX CELL DIVISION PROTEIN OF ESCHERICHIA COLI: IDENTIFICATION OF AMINO ACID RESIDUES CRITICAL FOR SEPTAL LOCALIZATION AND PEPTIDOGLYCAN BINDING

by

Kyle Brandon Williams

A thesis submitted in partial fulfillment
of the requirements for the Doctor of
Philosophy degree in Microbiology
in the Graduate College of
The University of Iowa

May 2010

Thesis Supervisor: Associate Professor David Weiss

Graduate College
The University of Iowa
Iowa City, Iowa

CERTIFICATE OF APPROVAL

PH.D. THESIS

This is to certify that the Ph.D. thesis of

Kyle Brandon Williams

has been approved by the Examining Committee
for the thesis requirement for the Doctor of Philosophy
degree in Microbiology at the May 2010 graduation.

Thesis Committee:

David Weiss, Thesis Supervisor

Steve Clegg

Michael Feiss

Peter Rubenstein

George Stauffer

To my wonderful Robin.

ACKNOWLEDGEMENTS

I would like to acknowledge my mentor, David Weiss. David has been an excellent person to learn from and has a wealth of scientific knowledge. He was shown me the importance of being thorough and thoughtful in my research. I cannot thank him enough for all of the advice and support he has given me during the years I've spent in the laboratory.

I have to thank the past and current members of the Weiss lab. Everyone I've had the chance to work with has made coming to work each day fun and entertaining. Past lab members Ryan Arends and Ryan Kustusch became much more than coworkers, they became great friends who have helped make my time in Iowa so enjoyable.

I would like to thank the members of my committee as well. Their comments and suggestions throughout the years have been very helpful. When working on a few highly specialized projects, it's easy to focus in too much at times. They have been extremely helpful in reminding me the importance of relating my research into the "bigger picture".

Two professors at Indiana University also should be noted. David White and Clay Fuqua were the first people who made me truly excited about science and provided me my first opportunity to work in a lab and conduct research. Their influence on my education was immense and I thank them both for helping me find my way.

I thank my wonderful family for all of their support throughout my life. My Mom and Dad have always been there for me and have given me every opportunity possible to pursue my interests. Over the last few years I have unfortunately lost several grandparents and a great grandmother, all of whom were very important in my life. I want to thank all of them for helping make me the person I am today. Our family is very close and it was a joy growing up with them in my life. I love them all and miss them greatly.

To my wife Robin, I want to thank you for all of your love and patience. There is no way I could have accomplished this, or made it through the last few months of writing this thesis, without you. No matter how rough of a day I had, I could always come home and go on a hard bike ride with you and all that stress would disappear. I can't imagine going through life without you with me and am excited for our future together.

TABLE OF CONTENTS

LIST OF TABLES

Table

LIST OF FIGURES

Figure

CHAPTER 1: INTRODUCTION

In the Weiss lab, we use the Gram-negative bacterium *Escherichia coli* as a model organism to study cell division. For a number of years, I have studied proteins from *E. coli* that are involved in various aspects of bacterial cell division. A common theme among these studies has been the peptidoglycan (PG) cell wall. My first work in the Weiss laboratory dealt with the cell division proteins FtsW and FtsI, two proteins involved in synthesizing new PG at the division site. Later, I focused on a group of newly discovered division proteins named DamX, DedD, and RlpA. These proteins contain a PG binding domain known as a SPOR domain. This introduction begins with a brief overview of some key aspects of cell division and progresses to specific background related to my research projects.

Overview of cell division

Genetic analysis of the cell division process in *E. coli* began in the 1960's and resulted in the isolation of "filamentation temperature sensitive" mutants (*fts*) (Hirota et al., 1968). These mutants exhibited normal morphology when grown at 30° C but formed long filaments upon a temperature shift to 42° C. These filaments still had regularly spaced nucleoids, indicating their primary defect was with septation rather than DNA metabolism. Eventually, upon extended growth at the higher temperature, the cells would lyse and die.

Now, some four decades later, cell division in *E. coli* is known to be mediated by over 20 proteins that localize to a ring like structure at the midcell, referred to as the septal ring or divisome (Figure 1.1, For recent reviews see: Goehring and Beckwith, 2005; Vicente and Rico, 2006; Arends et al., 2007). The septal ring is a large, complex, multi-protein structure that is responsible for many steps of the division process. About

half of the septal ring proteins are essential for viability. Mutants that lack these proteins form filaments and die. The remaining septal ring proteins are not essential, although mutants are typically elongated. In *E. coli*, the septum is assembled at the midcell and involves coordinated inward growth of all layers of the cell envelope. This entails remodeling of the cytoplasmic membrane, the PG cell wall, and the outer membrane. As one can imagine, this is a highly regulated and complex process that is not completely understood.

Among the major questions are: How do the proteins in the septal ring work together? Many interactions among these proteins have been reported (Di Lallo et al., 2003; Karimova et al., 2005; D'Ulisse et al., 2007; Muller et al., 2007; Maggi et al., 2008; Karimova et al., 2009; Arends et al., 2010). It remains unclear which interactions are authentic and what is their relevance. Also, does the current set of cell division proteins represent a complete list of the players involved? This seems unlikely, given that new cell division proteins continue to be identified (Gerding et al., 2009; Moll & Thanbichler, 2009; Tarry et al., 2009; Arends et al., 2010). Finally, what are the specific biochemical functions of the septal ring proteins? Some of the division proteins, like FtsZ, are relatively well understood (Graumann, 2007; Osawa et al., 2008), but others are enigmatic. A prime example would be FtsEX. These proteins are predicted to constitute an ABC transporter, and, in fact, lesions in FtsE's ATP binding site inhibit division (Arends et al., 2009).

Fts proteins and assembly of the septal ring

The first established event in bacterial cell division is assembly of a protein named FtsZ into a contractile ring at the division site (Aarsman et al., 2005). FtsZ is a tubulin-like protein and utilizes GTP hydrolysis to drive constriction of the septal ring (Osawa et al., 2008; Monahan et al., 2009; Shlomovitz & Gov, 2009). The FtsZ ring also

serves as a landing pad for recruitment of other division proteins to the division site (Den Blaauwen et al., 1999; Hale & de Boer, 1999).

The remaining proteins composing the septal ring can be divided into a number of functional groups. (i) FtsZ binding proteins have roles promoting FtsZ-ring assembly and recruitment of downstream division proteins. Examples of this class would be FtsA and ZipA. (ii) FtsK is a DNA translocase and facilitates chromosome segregation. (iii) Some proteins are involved in synthesis of new PG at the septum, such as FtsI and probably FtsW. (iv) There are several PG hydrolases, such as AmiC, which help to separate daughter cells and remodel the cell wall. (v) The Tol-Pal complex aids constriction of the outer membrane and has components that span all three layers of the cell envelope. (vi) As noted above, many division proteins have essentially no known functions.

Several different approaches have been used to define the assembly pathway of the septal ring. One of the methods used has been determining which proteins still localize to the septum when another division component is removed through inactivation or depletion (reviewed in: Buddelmeijer & Beckwith, 2002; Vicente & Rico, 2006; Arends et al., 2010). What has emerged from these studies is a largely linear pathway of ordered recruitment (Figure 1.2). These findings are compatible with models where septal ring assembly is driven by a cascade of pairwise protein – protein interactions.

Another approach has examined the timing of arrival of division proteins at the septal ring. This has been analyzed in both *E. coli* and *Bacillus subtilis* and the findings show there are distinct early and late recruitment events, as indicated in Figure 1.2A (Aarsman et al., 2005; Gamba et al., 2009). It appears the early proteins localize simultaneously to the septum. Following a several minute break where no new protein joins the late proteins are then recruited simultaneously. The significance of the break in the temporal recruitment remains unclear. Possibly the division proteins recruited early have to remodel the cell envelope, and that action takes time to complete. Another

possibility is that the septal ring itself must undergo a conformational change, which cannot occur until all early recruits are present, before the late proteins can join the ring.

Other work has focused more directly on which cell division proteins interact with each other, using two-hybrid systems and immunoprecipitation. These studies have revealed a network of interactions that is much more complex than might be predicted from the recruitment pathway work (Buddelmeijer & Beckwith, 2002; Di Lallo et al., 2003; Karimova et al., 2005; Goehring et al., 2006; Karimova et al., 2009). Figure 1.2B summarizes these interactions. Elucidating which of these interactions are authentic and how all of the division proteins work with each other has to be a major focus of the cell division field in the future.

Peptidoglycan

Peptidoglycan (PG), also referred to as murein, forms a large bag-like structure known as a sacculus. It encapsulates the entire surface of the cytoplasmic membrane, where it defines the cell's shape and protects it from internal turgor pressure (Weidel & Pelzer, 1964). In a Gram-negative bacteria, such as *E. coli*, the PG is located in the periplasmic space. PG is composed of repeating monosaccharide subunits of alternating β1,4-linked *N*-acetylglucosamine (Glc*N*Ac) and *N*-acetylmuramic acid (Mur*N*Ac). These subunits are crosslinked via short peptide sidechains, which extend from the Mur*N*Ac sugar (Schleifer & Kandler, 1972). The PG sacculus of *E. coli* is comprised largely of a single layer of PG, but there is evidence that some parts of the sacculus are multilayered (Prats & de Pedro, 1989; Labischinski et al., 1991).

Figure 1.3A shows the layout of a PG disaccharide, with peptide side chain, from *E. coli*. This unit is referred to as a PG monomer, since it is the basic building block for the cell's sacculus. The peptide sequence for *E. coli* is initially a pentapeptide carrying several rare D-amino acids, with a sequence of L-Ala–D-iGlu–m-A_2pm–D-Ala–D-Ala.

The terminal D-Ala is lost to enzymatic degradation or when the peptide sidechains are crosslinked, resulting in a tetrapeptide form (Vollmer & Bertsche, 2008). The peptide side chains are typically crosslinked together between the m-A_2pm on one chain and the D-Ala of another (Figure 1.3A), although m-A_2pm - m-A_2pm can also occur. Between 40-60% of peptide sidechains are crosslinked in an *E. coli* sacculus (Glauner et al., 1988). This crosslinking forms the net-like PG structure that contributes to the rigidity and strength of the sacculus. Also important for linking the PG to the outer membrane is a lipoprotein called Lpp, which becomes covalently attached to 5-9% of the m-A_2pm residues in the sacculus of *E. coli* (Hantke & Braun, 1973). These features combine to give the *E. coli* sacculus its strength and architecture.

PG biogenesis occurs in two distinct parts of the cell. Early steps occur in the cytoplasm and are involved in producing PG precursor molecules. This process is outlined in Figure 1.3B and reviewed in Vollmer (2007). Cytoplasmic PG precursor synthesis results in creation of undecaprenyl pyrophosphoryl-(Glc*N*Ac)Mur*N*Ac-pentapeptide, known as lipid II (this is essentially the PG monomer described above, covalently linked to a specialized C55 inner membrane lipid). The lipid II molecule is then translocated across the inner membrane, and enlargement of the PG sacculus takes place in the periplasm (van Heijenoort, 2001). The protein(s) responsible for moving lipid II across the inner membrane have not been identified, although a family of proteins named SEDS proteins is considered a likely candidate (Ikeda et al., 1989; Lara et al., 2005).

Once the lipid II precursor has been translocated, the final steps of PG synthesis occur in the periplasm. Here the PG monomers are polymerized into glycan strands (with an average length of 20-40 disaccharides in *E. coli*) by transglycosylases and their peptide sidechains are crosslinked by transpeptidases (Vollmer & Bertsche, 2008; Vollmer & Seligman, 2010).

In *E. coli* a few classes of proteins carry out these final steps of PG synthesis (reviewed in Vollmer, 2007). Class B High Molecular Weight Penicillin-Binding Proteins (PBPs), such as PBP2 and FtsI are monofunctional transpeptidases and can only catalyze the creation of peptide crosslinks. Class A High Molecular Weight PBPs, such as PBP1A, are dual function enzymes capable of transpeptidation and transglycosylation. There are also monofunctional transglycosylases in *E. coli*, such as MgtA, that contribute to PG synthesis (Di Berardino et al., 1996; Derouaux et al., 2008).

Regarding PG synthesis at the septum, a protein essential to this process is FtsI. FtsI is unique, in that it is required for septal PG synthesis but not for elongation of the lateral cell wall (Spratt & Pardee, 1975). FtsI is also known as penicillin-binding protein 3 (PBP3) and is a monofunctional transpeptidase (that will be discussed in more detail below). FtsI localizes to the septal ring, where it crosslinks septal PG and recruits FtsN to the division site (Adam et al., 1997; Addinall et al., 1997; Weiss et al., 1999; Wissel & Weiss, 2004). *E. coli* also has another monofunctional transpeptidase, PBP2. In contrast to FtsI, PBP2 is specifically required for crosslinking PG during elongation and not division (Wientjes & Nanninga, 1991). However, PBP2 has been reported to weakly localize to the septum and might be active there even though it is not required for septal PG synthesis (Den Blaauwen et al., 2003).

It is not clear which proteins are responsible for transglycosylation of septal PG. Some likely candidates in *E. coli* include the Class A High-Molecular-Weight PBPs, such as PBP1a, PBP1b, and PBP1c. These proteins are bifunctional transglycosylase / transpeptidase enzymes and are responsible for the majority of PG synthesis in the cell (Vollmer & Bertsche, 2008). Hints that PBP1b is involved include a report that overexpression of dominant negative forms of this protein caused *E. coli* cells to lyse at the division site (Meisel et al., 2003). Also, *B. subtilis* has several Class A HMW PBPs that localize to the septal ring, including a PBP1 homolog that shows very strong localization (Scheffers & Errington, 2004; Scheffers et al., 2004).

Besides the enzymes involved in PG synthesis, *E. coli* has ~ 20 PG hydrolayses (Vollmer & Bertsche, 2008). The PG hydrolases fall into three primary categories – lytic transglycolases (LT), *N*-acetylmuramyl-L-alanine amidases (amidases), and peptidases. During lateral growth of the cell wall, openings must be made in the net-like PG structure in order to insert new subunits. Likewise, at the septum, much remodeling of the PG must occur during division.

E. coli has several LTs, such as MltA and Slt70. These are muramidases that cleave the glycosidic linkage between the sugar PG subunits with concomitant formation of a 1,6-anhydro bond at the Mur*N*Ac residue (Holtje et al., 1975). There are examples, like EmtA, of endo specific LT activity (Kraft et al., 1998). Others, such as Slt70 and MltA, are exoenzymes that remove the sugar units from the end of the glycan strand (Vollmer, 2007).

E. coli has three amidases (AmiA, B, and C) that cleave the bond between the glycan backbone and the peptide sidechain. These enzymes play an important role during cell division. Some amidases localize to the septum, and mutants lacking all three amidases are incapable of separating after division, giving rise to long chains of cells (Heidrich et al., 2001; Bernhardt & de Boer, 2003; Uehara T, 2010).

The last class, the peptidases, has a similar function to the amidases. But, instead of cleaving the bond between the peptide and Mur*N*Ac, they cleave the bonds within peptides (either among the sidechain residues or at the linkage between two crosslinked sidechains). Examples of this category would be MepA and PBP4 (reviewed in Vollmer, 2007).

Remarkably, in one generation of growth, *E. coli* will turnover nearly half of its total PG (Goodell, 1985). The PG synthesis and degradation machinery must function in a concerted fashion in order to maintain the integrity of the sacculus throughout growth and division. An interesting observation about the spatial location of PG metabolism during the bacterial cell cycle has been reported. With the onset of division, the majority

of PG creation moves from being diffuse throughout the cell to predominantly localized at the septum (Wientjes & Nanninga, 1989). This switch to intense synthesis at the septum raises the possibility of accumulation of transient structures in the PG at the septum, an idea that will become important in later discussions.

The inner membrane proteins FtsW and FtsI

FtsW. FtsW is an essential inner membrane protein that belongs to an extensive family of proteins found in all bacteria possessing a PG cell wall (Ikeda et al., 1989; Margolin, 2000). This family of proteins is known as "SEDS" for shape, elongation, division, and sporulation and typically works together with a class B high molecular weight penicillin-binding protein (PBP) (Henriques et al., 1998). In fact, mutants with an inactivated SEDS gene have the same phenotypes as those lacking their corresponding PBP. In the *E. coli* genome there are genes coding for two independent pairs of such proteins, *ftsW – ftsI* and *rodA – pbpA* (Blattner et al., 1997). The FtsW/I pair is involved in cell division, while RodA/PBP2 are needed for proper elongation. There are over 3300 examples of the SEDS family in the Pfam database (Finn et al., 2008) and typically they occur in the same operon as their cognate PBP.

FtsW from *E. coli* is comprised of 414 amino acids and has a predicted topology with 10 transmembrane helices (TMHs) and a large periplasmic loop between TMH 7 and 8 (Lara & Ayala, 2002). Despite the fact this protein is widely conserved and distributed throughout bacterial species, there is only one established function for FtsW. Several years ago our laboratory showed that FtsW is required for recruitment of the septal specific transpeptidase FtsI to the division site (Mercer & Weiss, 2002). The role of FtsW in FtsI recruitment was further explored through a mutagenesis approach that suggested the loop between TMH 9 and 10 is important (Pastoret et al., 2004).

Moreover, FtsW and FtsI have been shown to interact in two-hybrid systems (Di Lallo et al., 2003; Karimova et al., 2005; Maggi et al., 2008).

It is unknown if FtsW has additional functions *in vivo*. There has been speculation that FtsW plays a role in translocation of the PG precursor lipid II to the periplasm (Ehlert & Holtje, 1996; Lara & Ayala, 2002). This hypothesis has been tested by looking at the effect of depleting FtsW on accumulation of nucleotide-linked PG precursors (Lara et al., 2005). The authors did not observe the expected buildup, arguing against the transport function. However, it is possible the deficiency was masked by the presence of RodA in the cells, which would likely be shuttling the same substrate.

FtsI. FtsI is a transpeptidase required for synthesis of septal PG and is also known a penicillin binding protein 3 (PBP3). FtsI has a relatively simple architecture consisting of a short N-terminal cytoplasmic tail, a single TMH, and a large periplasmic region containing a transpeptidase domain and a large domain of unknown function (Bowler & Spratt, 1989).

FtsI belong to the class B high molecular weight PBPs. These proteins are monofunctional transpeptidases and are different than class A PBPs, which have both transpeptidase and transglycosylase activities (Holtje, 1998). Also, in contrast to class A PBPs, which perform catalysis on the PG precursor molecule lipid II (Adam et al., 1997), the authentic substrate in the cell is not yet known.

As mentioned previously, the single TMH of FtsI is essential for targeting the protein to the septum (Wissel & Weiss, 2004; Wissel et al., 2005). Moreover, alanine scanning mutagenesis implicated one face of this helix in driving septal localization (Wissel et al., 2005). We believe this result argues strongly for a protein - protein interaction with another division protein, most likely FtsW (which has 10 TMHs).

The domain of unknown function has been proposed to interact with other division proteins, especially FtsN, which localizes directly following FtsI in the

recruitment pathway (Figure 1.2) (Marrec-Fairley et al., 2000; Wissel & Weiss, 2004). Also, there are data from two hybrid analysis that this domain interacts with FtsL (Karimova et al., 2005).

FtsN and other SPOR domain proteins

FtsN is a bitopic membrane protein that is essential for division (Figure 1.4) (Dai et al., 1993; Dai et al., 1996). How FtsN facilitates cell division is not clear. Because overproduction of FtsN rescues a variety of mutants with lesions in genes for other cell division proteins [*ftsA*(Ts), *ftsI*(Ts) *ftsQ*(Ts), *ftsEX* null, *ftsK* null, and *ftsP* (*sufI*) null strains], it seems likely that one function of FtsN is to improve the assembly and/or stability of the septal ring (Glauner, 1988; Dai et al., 1993; Draper et al., 1998; Geissler & Margolin, 2005; Goehring et al., 2007; Tarry et al., 2009). Also, a very recent report suggests that FtsN plays an important role in triggering constriction, probably by allosteric activation of some other component of the septal ring (Gerding et al., 2009).

A notable feature of FtsN is that it contains at its C terminus a peptidoglycan (PG) binding domain known as a SPOR domain (Pfam accession no. 05036) (Ursinus et al., 2004; Yang et al., 2004; Finn et al., 2008). SPOR domains are a domain of ~70 amino acids and are both common and widespread in bacteria. Currently there are over 2,000 proteins that contain a SPOR domain listed in the Pfam database. These proteins come from over 500 bacterial species. The domain is named after the founding member of the protein family, a *Bacillus subtilis* protein named CwlC that is produced late in the process of sporulation (Kuroda et al., 1993). CwlC, which consists of an N-terminal amidase domain and a C-terminal SPOR domain, facilitates release of the mature spore by degrading PG in the mother cell (Smith & Foster, 1995; Mishima et al., 2005). Solution structures, solved using nuclear magnetic resonance spectroscopy (NMR), have been reported in the literature for the SPOR domains from both FtsN and CwlC (Yang et

al., 2004; Mishima et al., 2005). A ribbon diagram of the CwlC structure is shown in Figure 1.4B. From this it can be seen the domain has a repeating βαβ topology, which forms an antiparallel β-sheet on one face flanked by a pair of α-helices on the other. Chapter 4 in this thesis will comment more specifically on the structure of SPOR domains.

E. coli has four proteins containing a SPOR domain: FtsN, DamX, DedD, and RlpA. The first three are inner membrane proteins, however RlpA is a lipid linked outer membrane protein. Recent reports from several laboratories, including ours, have shown that these and other SPOR domain proteins are likely involved in division (Gerding et al., 2009; Moll & Thanbichler, 2009; Arends et al., 2010). In particular, it was shown that DamX and DedD (fused to GFP) and RlpA (fused to mCherry) were able to localize to the midcell (Figure 1.5A). A *dedD* mutant, while viable, has mild division defects, yielding slightly filamentous cells. A *damX* mutant is normal in length but has increased sensitivity to the ionic detergent deoxycholate (Arends et al., 2010). Combing those two mutations results in a synergistic effect, producing cells longer than either of the single mutants alone (Gerding et al., 2009; Arends et al., 2010). No detectable defects were found when looking at an *rlpA* mutant, either by itself or in combination with *damX* and *dedD*.

Interestingly, numerous isolated SPOR domains, when fused to GFP, could still localize well to the division site. This was true for many examples, including the four SPOR domains found in *E. coli*, CwlC from *B. subtilis*, and even two SPOR domains from distantly related bacteria, *Aquifex aeolicus* and *Cytophaga hutchinsonii* (Figure 1.5B) (Deckert et al., 1998; Xie et al., 2007; Gerding et al., 2009; Arends et al., 2010). So, it would seem all of the septal targeting information needed for these proteins is provided in this small domain.

This finding begs the question of how the SPOR domains are targeting the septum. The canonical model in which septal localization is driven by protein-protein

interactions seems unlikely because the heterologous SPOR domains that localize in *E. coli* are too divergent, having less than 20% identity to any *E. coli* SPOR domain in pair-wise alignments (Arends et al., 2010). By way of comparison, heterologous FtsZ proteins that are ~50% identical to *E. coli* FtsZ fail to localize properly when produced in *E. coli* (Osawa & Erickson, 2006).

We hypothesize that SPOR domains bind preferentially to septal PG. In support of this idea, numerous SPOR domains bind PG when incubated with isolated sacculi (Ursinus et al., 2004; Gerding et al., 2009; Moll & Thanbichler, 2009; Arends et al., 2010). Moreover, according to one report, the sacculi must contain septal PG to see good binding (Ursinus et al., 2004), although we have not been able to reproduce that result (see Chapter 3). Nevertheless, one problem with the notion that SPOR domains bind septal PG is that there are no convincing reports showing septal PG is different from PG elsewhere in the cell (Glauner, 1988; Romeis et al., 1991; Obermann & Holtje, 1994; de Pedro et al., 1997; Ishidate et al., 1998). A likely reason is that septal PG might differ only in being enriched in a transient structure that arises during biogenesis of PG anywhere in the cell. Examples include multi-layered PG, glycan strands that have been extended but not yet crosslinked, PG that lacks Lpp, or degradation intermediates.

Two reports indicate that SPOR domains might target “naked” glycan strands that lack peptide sidechains. The evidence is as follows. First, the SPOR domain from FtsN binds to such structures provided they are at least 25 disaccharides in length (Ursinus et al., 2004). Second, septal localization of SPOR domains is not observed in an *E. coli* triple amidase mutant, which should be unable to generate “naked” glycan strands (Gerding et al., 2009). Third, in *E. coli* the amidase activity is concentrated at the septum (Kuroda et al., 1993; Bernhardt & de Boer, 2003; Priyadarshini et al., 2007). But there are some contradictory observations in the literature as well, including that nobody has ever demonstrated the existence of “naked” glycan strands in PG sacculi, let alone that such structures are enriched at the septum or absent in an amidase mutant. Moreover, the

SPOR domain of FtsN has also been reported to bind short muropeptides (Muller et al., 2007) and many potential binding substrates have never been tested, such as long glycan strands that still carry peptide side chains.

An overview of this thesis

Chapter two of this thesis describes a systematic mutagenesis of the 10 TMHs of FtsW for the purpose of identifying a TMH that interacts with FtsI. The data suggest the last TMH of FtsW (TMH-10) is specifically required for efficient localization of FtsI to the septal ring, but we were unable to show a direct interaction between TMH-10 of FtsW and the TMH of FtsI, despite some effort. Chapter three presents a characterization of the co-sedimentation assay used to study binding of SPOR domains to PG sacculi. The results imply co-sedimentation measures a general affinity of SPOR domains for PG rather than specific binding to septal PG. Chapter 3 also documents that many SPOR domains (not just the one from FtsN) bind PG. The fourth chapter is a structure-function study of the SPOR domain from DamX. The solution structure, as determined by NMR, reveals an RNP fold, while follow-up studies using site-directed mutants implicate a cleft formed by a curved β-sheet as the PG binding site. Notably, there is extensive overlap in residues important for septal localization and PG-binding, which supports the idea that SPOR domains localize to the septal ring by binding to septal PG. Finally, appendixes describe (i) features of the SPOR domain from DamX that did not fit conveniently into chapter four and (ii) results from two-hybrid assays of DamX and DedD against other known division proteins. Some of the work presented in this thesis has been published (Arends et al., 2010).

Figure 1.1. The septal ring. A. Overview of the proteins involved in cell division in *E. coli*. Proteins are shown from left to right in their order of recruitment to the septal ring, with FtsZ being the first component to arrive at the site. Proteins given a single letter designation are "Fts" proteins. OM, outer membrane; CM, cytoplasmic membrane; PG, peptidoglycan cell wall. B. GFP-FtsL fusion protein in *E. coli*. The image was taken using deconvolution microscopy and shows a pattern of fluorescence localization to a ring structure at the midcell. This ring structure is referred to as the septal ring (Image modified from (Ghigo et al., 1999)).

A

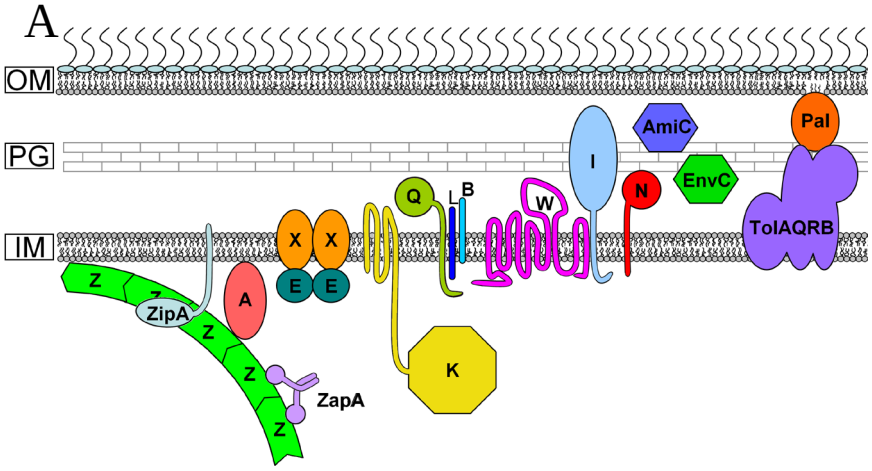
OM
PG
IM
AmiC
Pal
I
EnvC
N
Q
L
B
W
TolAQRB
X
X
E
E
A
ZipA
Z
Z
Z
Z
Z
ZapA
K

B


Septal
Ring

Figure 1.2. Assembly of the septal ring. A. Recruitment hierarchy of *E. coli* cell division proteins as determined by localization dependencies. B. Reported interactions among Fts proteins through two-hybrid analysis (see text for source references). Lines connect proteins reported to interact in at least one assay, while circular arrows indicate self-interaction (e.g., homodimerization).

A

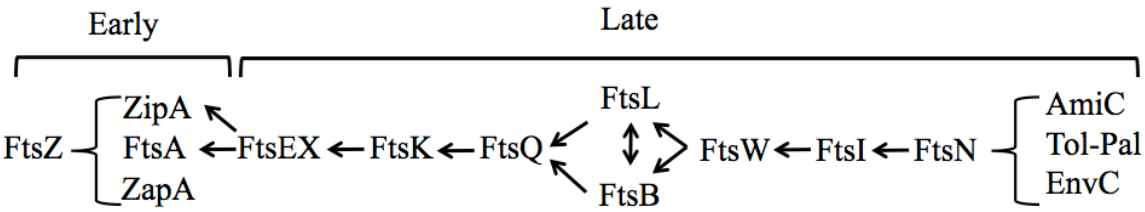
Early
Late
FtsZ
ZipA
FtsA
ZapA
FtsEX
FtsK
FtsQ
FtsL
FtsB
FtsW
FtsI
FtsN
AmiC
Tol-Pal
EnvC

B

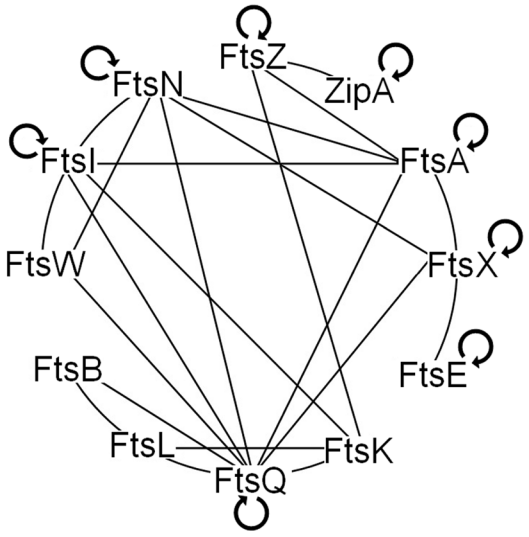
FtsZ
ZipA
FtsN
FtsI
FtsA
FtsW
FtsX
FtsE
FtsB
FtsL
FtsK
FtsQ

Figure 1.3. Peptidoglycan in *E. coli*. A. Structure of peptidoglycan. Left: Layout of a PG monomer. This unit consists of alternating *N*-acetylglucosamine (Glc*N*Ac) and *N*-acetylmuramic acid (Mur*N*Ac). Mur*N*Ac residues can have the indicated peptide side chain attached. Right: Peptide sidechains can be crosslinked by joining the D-Alanine position of one sidechain to the meso-diaminopimelic acid position of another chain. B. Mechanism of PG synthesis. Cartoon of how Lipid II is synthesized and translocated to the periplasm during PG synthesis in the *E. coli* cell. The enzyme responsible for the flippase activity is not yet known, although SEDS family proteins such as FtsW might accomplish this function. UDP-G, UDP-*N*-acetylglucosamine.

A

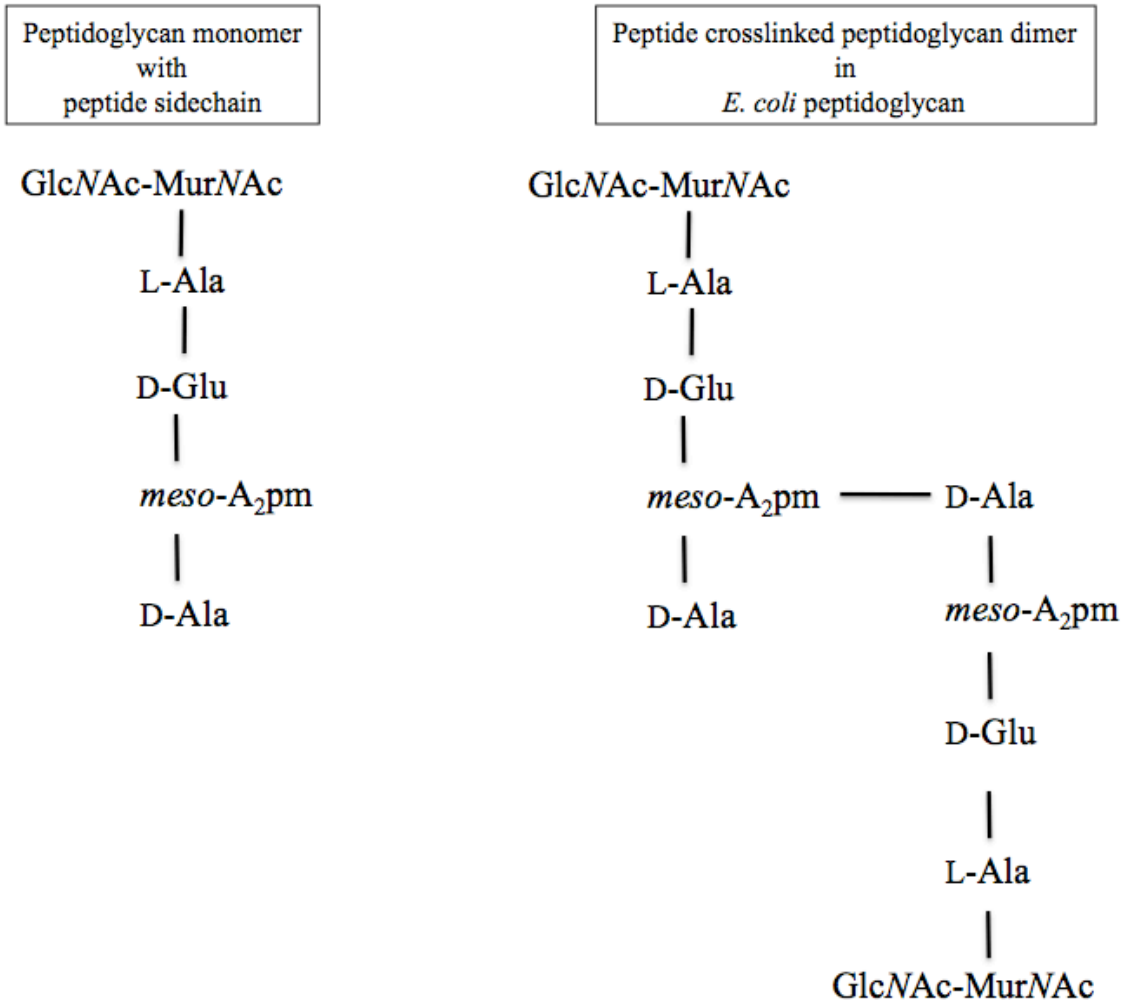
Peptidoglycan monomer with peptide sidechain
Peptide crosslinked peptidoglycan dimer in *E. coli* peptidoglycan
GlcNAc-MurNAc
L-Ala
D-Glu
meso-A2pm
D-Ala
GlcNAc-MurNAc
L-Ala
D-Glu
meso-A2pm
D-Ala
D-Ala
meso-A2pm
D-Glu
L-Ala
GlcNAc-MurNAc

B

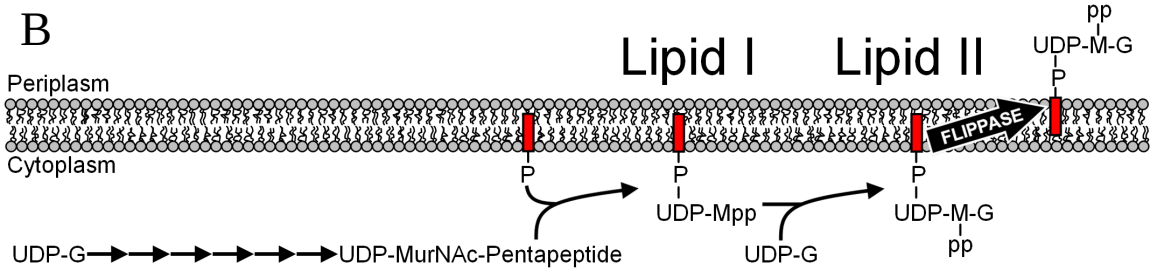
Lipid I
Lipid II
pp
UDP-M-G
P
Periplasm
FLIPPASE
Cytoplasm
P
P
P
UDP-Mpp
UDP-M-G
pp
UDP-G
UDP-MurNAc-Pentapeptide
UDP-G

Figure 1.4. The SPOR domain. A. The four SPOR domain proteins in *E. coli*. Membrane topology and number of amino acids in each domain as retrieved from UniProt release 15.7 (http://www.uniprot.org) or the GTOP update of 15 December 2008 (http://spock.genes.nig.ac.jp/_genome/gtop.html). N, amino terminus; CM, cytoplasmic membrane; OM, outer membrane. RlpA has a covalently attached lipid at its amino terminus. B. Ribbon diagram of the SPOR domain from the *B. subtilis* protein CwlC, based on the solution structure determined from NMR (Mishima et al., 2005). Cartoon was generated with Pymol from PDB ID 1x60 (DeLano, 2002), α-helices and β-strands are numbered from N to C-terminus as indicated.

A

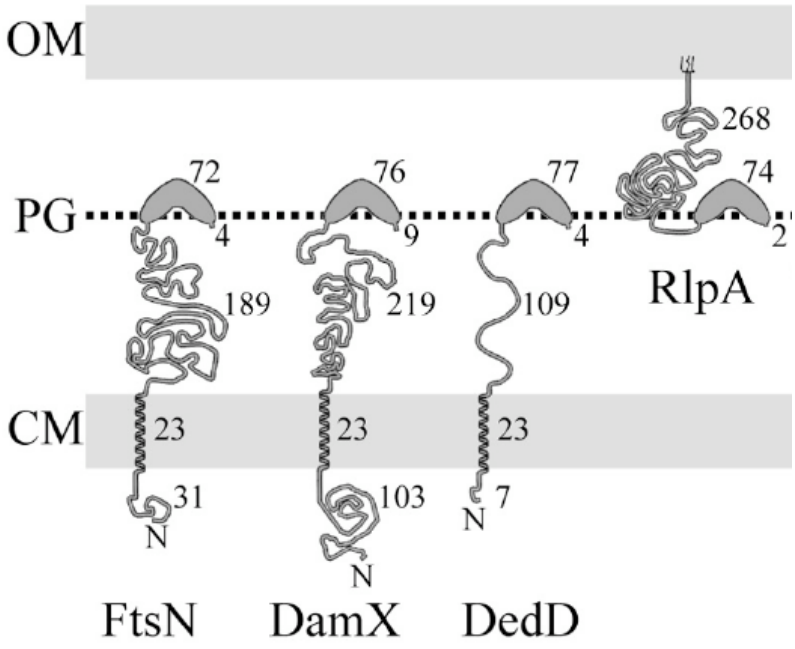
OM
PG
CM
72
4
76
9
77
4
74
2
268
189
219
109
RlpA
23
23
23
31
103
7
N
N
N
FtsN
DamX
DedD

B

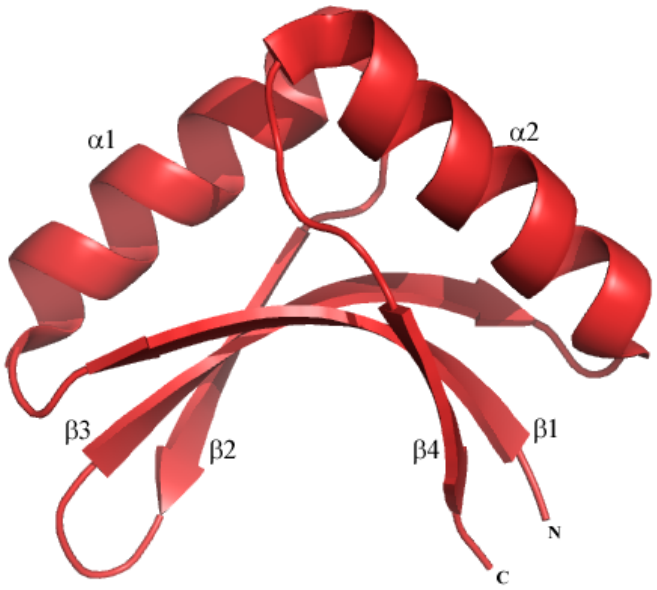
α1
α2
β3
β2
β4
β1
N
C

Figure 1.5. Localization of SPOR domain proteins. A. Full-length SPOR domain proteins localize to the septal ring. Fluorescence micrographs of live cells producing the indicated GFP or RFP fusion protein. B. Isolated SPOR domains localize to the septal ring. Fluorescence micrographs of live cells producing the indicated GFP fusion protein from a plasmid. These GFP fusions were targeted to the periplasm via the TAT system. Figure adapted form Arends *et al*, 2010. Bar, 5μm.

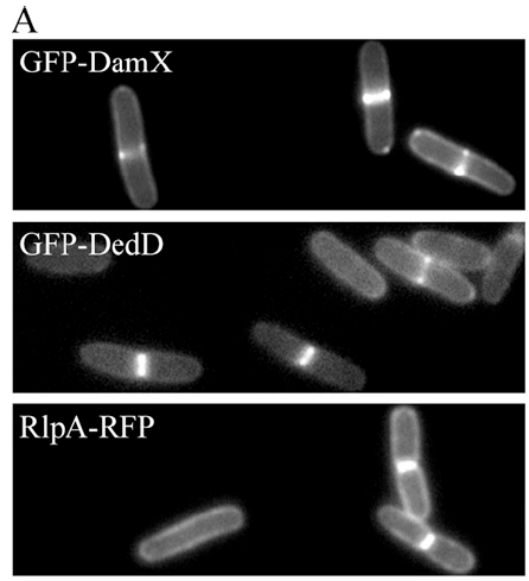
A
GFP-DamX
GFP-DedD
RlpA-RFP

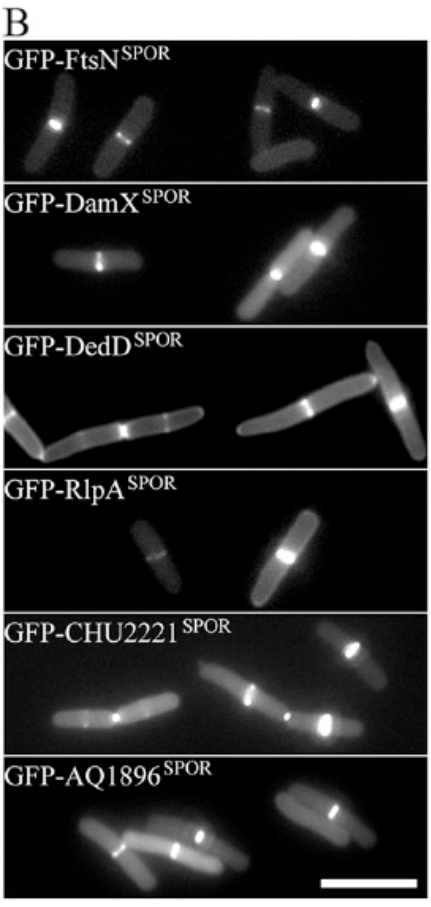
B
GFP-FtsN SPOR
GFP-DamX SPOR
GFP-DedD SPOR
GFP-RlpA SPOR
GFP-CHU2221 SPOR
GFP-AQ1896 SPOR

CHAPTER 2: GENETIC ANALYSIS OF THE CELL DIVISION PROTEIN FTSW AND ITS INTERACTION WITH FTSI (PBP3)

Introduction

As discussed in Chapter 1, cell division in bacteria is a complex process involving over 20 known proteins in *E. coli*. These proteins must function in a concerted fashion to synthesize all three layers of the cell envelope in order to gives rise to two new daughter cells. Two of the proteins involved in this process are FtsW and FtsI.

FtsI is a class B high molecular weight PBP (see Chapter 1 for more information on FtsI) that localizes to the division site, where it is essential for crosslinking newly synthesized PG at the septum (Adam et al., 1997; Weiss et al., 1999; Arends, 2007). In terms of structure, FtsI is a bitopic membrane protein with a small cytoplasmic domain, a single transmembrane (TM) helix, and a large periplasmic region that contains both a domain of unknown function and a transpeptidase catalytic domain (Bowler & Spratt, 1989; Goffin et al., 1996; Goffin & Ghuysen, 1998).

Several lines of evidence indicate that FtsI is targeted to the septal ring by its TM. First, random mutagenesis followed by a screen for localization-defective mutants returned only lesions in the TM (Wissel & Weiss, 2004). Second, a 26 amino acid fragment of FtsI that includes the TM and little if any flanking sequence localized to the septal ring, albeit poorly (Wissel et al., 2005). Third, alanine-scanning mutagenesis of the TM revealed that residues critical for septal localization cluster on one face of the helix, suggestive of a protein-protein interaction (Wissel et al., 2005). Because FtsI does not interact with itself in one two-hybrid system (Di Lallo et al., 2003; Karimova et al., 2005), but does interact modestly in another (Di Lallo et al., 2003), it is unclear at this point if the TM could mediate dimerization of FtsI. However, we suspect it (or a

complex consisting of two FtsI TM dimers) interacts with a TM from another division protein; the leading candidate is FtsW.

FtsW belongs to a large family of polytopic membrane proteins found in all bacteria that contain a PG cell wall. This family is named SEDS, for shape, elongation division and sporulation (Henriques et al., 1998). The founding members of the SEDS family are FtsW and RodA of *E. coli*, and SpoVE of *Bacillus subtilis* (Ikeda et al., 1989; Boyle et al., 1997; Henriques et al., 1998). These proteins are required for PG synthesis during elongation (RodA), division (FtsW) and sporulation (SpoVE). Each SEDS protein appears to work together with a cognate class B penicillin-binding protein (PBP) that catalyzes the formation of cross links in PG. Examples of such pairs include RodA-PBP2, FtsW-FtsI (also called PBP3) and SpoVE-SpoVD. Typically a SEDS-PBP pair is encoded in the same operon and inactivation of either results in the same phenotype.

Most SEDS proteins contain 10 transmembrane helixes (TMs) (Gerard et al., 2002; Lara & Ayala, 2002). Because of their complex transmembrane structure and involvement in PG synthesis, it has been suggested that SEDS proteins might transport Lipid II (a precursor for PG synthesis) across the cytoplasmic membrane (Ishino et al., 1986; Ikeda et al., 1989; Ehlert & Holtje, 1996). Efforts to prove this have yet to succeed (Lara et al., 2005) and more recently it has been proposed that MurJ family proteins are the "missing" Lipid II flippases (Ruiz, 2008; Ruiz, 2009), although this too has been challenged (Fay & Dworkin, 2009; Vasudevan et al., 2009).

The one reasonably well-established function for SEDS proteins is in recruitment of their cognate transpeptidases to the correct place in the cell. In particular, our lab demonstrated that FtsW is needed for recruitment of FtsI to the septal ring, while Dworkin and co-workers showed that SpoVE recruits SpoVD to the outer forespore membrane (Mercer & Weiss, 2002; Real et al., 2008). Moreover, several studies have reported that FtsW and FtsI homologs from a variety of organisms interact either in two hybrid systems (Di Lallo et al., 2003; Karimova et al., 2005) or by immunoprecipitation

(Datta et al., 2006; Maggi et al., 2008). These considerations led us to undertake a systematic mutagenesis of the TMs of FtsW as an approach for characterizing the FtsW-FtsI interaction in molecular detail.

Materials and Methods

Media. *E. coli* strains were grown in Luria-Bertani (LB) medium containing 10 g tryptone, 5 g yeast extract, and 10 g NaCl per liter. Plates contained 15 g agar per liter. Ampicillin was used at 200 µg/ml and spectinomycin at 100 or 35 µg/ml for plasmids or chromosomal alleles, respectively. Kanamycin was used at 40 µg/ml and chloramphenicol at 30 µg/ml.

Strains. Strains used in this study are listed in Table 2.1. All two-hybrid analyses were carried out in *E. coli* stain DMH1 (Karimova et al., 2000).

Plasmids. Plasmids used in this study are listed in Table 2.2. Plasmids were constructed by PCR using VENT DNA polymerase (New England Biolabs) and sequenced to verify their integrity. All primers are listed in Table 2.3 and were obtained from Integrated DNA Technologies (Coralville, IA).

Generation of triple alanine substitutions in FtsW TMs. Amino acid substitutions in three consecutive residues in each of the 10 transmembrane helices (TMs) were done using site directed mutagenesis and megapriming (Sarkar & Sommer, 1990). Megaprimers for creating the 3 alanine substitutions were generated using the primer pairs listed below and pDSW311 as template: TMH1; P845 and GFP666F, TMH2; P846 and GFP666F, TMH3; P847 and GFP666F, TMH4a; P869 and GFP666F, TMH4b; P870 and GFP666F, TMH5; P871 and P874, TMH6; P872 and P874, TMH7; P873 and P875, TMH8; P848 and P415, TMH9; P849 and P415, TMH10; P850 and P415. These

megaprimers were then purified with a PCR cleanup kit and used with either primer P415 or GFP666F in another round of PCR with pDSW311 as template. This created full length *ftsW* PCR product with the desired mutations and restriction sites for EcoRI (5') and HindIII (3').

Plasmids for localization of GFP-FtsW. The *ftsW* 3-ala PCR products were digested with EcoRI and HindIII and ligated into the vector pDSW311 that had been cut with EcoRI and HindIII. The resulting plasmids contained *gfp* fused to the 5' end of the mutated *ftsW*.

Plasmids for studying recruitment of GFP-FtsI. Three tandem copies of the hemagglutinin tag (3xHA) were amplified by PCR using pMPY-3xHA as template and primers P902 plus P903. The 115 bp product was purified using a PCR cleanup kit (Qiagen) and used as a megaprimer, with P415, for amplifying *ftsW* from pDSW311. The ~1,350 bp product was then digested with MfeI and HindIII and ligated into the pAM238 vector, which had been cut with EcoRI and HindIII. This leaves an EcoRI site between the HA tag sequence and the start of *ftsW*. This restriction site was used with the HindIII site to clone the collection of 3 alanine substitutions (described above) into this vector.

Plasmids for testing FtsW's interaction with FtsI. pKT25-*ftsW* was cut with BamHI and KpnI. The vector was gel-purified (Qiagen). The various mutated forms of *ftsW* (described above) were then amplified using PCR and the primers P414 and P415. The resulting ~1,250 bp product was then cut with the same enzymes and ligated into the purified vector. pUT18c-*ftsI* was obtained from the Ladant laboratory (Karimova et al., 2005).

Plasmids for testing mutant FtsI proteins in the two-hybrid system. Primers P1100 and P1096 were used in a PCR reaction, with pDSW521 (P_{206}-*gfp-ftsI*) as template, to amplify a fragment of *ftsI* that encodes the first 50 amino acids of the protein. This fragment was purified using a PCR cleanup kit (Qiagen) and cut with BamHI and

KpnI and ligated into pUT18c that had been cut with the same enzymes. The resulting plasmid was named pDSW1160.

pDSW1161 and pDSW1162 (which encode the first 80 and 239 amino acids of FtsI, respectively) were created in a similar manner. For pDSW1161 the primers used were P1100 and P1097. For pDSW1162, primers P1100 and P1098 were used.

In order to generate a full length *ftsI* that encodes an L39P amino acid substitution, primers P1100 and P1099 were used to amplify the mutant allele from pDSW566. The fragment was purified using a PCR cleanup kit and digested with BamHI and KpnI and ligated into pUT18c that had been cut with the same enzymes. The resulting plasmid was named pDSW1163.

pDSW1164 encodes for a full-length version of FtsI that has an extra leucine residue inserted at residue 41. This plasmid was generated as described for pDSW1163. However, pLD75 was used as template for amplifying the mutant allele.

General microscopy methods. Our microscope, camera, and software have been described previously, as has the fixation of cells with paraformaldehyde (Mercer & Weiss, 2002; Arends et al., 2009; Tarry et al., 2009; Arends et al., 2010).

Localization of 3-alanine lesions of FtsW. The *gfp-ftsW* plasmids were transformed into wild type *E. coli* strain DHB4. Transformants were grown overnight at 30° C in LB supplemented with ampicillin to maintain the plasmid. The following morning, cells were subcultured 1:200 into fresh media and allowed to grow to an OD_{600} of ~0.5. At that time cells were harvested and fixed in paraformaldehyde/glutaraldehyde and attached to glass slides for imaging GFP. Samples were also taken for Western blotting.

Localization of the GFP-FtsW fusions was also tested in the FtsW depletion strain EC850, which has a wild type copy of *ftsW* under the control of an arabinose inducible

promoter. EC850 was transformed with the *gfp-ftsW* constructs or an empty *gfp* vector (negative control). Transformants were grown overnight at 30° C with 0.2% arabinose (to express wild type FtsW) and ampicillin and chloramphenicol for plasmid maintenance. The overnight cultures were then diluted 1:50 and grown with 0.02% arabinose until their OD_{600} reached ~0.5. At this time they were shifted to growth with 0.2% glucose and no arabinose and expression of the *gfp-ftsW* allele to be tested was induced with the addition of 0.1 mM IPTG. After about 2 hours, the derivative carrying the empty *gfp* vector had become filamentous (~20 μm), which implied that cells were successfully depleted of wild type FtsW. At this time, all cultures were fixed for microscopy.

Recruitment to the septum of GFP-FtsI by FtsW. The 3xHA tagged *ftsW* 3-ala constructs and an empty vector control were transformed into EC1655, an FtsW depletion strain that has *gfp-ftsI* integrated onto the chromosome in single copy. Transformants were grown as described above for localizing GFP-FtsW in EC850, except that spectinomycin and chloramphenicol were used for plasmid maintenance. In this case, addition of IPTG induced expression of both 3xHA-*ftsW* from a plasmid and the *gfp-ftsI* from the chromosome. Cells were fixed for microscopy, and samples were taken for Western blot analysis to verify production the 3xHA-FtsW protein.

Bacterial two-hybrid analysis. Transformants of DHM1 carrying appropriate plasmid pairs (derivatives of pUT18c and pKT25) were streaked onto plates of LB medium containing ampicillin (200 μg/ml) and kanamycin (40 μg/ml), and the plates were incubated for 2 or 3 days at 30°C. Three to five colonies were used to inoculate 5 ml of LB medium containing ampicillin and kanamycin plus 0.5 mM IPTG, and the cultures were grown on a roller at 30°C for 16 h to an OD_{600} of 0.6 to 0.8. Then duplicate 15-μl culture samples were assayed for β-galactosidase activity by standard procedures

(Miller, 1972). All assays were repeated at least three times (on different days).

Western blotting. For Western blotting, typically 1 ml of culture at an OD_{600} of 0.5 was centrifuged, and the resulting cell pellet was taken up into 0.5 ml of sodium dodecyl sulfate-polyacrylamide gel electrophoresis (SDS-PAGE) loading buffer. Samples were boiled, and 10-µl aliquots were subjected to SDS-10% PAGE. Proteins were then transferred onto nitrocellulose and detected by standard methods. Rabbit anti-GFP antibodies were obtained from W. Margolin and used at a dilution of 1:2,500. Mouse anti-HA serum (Covance) was used at a 1:10,000 dilution. The secondary antibody was horseradish peroxidase-conjugated goat anti-rabbit antibody (1:8,000; Pierce) or goat anti-mouse antibody (1:5000; Molecular Probes), which in turn was detected with SuperSignal Pico West chemiluminescent substrate (Pierce). Blots were visualized with an LAS-1000 luminescent imager from Fuji (Stamford, CT).

Results

Phenotypes of FtsW derivatives with mutant TMs. We mutagenized each of FtsW's 10 transmembrane helices by substituting three consecutive residues in the middle of each TM for alanine, except in the case of TM4, where two 3-ala constructs were made (black circles in Figure 2.1A). TM4 is predicted to contain highly conserved charged residues, so we were concerned that the 3-ala substitutions might disrupt assembly of the protein into the membrane. The full set of mutant proteins was cloned into two different vectors, creating fusions to GFP or three tandem copies of the hemagglutinin epitope tag (3xHA), respectively. Western blotting with anti-GFP and anti-HA antibodies verified wild type and all mutant proteins were produced at similar levels (Figure 2.2).

The FtsW derivatives were assayed for septal localization, ability to recruit FtsI to the septal ring, and complementation of an FtsW depletion strain. Only three of the mutant proteins had noteworthy defects (Figures 2.1B, 2.3, and 2.4). The TM1 mutant complemented weakly, did not localize very efficiently and failed to recruit FtsI (presumably as a consequence of its poor localization). We infer that TM1 plays a critical role in assembly of FtsW into the membrane or targeting FtsW to the septal ring. The TM4a mutant protein failed to support colony formation despite the fact that it localized to the septal ring and recruited FtsI. Perhaps TM4 is involved in the putative Lipid II transport activity of FtsW. The final interesting protein was the TM10 mutant, which localized well but did not support efficient recruitment of FtsI to the septal ring. The TM10 protein barely supported division in a complementation assay and was a mild dominant negative when co-expressed with wild type (note the elongated cell in the DHB4 background in Figure 2.3). This phenotype is what we would expect of an FtsW protein that is specifically defective in interaction with FtsI. Pastoret et al. (2004) reported a similar phenotype for a mutant FtsW with two amino acid substitutions in the periplasmic loop connecting TM9 to TM10, which led these authors to suggest the TM9-TM10 loop interacts with FtsI (which they called PBP3).

Two-hybrid analysis. To try to get further evidence that TM10 of FtsW interacts with the lone TM of FtsI, we turned to a bacterial two-hybrid system that had been used previously to show FtsW interacts with FtsI (Karimova et al., 2005). First, we confirmed the previously reported FtsW-FtsI interaction (Figure 2.5), which was stronger even than the positive control (two leucine zipper domains) (Karimova et al., 2000). Next, we surveyed our collection of FtsW 3-ala proteins. Lesions in TM1, 5, 6 and 10 all reduced the apparent interaction with FtsI by 2- to 4-fold, with the TM10 mutant protein exhibiting the weakest interaction (Figure 2.5). While generally consistent with our hypothesis, the complexity of these results makes it difficult to draw firm conclusions.

We also used the two-hybrid system to test the ability of several FtsI derivatives to interact with FtsW. Lesions in the TM of FtsI that prevent septal localization (Wissel & Weiss, 2004) also abrogated the interaction (Figure 2.6; see Leu 39 to Pro, or lengthening the TM by insertion of a Leu at position 41). Thus, the TM of FtsI appears to be necessary for the interaction with FtsW. An FtsI protein truncated at residue 50, designated 50-stop, failed to interact with FtsW in the two-hybrid system (Figure 2.6). This fragment encodes the entire cytoplasmic domain and TM and localizes to the septal ring, albeit weakly (Wissel et al., 2005). To observe an interaction with FtsW, it was necessary to include more of the periplasmic domain (Figure 2.6; e.g., 80-stop and 239-stop). In toto, these findings argue that FtsI must have an intact TM to interact with FtsW but the TM itself is not sufficient—portions of the periplasmic domain immediately following the TM are needed too. These data are also consistent with a report by Karimova *et al* (2005) in which they showed a fragment of FtsI consisting of residues 1-70 could interact with FtsW, but fragments made up of residues 1-42 or 19-51 (both of which maintain the TM) were unable to interact with FtsW.

Discussion

Systematic mutagenesis of the TMs of FtsW has revealed three TMs that may play specific roles in FtsW function.

(i) TM1 is important for septal localization. One interesting possibility is that TM1 of FtsW interacts with a septal ring component like FtsQ, FtsL or FtsB—these proteins form a complex that has been implicated in recruitment of FtsW to the septal ring (Goehring et al., 2006; Gonzalez et al., 2010).

At this point, we do not know if the lesions in TM1 of FtsW are blocking the protein's ability to interact with other cell division proteins or simply preventing it from properly inserting into the membrane. We do know that when expressed from a plasmid,

the mutant protein appears as stable as wild-type (Figure 2.2). But, we would need to probe the membrane fraction from cells expressing the mutant protein to address the abundance at that site.

One interesting way of following up on the TM1 localization phenotype would be testing this mutant protein for its ability to interact with the cell division proteins directly upstream in the recruitment pathway (FtsQLB) using the two-hybrid assay. However, in the two-hybrid system we have chosen to use, FtsW does not interact with FtsB and only weakly interacts with FtsQ and FtsL (Karimova et al., 2005), despite the *in vivo* interactions reported above. The modest levels of interaction FtsW shows with FtsQ and FtsL might prove problematic in interpreting results from an FtsW mutant. However, in another two-hybrid system (based on phage repressors) FtsW has been shown to interact with FtsQ, FtsL, and FtsB (Di Lallo et al., 2003). Perhaps follow-up work could be done using that system to further explore the role of TM1 in FtsW midcell targeting.

(ii) TM4 is essential for FtsW function. The TM4a 3-ala protein failed to rescue an FtsW-depletion strain, despite being present in normal amounts. Moreover, the protein localized to the septal ring and recruited FtsI. A noteworthy feature of TM4 is that it contains highly conserved charged residues. The properties of the TM4 mutant are consistent with this being a site of Lipid II interaction, although other interpretations cannot be excluded.

Working with most SEDS proteins is often complicated by their essential nature for the organism. However, as noted earlier, the sporulation related SEDS proteins SpoVE is non-essential and has been studied in *B. subtilis* (Real et al., 2008). Perhaps the information on the 4th TM's role in activity from our study could be applied to the SpoVE system. Analogous lesions could be engineered into SpoVE's corresponding TM and spore formation phenotypes studied. This approach would bypass the difficulties of working with depletion strains when studying the essential SEDS proteins, such as FtsW and RodA.

(iii) TM10 is involved in recruitment of FtsI to the septal ring. The TM10 3-ala protein localized to the septal ring but did not to recruit FtsI efficiently, resulting in a mild dominant negative phenotype. In a two-hybrid assay, the TM10 3-ala protein interacted only weakly with FtsI. Efforts to demonstrate a direct interaction using cysteines engineered into TM10 of FtsW and the lone TM of FtsI have been unsuccessful (not shown). While some of those difficulties were likely related directly to FtsW's problematic behavior in biochemical analysis (problems transferring protein from gels to membranes, aggregation in gel loading wells, inability to boil samples, among others), the possibility remains that the TM of FtsW doesn't make direct contact with the TM of FtsI.

(iv) Several observations argue that the region of FtsI's periplasmic domain closest to the TM also contributes to septal localization and interaction with FtsW. The inability of the P50-stop truncation of FtsI to interact with FtsW in the two hybrid analysis and the report from Nguyen-Disteche's laboratory that mutations in the loop region between FtsW's TM9 and 10 were important for FtsI recruitment (Pastoret et al., 2004) support this possibility. However, it is clear that the TM of FtsI is still critical for the FtsW interaction. Either of the mutant forms of FtsI with an altered TM failed to interact with FtsW in the two-hybrid system (Figure 2.6). These observations are consistent with results from Mark Wissel in which those same mutant FtsIs failed to localize to the division site (Wissel et al., 2005).

Table 2.1. Strains used in this study

Strain	Relevant features	Source or reference
DHB4	F′ *lacI*^{q} pro/λ^{-} Δ*lacX74 galE galK thi rpsL phoR* Δ*phoA*(PvuII) Δ*malF3*	Boyd et al., 1987
EC850	*ftsW::kan* / pBAD33-*ftsW*	Mercer et al., 2002
EC1655	W3110 Δ*lac*U169 *gal*490 Δ*fts*W ϕ80::*gfp-ftsI* / pBAD33-*ftsW*	Lab Collection
DHM1	*glnV44*(AS) *recA1 endA gyrA96 thi-1 hsdR17 spoT1 rfbD1 cya-854*	Karimova et al, 2000

Table 2.2. Plasmids used in the study

Plasmid	Relevant features	Source or reference
pDSW311	P_{206}-*gfp*-*ftsW* Amp^r	Mercer and Weiss, 2002
pAM238	pACYC184 derivative, $lac_{UV5}p$ Spc^r	Kadokura et al., 2004
pMPY-3xHA	3x-HA tag vector	Schneider, 1995
pUT18c	BACTH vector for fusion of target proteins to *B. pertussis cya* gene T18 fragment; P_{lac}::$cya^{675-1197}$-MCS pUC ori Ap^r	Karimova et al, 2000
pKT25	BACTH vector for fusion of target proteins to *Bordetella pertussis cya* gene T25 fragment; P_{lac}::cya^{1-675} p15 ori Km^r	Karimova et al, 2000
pDSW824	pDSW311(3-ala 1)	This work
pDSW825	pDSW311(3-ala 3)	This work
pDSW826	pDSW311(3-ala 8)	This work
pDSW827	pDSW311(3-ala 9)	This work
pDSW828	pDSW311(3-ala 10)	This work
pDSW829	pDSW311(3-ala 4a)	This work
pDSW830	pDSW311(3-ala 4b)	This work
pDSW832	pDSW311(3-ala 2)	This work
pDSW833	pDSW311(3-ala 5)	This work
pDSW834	pDSW311(3-ala 6)	This work
pDSW835	pDSW311(3-ala 7)	This work
pDSW836	pAM238-3xHA-*ftsW*	This work
pDSW920	pKT25-*ftsW*	This work
pDSW921	pDSW920(3-ala 8)	This work
pDSW922	pDSW920(3-ala 10)	This work
pDSW970	pDSW920(3-ala 1)	This work
pDSW971	pDSW920(3-ala 2)	This work
pDSW972	pDSW920(3-ala 3)	This work
pDSW973	pDSW920(3-ala 4a)	This work
pDSW974	pDSW920(3-ala 4b)	This work
pDSW975	pDSW920(3-ala 5)	This work
pDSW976	pDSW920(3-ala 6)	This work
pDSW977	pDSW920(3-ala 7)	This work
pDSW978	pDSW920(3-ala 1)	This work

Table 2.2. continued

Plasmid	Relevant features	Source or reference
pDSW1149	pAM238-3xHA-*ftsW*(3-ala 1)	This work
pDSW1150	pAM238-3xHA-*ftsW*(3-ala 2)	This work
pDSW1151	pAM238-3xHA-*ftsW*(3-ala 3)	This work
pDSW1152	pAM238-3xHA-*ftsW*(3-ala 4a)	This work
pDSW1153	pAM238-3xHA-*ftsW*(3-ala 4b)	This work
pDSW1154	pAM238-3xHA-*ftsW*(3-ala 5)	This work
pDSW1155	pAM238-3xHA-*ftsW*(3-ala 6)	This work
pDSW1156	pAM238-3xHA-*ftsW*(3-ala 7)	This work
pDSW1157	pAM238-3xHA-*ftsW*(3-ala 8)	This work
pDSW1158	pAM238-3xHA-*ftsW*(3-ala 9)	This work
pDSW1159	pAM238-3xHA-*ftsW*(3-ala 10)	This work
pDSW1160	pUT18c-*ftsI*(P50 truncation)	This work
pDSW1161	pUT18c-*ftsI*(R80 truncation)	This work
pDSW1162	pUT18c-*ftsI*(R239 truncation)	This work
pDSW1163	pUT18c-*ftsI*(L39P)	This work
pDSW1164	pUT18c-*ftsI*(+L41)	This work

Table 2.3. Primers used in the study

Primer	Sequence[a]
P415	GCGAAGCTTCTAGATCATCGTGAACCTCGTACAAACGC
GFP666F	GAGACCACATGGTCCTTCTTGAG
P845	AAAGCCAATCGCCGCGGCCGCGGTCAGCCACAGTAA
P846	CAGCGTAATGATCGCAGCGGCCGCCGCCAAAATCAGATA
P847	GACGATCATCAGCAGAGCGGCCGCTCCGAGCAGCATCGT
P848	GTCGGTGTGGTGCTGGCGGCCGCTATGGTATTCTTCGTC
P849	TCTATTGGCATCTGGGCGGCCGCTCAGGCGCTGGTTAAC
P850	TACGGTGGTTCGAGCGCGGCCGCTATGTCGACAGCCATC
P869	AAACAGCGACAGTTTAGCGGCCGCCGCAGGCTGGATACG
P870	GGCGATATAGCAAAAAGCGGCCGCTTTTGTCAGCTCCGC
P871	TAACACTGCCAACACAGCGGCCGCGCCCATCGGTTTCAG
P872	CAGGAACAACATCGCAGCGGCCGCCACAAACAACACCAC
P873	CAGCAACACAACCGCTGAAATGCCCATACCGATAATGGC
P874	CTTCTTCGCGAAGCGTGA
P875	CGAAGTACGTAATAACCT
P880	CGTGAATTCGCGGCGGCCGCTAAACTGTCGCTGTTTTGC
P881	CGTGAATTCAAAGCGGCCGCTTTTTGCTATATCGCCAAC
P882	CGTGAATTCGGCGCGGCCGCTGTGTTGGCAGTGTTACTG
p902	AGTCAATTGTTACCCATACGATGTT
P903	AACGCATGTTGTTGTTGTTGAATTCAGCGTAATCTGGAACGTC
P912	GCATGAATTCTTACGATCTGCC
P913	TCGACTCTAGAGAAAGCAGCGCGC
P914	GCTCGGTACCTTCATCGTGAAC
P915	TCGACTCTAGAGATGCGTTTATCT
P993	ACTAAGCTTTCATCGTGAACCTCGTACAA
P994	AGTGGTACCTTACCCATACGATGTT
P1021	TACGGTGGTTCGAGCTTACTGATTTGCTCGACAGCCATC
P1022	TACGGTGGTTCGAGCTTACTGTGCATGTCGACAGCCATC
P1023	TACGGTGGTTCGAGCTTATGCATTATGTCGACAGCCATC
P1024	TACGGTGGTTCGAGCTGCCTGATTATGTCGACAGCCATC
P1025	TACGGTGGTTCGTGCTTACTGATTATGTCGACAGCCATC
P1033	CTTAGGTACCGTTCATCGTGAACCTCGTACAA
P1034	CTAGAGGATCCCATGCGTTTATCTCTC
P1057	AGCGCCAGGCAAATACAGCC
P1058	GGAGAATACAGCAGCATAACAACG
P1059	GCCGCATAAGCACGCAAAACG

Table 2.3. continued

Primer	Sequence[a]
P1060	CAGGAGAATAGCGCCGCATAA
P1061	GAATACAGCCGGCTAACAACGC
P1096	CTTAGGTACCCGGGGAGATAACTTGTA
P1097	CTTAGGTACCGCGACCAGAACGGTCAGTA
P1098	CTTAGGTACCCAGGCGTTCATCAATACTC
P1099	CTTAGGTACCTTACGATCTGCCACCTG
P1100	CTAGAGGATCCCAAAGCAGCGGCGAAA

[a] DNA sequence is given in the 5’ to 3’ direction for all primers.

Figure 2.1. Overview of FtsW. A. Model of FtsW. Residues conserved among different γ-proteobacteria are shown in green. Residues targeted for alanine substitution are shown in bold black outline. B. Table summarizing phenotypes observed in this study.

A

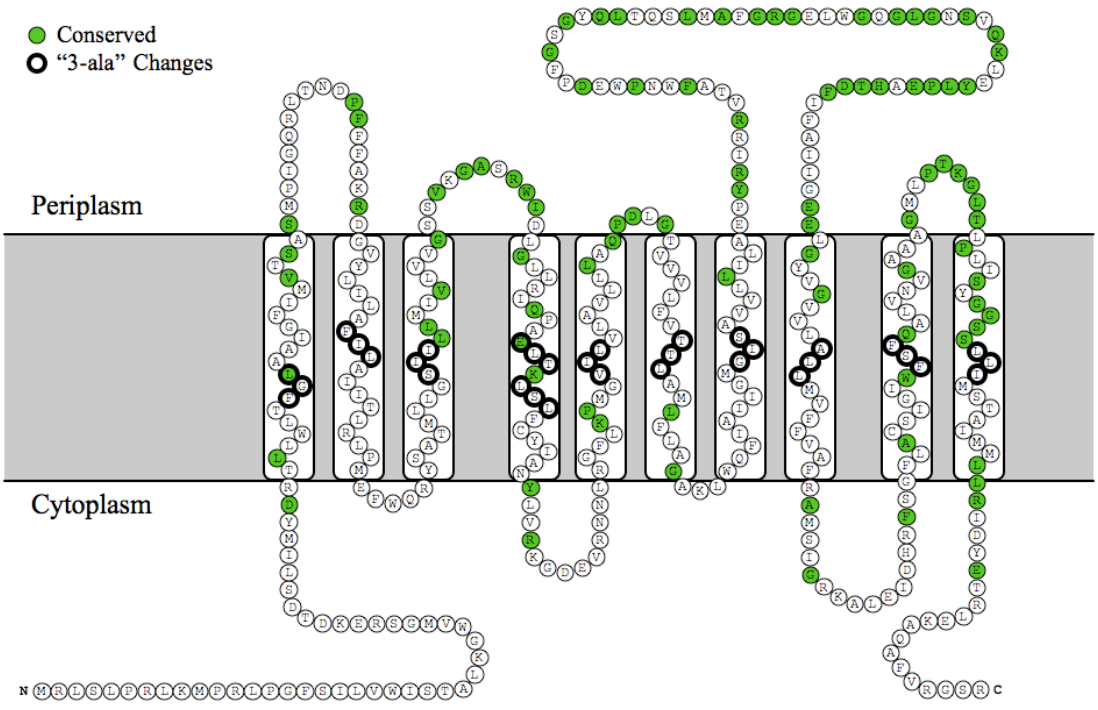

B

Summary of FtsW 3 alanine lesion phenotypes

Lesion	Localization DHB4	Localization Depletion	FtsI Recruitment[a]	Complementation	Protein Stability
WT	45%	38%	+++	+++	+
TMH1	<1%	10%	-	+[b]	+
TMH2	45%	15%	+++	+++	+
TMH3	51%	15%	+++	+++	+
TMH4a	25%	17%	+++	-[c]	+
TMH4b	30%	6%	+++	++	+
TMH5	24%	30%	+++	+++	+
TMH6	30%	30%	+++	+++	+
TMH7	36%	17%	+++	+++	+
TMH8	36%	28%	+++	+++	+
TMH9	32%	12%	+++	+++	+
TMH10	89%	90%	+	+[b]	+

[a] FtsI recruitment measured as spacing of bands of GFP-FtsI fluorescence in cells. "+++" was assigned to cells expressing wild-type FtsW and represents ~11 microns per GFP band. "+" assigned to TMH10 mutant represents ~23 microns per band. The TMH1 mutant showed extremely low levels of GFP-FtsI recruitment.

[b] Cells appeared filamentous when examined with phase contrast microscopy.

[C] No colony formation on plates, but only modest filamentation in liquid culture.

Figure 2.2. Steady state protein levels of FtsW. A. Levels of the GFP-FtsW fusion proteins (blot probed with anti GFP primary antibody). B. Levels of the 3xHA tagged FtsW fusion proteins (blot probed with anti HA monoclonal antibody).

A.

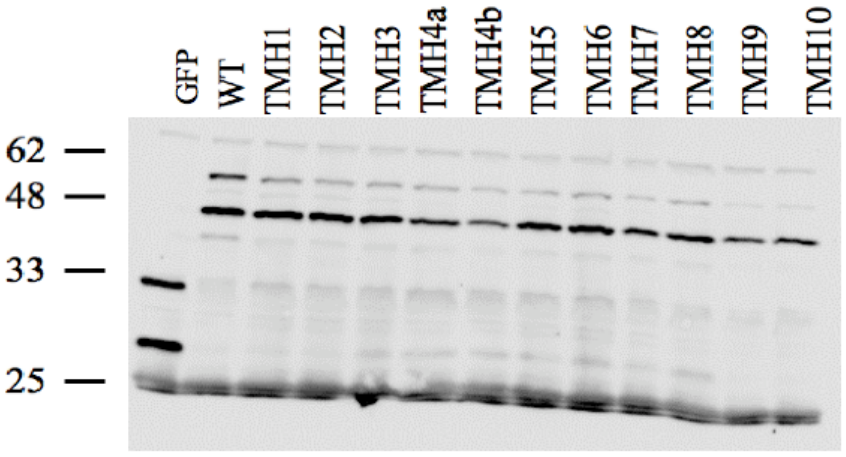
GFP
WT
TMH1
TMH2
TMH3
TMH4a
TMH4b
TMH5
TMH6
TMH7
TMH8
TMH9
TMH10
62
48
33
25

B.

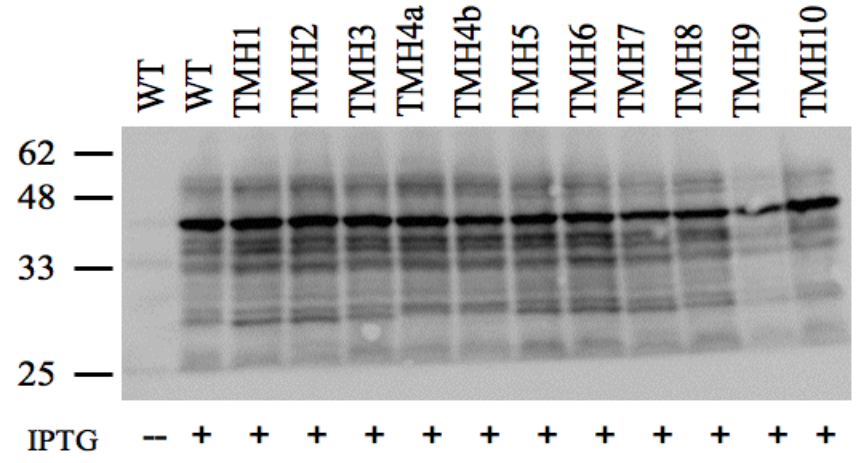
WT
WT
TMH1
TMH2
TMH3
TMH4a
TMH4b
TMH5
TMH6
TMH7
TMH8
TMH9
TMH10
62
48
33
25
IPTG
– + + + + + + + + + + + +

Figure 2.3. Localization of selected GFP-FtsW proteins with TMH lesions. Constructs were expressed either in a strain background (DHB4) with native FtsW present or after depletion of native FtsW (by growing EC850 transformants in LB glucose).

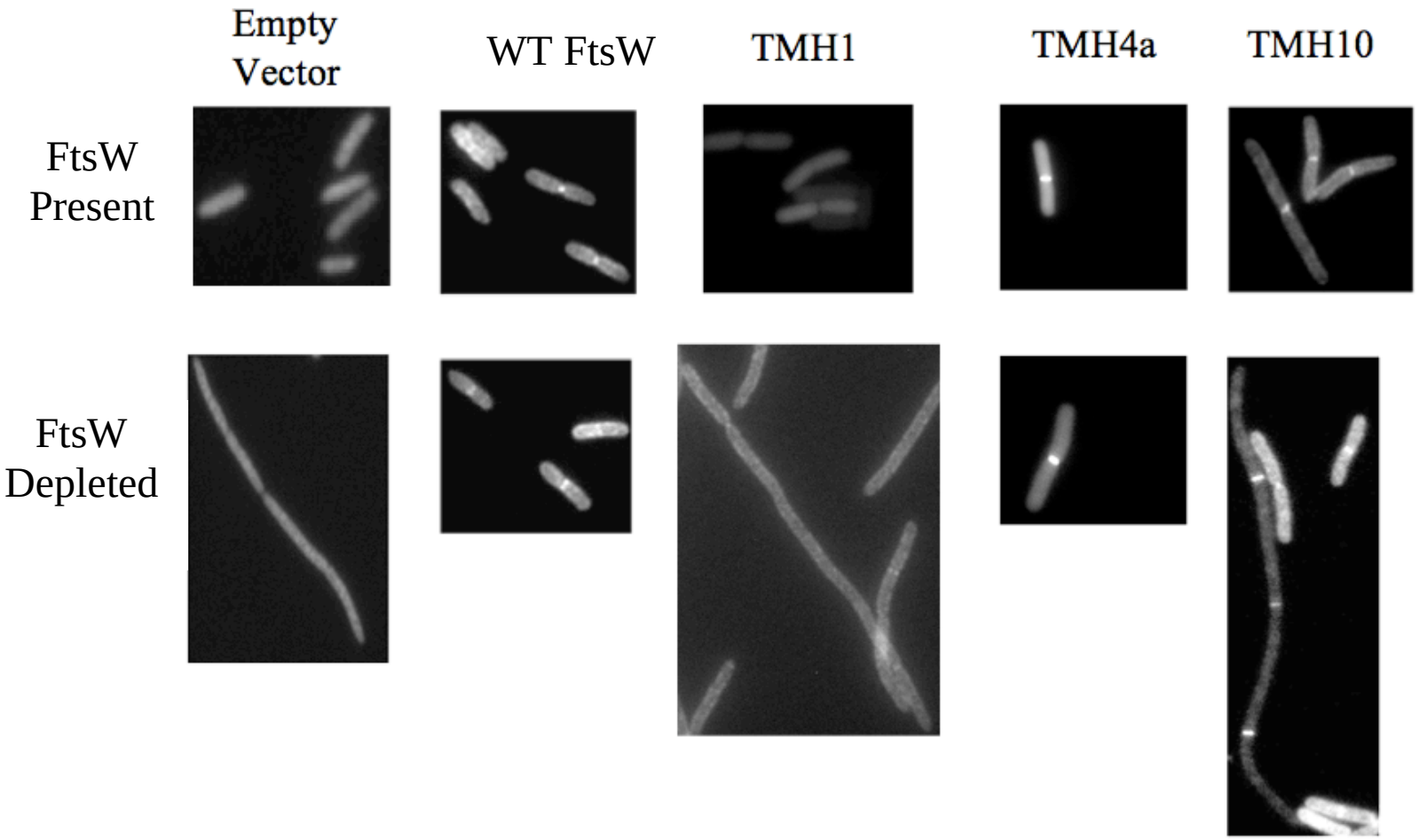
Empty Vector
WT FtsW
TMH1
TMH4a
TMH10
FtsW Present
FtsW Depleted

Figure 2.4. Recruitment of GFP-FtsI by FtsW TM mutant proteins. Cultures were grown in LB glucose to deplete wild-type FtsW. IPTG was added to induce *gfp-ftsI* and the plasmid-borne *ftsW* allele indicated. None = no addition of IPTG; this was done to monitor formation of filamentous cells.

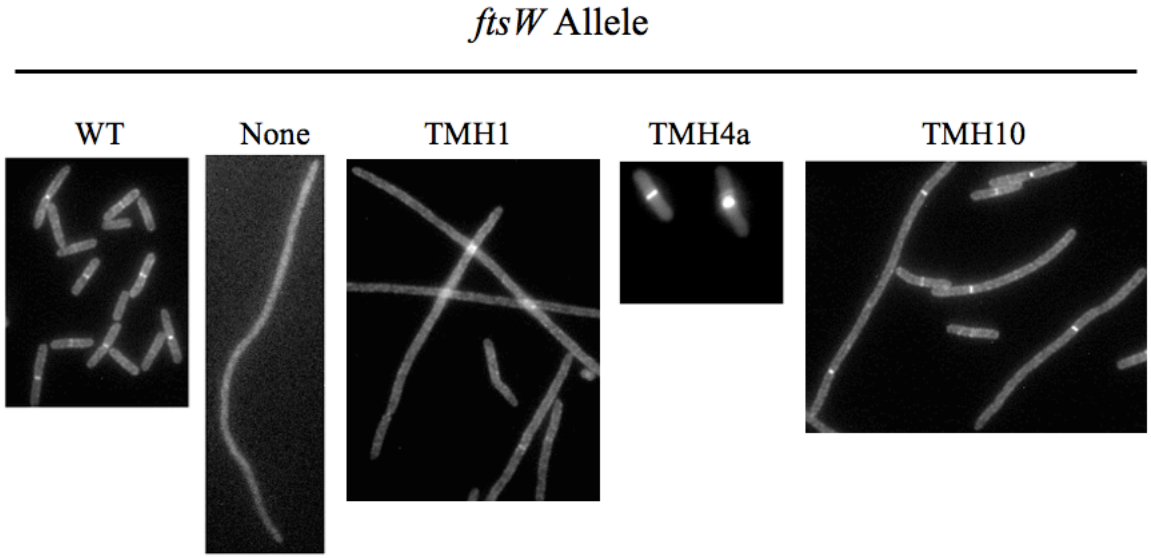
ftsW Allele
WT
None
TMH1
TMH4a
TMH10

Figure 2.5. Bacterial two-hybrid analysis of FtsW TMH lesions. A set of 10 FtsWs with 3 alanine substitutions in each TMH was tested against FtsI. *ftsW* derivatives were located on the pKT25 plasmid and *ftsI* on the pUT18c vector. Negative control = empty vectors. Positive control = two leucine zipper proteins known to interact (Karimova et al., 2000).

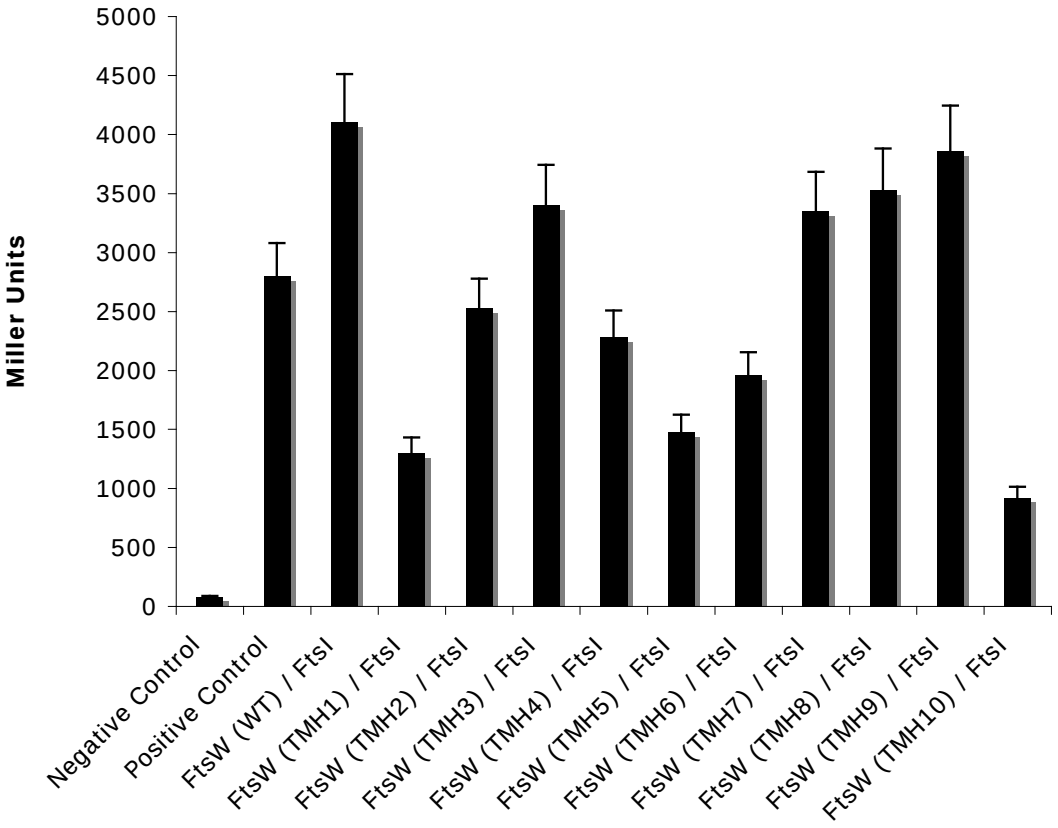
Miller Units
5000
4500
4000
3500
3000
2500
2000
1500
1000
500
0
Negative Control
Positive Control
FtsW (WT) / FtsI
FtsW (TMH1) / FtsI
FtsW (TMH2) / FtsI
FtsW (TMH3) / FtsI
FtsW (TMH4) / FtsI
FtsW (TMH5) / FtsI
FtsW (TMH6) / FtsI
FtsW (TMH7) / FtsI
FtsW (TMH8) / FtsI
FtsW (TMH9) / FtsI
FtsW (TMH10) / FtsI

Figure 2.6. FtsI. A. Domain structure of FtsI (modified from Wissel *et al.*, 2005). B. Bacterial two-hybrid analysis of FtsI mutant/truncation collection against FtsW. Assays conducted as per analysis shown in Figure 2.5. *ftsI* variants are located on the pUT18c vector. Positive and negative controls as in Figure 2.5.

A.

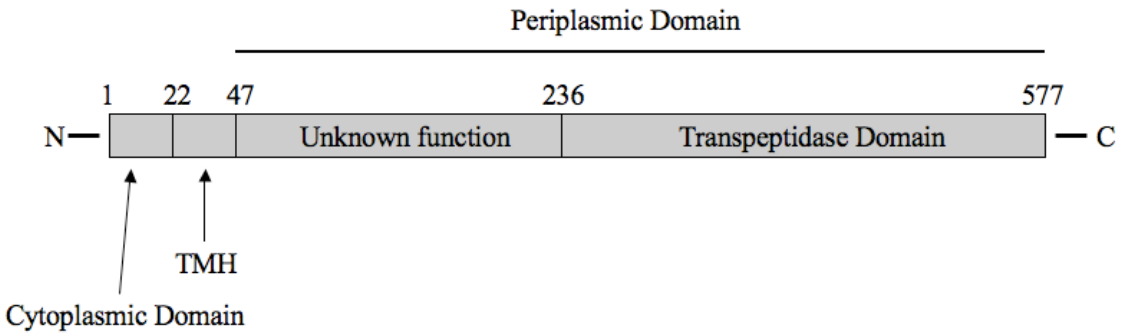
Periplasmic Domain
1
22
47
236
577
N
Unknown function
Transpeptidase Domain
C
TMH
Cytoplasmic Domain

B.

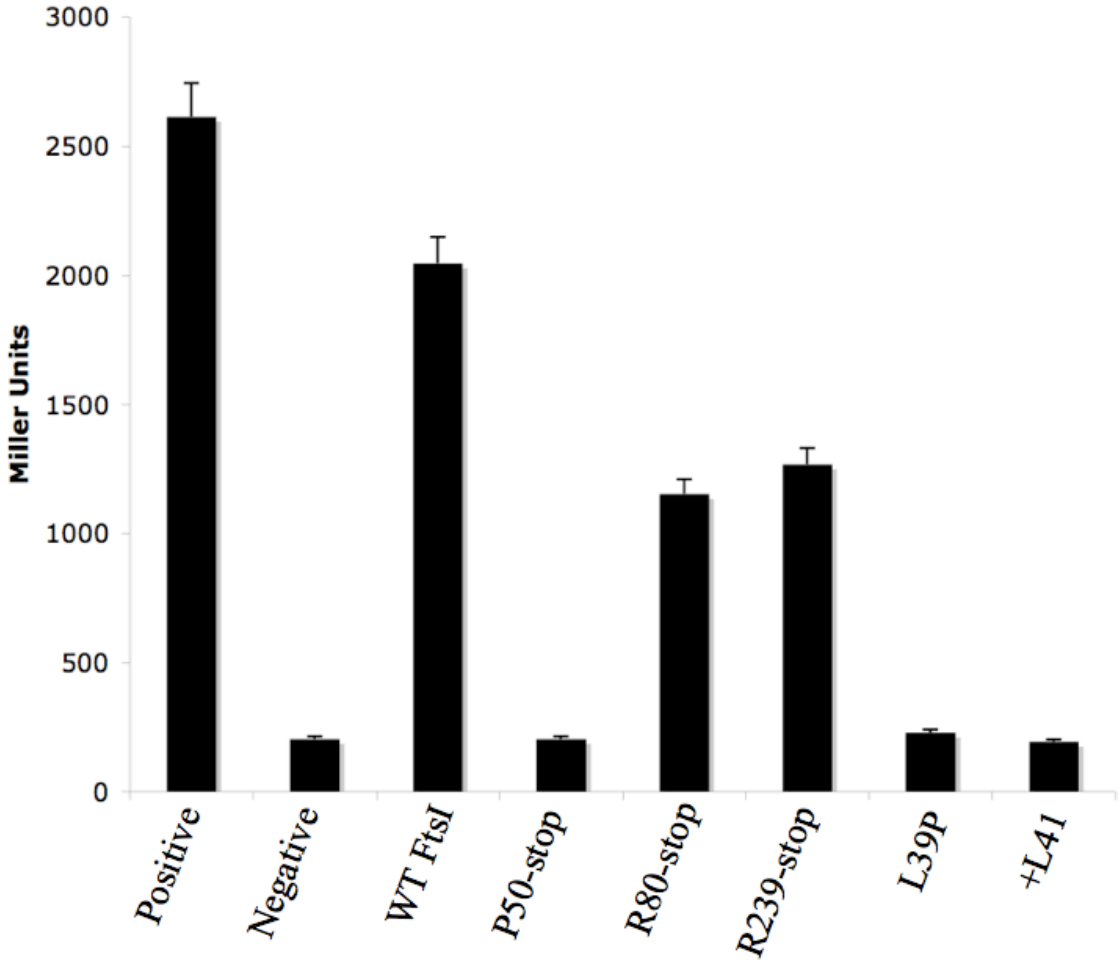
3000
2500
2000
1500
1000
500
0
Miller Units
Positive
Negative
WT FtsI
P50-stop
R80-stop
R239-stop
L39P
+L41

CHAPTER 3: CHARACTERIZATION OF A PEPTIDOGLYCAN BINDING ASSAY USING PURIFIED SPOR DOMAINS

Introduction

Although SPOR domains are described in databases such as Pfam and Interpro as being involved in binding peptidoglycan, this activity has only been demonstrated biochemically for the SPOR domain from FtsN from two species, *E. coli* and *Caulobacter crescentus* (Ursinus et al., 2004; Moll & Thanbichler, 2009). In both cases binding was demonstrated by showing that a purified His_6-tagged SPOR domain co-sedimented with whole PG sacculi during ultracentrifugation. Essentially the same assay has also been used to show that a PASTA domain from a *Mycobacterium tuberculosis* kinase also binds to PG (Shah et al., 2008). Unfortunately, none of these publications did a very thorough job of characterizing the co-sedimentation assay, so it is not entirely clear how robust the assay is or what exactly it measures.

Both our lab and Piet de Boer's recently demonstrated that numerous SPOR domains localize to the division site when produced in growing *E. coli* cells (Gerding et al., 2009; Arends et al., 2010). Both labs also hypothesized that SPOR domains are recruited to the division site by binding preferentially to septal PG. One problem with this hypothesis, however, is that PG in the division septum is generally considered to be identical to PG elsewhere around the cell (Hungerer & Tipper, 1969; Glauner et al., 1988; Obermann & Holtje, 1994; Signoretto et al., 1996; Ishidate et al., 1998; Lara et al., 2005). We think there must be differences, and hope that studying the SPOR:PG interaction in detail will reveal what these differences are.

In this chapter we describe our efforts to characterize the co-sedimentation assay that we and others have used to document binding of proteins to PG. We then use this assay to explore some of the structural features of PG that might be recognized by SPOR

domains. We also demonstrate that a wide range of SPOR domains bind PG. In this context, it is important to note that the ideal assay would be quantitative and minimize the amount of PG used per reaction, because purification of PG from *E. coli* is very time consuming and the yield is low. Other desirable characteristics included robustness with respect to pH and salt concentrations, linearity with protein, and specificity. By specificity we mean two things. First, only authentic PG binding proteins should co-sediment with the sacculi under the assay conditions employed. Second, SPOR domains should bind to purified PG sacculi the same way they bind to PG in live cells. The results presented below show that our assay is reasonably well behaved in all respects, except one—binding of SPOR domains to isolated sacculi does not appear to reflect specific binding to only the septal PG in those sacculi.

Materials and Methods

Media. *E. coli* strains were grown in Luria-Bertani (LB) medium containing 10 g tryptone, 5 g yeast extract, and 10 g NaCl per liter. Plates contained 15 g agar per liter. Ampicillin was used at 200 µg /ml.

Strains. Strains used in this study are listed in Table 3.1. *Aquifex aeolicus* DNA was obtained from R. Huber, *Cytophaga hutchinsonii* ATCC 33406 was obtained from the American Type Culture Collection, *Vibrio parahaemolyticus* LM5674 was obtained from L. McCarter, *Staphylococcus aureus* SH1000 was obtained from A. Horswill, and *Bacillus subtilis* PY79 was obtained from C. Ellermeier.

Plasmids. Plasmids used in this study are listed in Table 3.2. Plasmids were constructed by PCR using VENT DNA polymerase (New England Biolabs) and sequenced to verify their integrity. All primers were obtained from Integrated DNA

Technologies (Coralville, IA). In the following descriptions, restriction sites incorporated into primers are underlined. pDSW1000 [P_{T5}::*His*$_6$-*damX*(338-428)] was constructed using primers P1144 (GCCGGATCCAACAACAACGGTTCGTTGAAATCGGCA) and P1137 (CTGAAGCTTACTTCAGATCGGCCTGTACCT) to amplify the last 90 codons of *damX* with pDSW918 as the template. The 301-bp product was cut with BamHI and HindIII and ligated into the corresponding sites of pQE80L. pDSW1002 [P_{T5}::*His*$_6$-*dedD*(141-220)] was constructed by amplifying the last 80 codons of *dedD* from plasmid pDSW937 with primers P1125 (GCCGGATCCAACAACAACGGTAAAGCCTATGTTGTG) and P1126 (GCCAAGCTTTAATTCGGCGTATAGCCCATT). The 269-bp product was cut with BamHI and HindIII and ligated into the corresponding sites of pQE80L. pDSW1003 [P_{T5}::*His*$_6$-*rlpA*(283-362)] was constructed by amplifying the last 80 codons of *rlpA* from plasmid pDSW931 with primers P1127 (GCCAGATCTAACAACAACGTCTCGCAAAGCGCCAGC) and P1128 (GCCAAGCTTTACTGCGCGGTAGTAATAAAT). The 269-bp product was cut with BglII and HindIII and ligated into the BamHI and HindIII sites of pQE80L. pDSW1114 [P_{T5}::*His*$_6$-*aq1896*(254-342)] was constructed by amplifying the last 89 codons of *aq1896* from *A. aeolicus* chromosomal DNA with primers P1223 (GCCGGATCCAACAACAACATCCCAAGAGTGCATAAA) and P1224 (CTGAAGCTTATCACTTGATTTCAACGACGAA). The 298-bp product was cut with BamHI and HindIII and ligated into the corresponding sites of pQE80L. pDSW1113 [P_{T5}::*His*$_6$-*chu2221*(161-249)] was constructed by amplifying the last 89 codons of *chu2221* from chromosomal DNA of *C. hutchinsonii* ATCC 33406 with primers P1229 (GCCGGATCCAACAACAACTTCTATTCTACTAAATTGGAG) and P1230 (CTGAAGCTTATTTTGGAGATAGGATCACACT). The 295-bp product was cut with BamHI and HindIII and ligated into the corresponding sites of pQE80L. pDSW1115 [P_{T5}::*His*$_6$-*vpa1294*(37-134)] was constructed by amplifying the last 97 codons of

vpa1294 from chromosomal DNA of *V. parahaemolyticus* strain LM5674 using primers P1317 (GCCGGATCCAACAACAACGCATACGGCTACCTGAATCCC) and P1318 (CTGAAGCTTAGCGCATTCTCACGACACTAG) and ligated into the corresponding sites of pQE80L.

Purified proteins. MBP2* was purchased from New England Biolabs (Beverly, MA). FtsZ was overproduced and purified as described previously (RayChaudhuri & Park, 1992), except that Q-Sepharose Fast-Flow was substituted for DEAE-Sephacel. His_6-tagged SPOR domains were overproduced in and purified from *E. coli* BL21 transformants by cobalt affinity chromatography on Talon affinity resin according to instructions from the manufacturer (Clontech, Mountain View, CA). The purified proteins were dialyzed into storage buffer (50 mM Tris-HCl, 200 mM NaCl, 5% glycerol, pH 7.5), and aliquots were stored at –80°C until needed. A 0.5-liter culture yielded 4 mg purified protein as determined by ultra violet absorption at 280 nm with a Nanodrop Spectrophotometer (Thermo). Extinction coefficients for each His_6-SPOR domain were calculated from their sequences using ProtPram (Wilkins et al., 1999). Protein purity was >95% as judged by SDS-PAGE.

Purification and quantification of PG. Cells of wild type *E. coli* (EC251) for isolation of PG sacculi were grown at 30°C and 210 rpm in 2 L flasks containing 0.5 L of LB. Typically two cultures at an OD_{600} ~ 0.8 were harvested per preparation. Purification of PG sacculi involved boiling cells in SDS and multiple enzymatic treatments (Pronase, Amylase, DNase, RNase) essentially as described (Glauner, 1988). PG was quantified for us by David Popham (Virginia Tech) by quantifying muramic acid. Briefly, samples of purified PG were suspended in 6 N HCl and hydrolyzed at 95°C for 4 h. Hydrolysates were subjected to amino sugar analysis (González-Castro, 1997) and quantified relative to purified standards processed in parallel. The values furnished to us by Dr. Popham were nmol of NAG per µl of sample. To convert nmol of NAG to a

weight basis, we took advantage of the fact that, to a good approximation, PG is a repeating structure composed of NAG-NAM(tetrapeptides). Thus, there are as many nmols of NAG as there are nmols of NAG-NAM(tetrapeptide). The mass of a NAG-NAM(tetrapeptide) is 985 g/mol, so a PG sample that has 1 nmol of NAG per µl has 985 ng (or 0.985 µg) of NAG-NAM(tetrapeptide) per µl. For generation of PG from filamentous *E. coli* cells that lack division septa, strain EC309 (*ftsZ*(Ts)), was used. Cells were grown at 30° C until an OD_{600} of 0.4 was reached. At that time the temperature was shifted to 42° C. After one hour of growth at 42° C, cells appeared filamentous under light microscopy, with an average length of ~17 µm. PG was then prepared from these cells as described above.

PG binding assays. Our standard binding assay was conducted in 25 mM potassium phosphate, pH 7.5, and 200 mM NaCl. A standard assay mixture contained 12 µg protein and 75 µg PG in a total volume of 100 µl. This is equivalent to ~1 nmol of His_6-$DamX^{SPOR}$ and ~75 nmol of NAM-NAG disaccharide units. As a control, assay mixtures that lacked PG were also prepared. Mixtures were incubated for 1 h on ice and then centrifuged at 4°C in a Beckman TLA-55 rotor at 50,000 rpm (average *g* force, 112,000 x *g*) for 45 min. The supernatant was recovered and saved for analysis. The PG pellet was washed by suspending it in 100 µl of cold assay buffer and centrifuging as described above. The wash supernatant was also saved. The PG pellet was again suspended in 100 µl of binding buffer. Aliquots of all three fractions (supernatant, wash, pellet) were analyzed by SDS-15% PAGE. Gels were stained with Coomassie Blue (GelCode Blue from Pierce, Rockford, IL) and scanned using a Typhoon 8610 Imager (GE Healthcare) with the following instrument settings: excitation laser, 532 nm; emission filter, 560 nm, long pass; photomultiplier, 600 V; and pixel size, 100 µm. ImageQuant software was used to quantify fluorescence signals. Because there was not

much protein in the wash, in later versions of the assay we pooled the initial supernatant and wash fractions before loading the gels.

Results

Comparison of published assay conditions. Our assay was based on published versions of the procedure, which we now summarize. Ursinus *et al* (2004) incubated 3 µg of protein with 100 µg PG in a buffer containing 10 mM Tris-maleate (pH 6.8), 10 mM $MgCl_2$, 50 mM NaCl, and 0.02% NaN_3. Protein was detected by Western blot or by staining gels with zinc. Photos of representative gels were published, but there was no quantification. Möll and Thanbichler (2009) used this same buffer/salt but roughly four fold more PG. Protein was detected by Western blotting, and a picture of the blot was published. Shah et al. (2008) used 50 µg protein and 5 mg PG (Shah et al., 2008) but did not specify volumes, buffer or salt conditions. Gels were stained with GelCode Blue (Thermo) and scanned, with results presented as a (quantitative) bar graph. In summary, the most striking differences among these assays related to the amounts of protein and PG used.

Of the three published studies, only Ursinus et al. (2004) included specificity controls. To demonstrate specificity with respect to protein, they used a mixture of protein molecular weight standards purchase from BioRad. They did not show the result, but said that some of these control proteins co-sedimented with PG, which could be worrisome, depending on the extent of the binding. Ursinus et al. also presented evidence that co-sedimentation of FtsN's SPOR domain reflects binding to septal PG. This was accomplished by showing that only about half as much SPOR domain bound when sacculi were prepared from non-dividing cells. The non-dividing cells were obtained by treating a culture with furazlocillin, a ß-lactam that inactivates FtsI (also known as penicillin-binding protein 3).

Development and characterization of our assay. Since PG from *E. coli* is a limiting resource, we chose to use a lower amount (75 µg) than the above reports for our assays. For instance, the 5 mg used in one experiment by Shah et al. (2008) would consume nearly all the PG purified from 2 liters of *E. coli*. (Note that Shah et al. were working with *B. subtilis*, which has more than 10-fold more PG per cell than does *E. coli*.) We also decided to switch to a phosphate buffer, since Tris-based buffers do not function that well at pH 6.8 and we wished to assay a variety of pH levels. Tris is also more affected by temperature changes.

An overview of our assay is presented in Figure 3.1. Our findings when His_6-$DamX^{SPOR}$ was tested at various pH and salt conditions are summarized in Table 3.3. Briefly, about 60% of the input protein bound to PG at pH 6.5, 7.0 and 7.5, but only ~30% bound at pH 8.0. Likewise, when the pH was 7.5, ~60% of the protein co-sedimented with PG at 50 and 200 mM NaCl, but this dropped to ~30% at 500 mM NaCl. Inclusion of 20 mM imidazole had little or no effect on binding to PG, arguing that binding is not driven by a non-specific interaction of the His_6 tag with the sacculus.

The effect of protein concentration on binding was assayed in mixtures containing 75 µg of PG, 25 mM $NaPO_4$ buffer (pH 7.5) and 200 mM NaCl. Binding increased rather linearly with protein over the entire range assayed, which was from 3 µg to 36 µg (Fig. 3.2). Nevertheless, the fraction of input protein that co-sedimented with PG decreased slightly above 12 µg (Table 3.3).

Binding of $DamX^{SPOR}$ to different PG preparations. As an initial approach to identifying the chemical features of PG that constitute a binding site for the SPOR domain of DamX, we assayed co-sedimentation with PG prepared from different sources. A PG preparation expected to lack septal PG was prepared from an *ftsZ*(Ts) mutant that had been grown at the non-permissive temperature until the cells were ~17 um long. Interestingly, $DamX^{SPOR}$ bound as well to PG from these nondividing cells as to PG from

wild type cells that were dividing normally (Table 3.3). This result suggests the pull down assay measures a general affinity of the protein for PG rather than specific binding for septal PG.

We took advantage of the structural diversity that exists naturally among different bacterial species to explore the potential relevance of the peptide cross-link. To this end, we isolated sacculi from *Bacillus subtilis*, *B. sphaericus*, and *S. aureus*. *B. subtilis* and *E. coli* use the same cross-link; the ε-amino group of a diaminopimelic acid in position 3 is joined directly to the carboxylate of D-Ala in position 4 (Atrih et al., 1999). Nevertheless, in *B. subtilis* almost all of the peptide side-chains are cross-linked whereas in *E. coli* only about half are cross-linked. This difference arises because *B. subtilis* PG is much thicker than *E. coli* PG (~15 vs. ~1 layer). *B. sphaericus* is like *B. subtilis* except that the L-*meso*-diaminopimelic acid in the third position is replaced with L-lysine. *S. aureus* also has a multi-layer, extensively cross-linked sacculus as well as the L-lysine substitution but differs in having a penta-glycine bridge in the cross link (Rogers, 1980).

The SPOR domain from DamX bound PG from either of the two *Bacillus* species about as well as that from *E. coli*, but about 30% less protein bound to *S. aureus* (Figure 3.3). Interestingly, *S. aureus* lacks any proteins with identifiable SPOR domains (See Discussion).

PG binding is a general activity of SPOR domains. As noted in the introduction, the generalization that SPOR domains bind PG is based on studies of the SPOR domain of FtsN from two different bacterial species (Ursinus et al., 2004; Moll & Thanbichler, 2009). Our studies up to this point clearly show that the SPOR domain from *E. coli* DamX also binds PG. In order to determine whether PG binding is a general property of SPOR domains, we purified and tested His_6-tagged SPOR domains from five additional proteins: DedD, RlpA, VPA1294, CHU2221, and AQ1896 proteins. In each case, ~80% of the SPOR domain protein was recovered in the PG pellet (Figure 3.4),

whereas all of the protein remained in the soluble fraction when the sample was centrifuged in the absence of PG (data not shown). As a negative control, we performed similar pulldown assays with maltose binding protein (MBP) and FtsZ. Only ~20% of these proteins copelleted with PG (Figure 3.4), and neither was detected in the pellet when the sample was centrifuged in the absence of PG (data not shown).

Discussion

Based on the studies described above, we settled on the following conditions as a "standard" co-sedimentation assay: 12 µg protein, 75 µg PG, 25 mM $NaPO_4$ buffer (pH 7.5), 200 mM NaCl, in a final reaction volume of 100 µl. The amounts of protein and PG were chosen to be high enough to readily detect and quantify both the bound and unbound protein using Coomassie-stained gels. The buffer conditions were chosen to support efficient binding, with up to about 80% of the input protein co-sedimenting with the PG. Under these conditions binding was roughly linear with protein, which makes the assay suitable for asking whether different forms of PG or mutant SPOR domains bind less well. Although the amount of input protein could easily be increased beyond 12 µg, this would seem to be a waste of protein. At the lower extreme, we find that 3 µg of input protein is the minimum we can use given our detection methods. We think it would be possible to lower the amount of input protein using other detection methods such as Western blotting or if protein samples were concentrated by TCA precipitation prior to loading gels. The drawback to these methods for quantitative work is that every manipulation introduces potential for errors. In this context it is worth noting that we tried staining our gels with silver rather than Commassie but encountered problems with high background that interfered with quantification.

Using the data from our titration experiment, we estimate there are at least 90,000 binding sites per sacculus, although the true value is likely to be much higher given that

the assay did not reach saturation. The value of 90,000 was arrived at as follows. When 36 µg of protein was used, about 18.5 µg was recovered in the pellet with the PG, which corresponds ~2 nmol of His_6-$DamX^{SPOR}$. That assay contained 75 µg of PG, which corresponds to ~75 nmol of disaccharide peptide units. Thus, the amount of protein recovered in the pellet was equivalent to ~3% of the disaccharide peptide units. The average *E. coli* sacculus contains 3×10^6 disaccharide peptide units (Wientjes et al., 1991). Three percent of 3×10^6 corresponds to 90,000.

In vivo SPOR domains probably bind preferentially to septal PG. Nevertheless, DamX's SPOR domain bound equally well to PG from wild type and filamentous cells of an *ftsZ*(Ts) mutant that should not have contained any septal PG. Curiously, Ursinus *et al.* reported that the SPOR domain from FtsN bound better to wild type PG than to PG from filamentous cells (Ursinus et al., 2004). Based on this, they inferred that FtsN's SPOR domain binds mainly septal PG in the pull down assay. Our findings argue otherwise. We cannot account for this discrepancy, but it is possible that FtsN's SPOR domain behaves differently from DamX's. Alternatively, it should be noted that Ursinus *et al.* generated filamentous *E. coli* by using an antibiotic that inhibits the transpeptidation activity of FtsI.

Prior to this study, only two SPOR domains had been shown to bind PG in a purified system, and both of these domains were derived from FtsN proteins (Ursinus et al., 2004; Moll & Thanbichler, 2009). Here we extended this finding to six additional SPOR domains, three from *E. coli* and one each from *V. parahaemolyticus*, *C. hutchinsonii*, and *A. aeolicus*. These findings establish that PG binding is a general property of SPOR domains. We have also demonstrated that all of these SPOR domains can also localize to the division site when expressed in *E. coli* (Arends et al., 2010). Taken together, these findings suggest septal localization is driven by binding to septal PG. Chapter 4 of this thesis describes our efforts to explore this link and identify

structural features of the SPOR domain that are important for protein function both *in vivo* and *in vitro*.

Some follow up work should be focused on better understanding the limitations of our binding assay. It should be possible to fully saturate the PG with protein and quantify the number of binding sites per sacculus, at least in the co-sedimentation assay. Conversely, if we were able to use much less protein in the assay, differences between wild type and "long cell" PG might become evident. Using less protein will require switching to Western blotting, or concentrating samples prior to analysis.

Preliminary work using PG isolated from a variety of organisms revealed that $DamX^{SPOR}$ bound equally well to PG from *E. coli*, *B. subtilis* and *B. sphaericus*, but less well to PG from *S. aureus*. In terms of structure, the most profound difference between *S. aureus* PG and all the rest is that the cross-link in *S. aureus* includes a penta-glycine bridge (Rogers, 1980). *S. aureus* sacculi may also have more curvature since the organism is coccus shaped. All other sacculi tested were from rod-shaped bacteria. This poor binding of $DamX^{SPOR}$ to *S. aureus* sacculi suggest that the cross-link is part of the binding site or the three-dimensional arraignment of the PG subunits may affect affinity. Interestingly, BLAST searches of *S. aureus* genomes failed to identify any SPOR domains (K. Williams, unpublished). It would be interesting to ask whether SPOR domains for heterologous organisms localize to division sites if produced in *S. aureus*.

Table 3.1. Strains used in this study

Strain	Relevant features	Source or reference
BL21 (λ DE3)	*ompT gal dcm hsdS$_B$*(r_B^- m_B^-) l (P_{lacUV5}::T7 gene 1)	Novagen
EC251	K-12 wild type MG1655	Lab collection
LM5674	V. parahaemolyticus *ΔopaR1* (translucent cell type)	Linda McCarter
ATCC 33406	*C. hutchinsonii*	American Type Culture Collection
SH1000	*Staphylococcus aureus* wild type lab strain, *rsbU+*	Alex Horswill
PY79	*Bacillus subtilis* wild type lab strain	Craig Ellermeier
13A82	*Bacillus sphaericus* Serotype 51, 5b	Patrick Eichenberger

Table 3.2. Plasmids used in the study

Plasmid	Relevant features	Source or reference
pDSW918	P_{204}::*gfp-damX lacI*^{q} *bla* pBR ori	Arends et al., 2010
pDSW931	P_{206}::*rlpA-rfp lacI*^{q} *bla* pBR ori	Arends et al., 2010
pDSW937	P_{204}::*gfp-dedD lacI*^{q} *bla* pBR ori	Arends et al., 2010
pDSW1000	pQE80L-*damX*(338–428)	This work
pDSW1002	pQE80L-*dedD*(141–220)	This work
pDSW1003	pQE80L-*rlpA*(283–362)	This work
pDSW1113	pQE80L-*chu2221*(161–249)	This work
pDSW1114	pQE80L-*aq1869*(254–342)	This work
pDSW1115	pQE80L-*vpa1294*(37–134)	This work
pQE80L	Carries T5 promoter and *lac* operators; *lacI*^{q} ColE1 ori Ap^{r}	Qiagen

Table 3.3. Development of PG binding assay

PG source[a]	Input protein	pH	NaCl concentration	% Protein in pellet[b]
Wild type	9 μg	6.5	50 mM	55.6
Wild type	9 μg	7.0	50 mM	61.2
Wild type	9 μg	7.5	50 mM	67.6
Wild type	9 μg	8.0	50 mM	28.5
Wild type	9 μg	7.5	50 mM	75.6
Wild type	9 μg	7.5	50 mM[c]	65.8
Wild type	9 μg	7.5	200 mM	67.0
Wild type	9 μg	7.5	500 mM	27.3
Wild type	3 μg	7.5	200 mM	64.0
Wild type	6 μg	7.5	200 mM	70.4
Wild type	12 μg	7.5	200 mM	74.7
Wild type	24 μg	7.5	200 mM	45.8
Wild type	36 μg	7.5	200 mM	51.4
ftsZ(Ts)	12 μg	7.5	200 mM	78.2

[a] Whole PG sacculi isolated from EC251 (wild type), or EC309 (*ftsZ*(Ts)).

[b] As determined by SDS-PAGE of the supernatant, wash and pellet fractions.

[c] This trial was done using 50 mM NaCl with the addition of 20 mM imidazole.

Figure 3.1. PG binding reactions. A. An overview of PG binding assay protocol. B. Representative results from a peptidoglycan (PG) binding assay using wild type $DamX^{SPOR}$ domain protein. SDS-PAGE gel stained with coomassie blue shows ~80% of the protein present in the PG pellet. A control from which PG was omitted shows that sedimentation is PG-dependent.

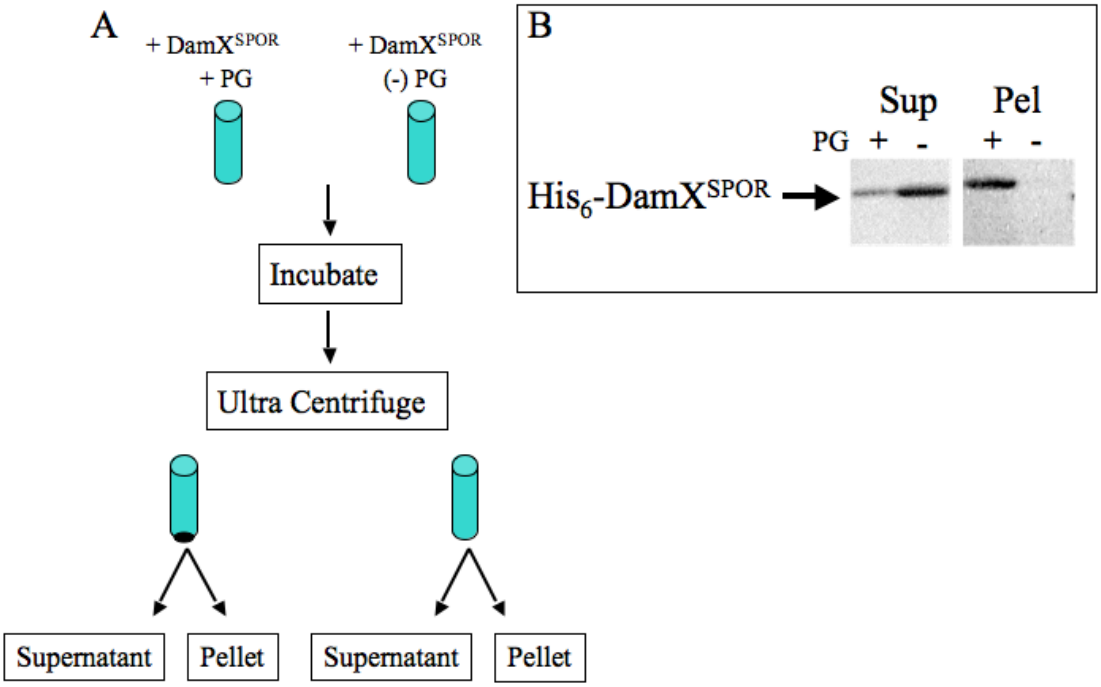
A
+ DamX^SPOR
+ PG
+ DamX^SPOR
(-) PG
Incubate
Ultra Centrifuge
Supernatant
Pellet
Supernatant
Pellet
B
Sup
Pel
PG + - + -
His6-DamX^SPOR

Figure 3.2. PG binding reaction titration. Graph shows the amount of His_6- $DamX^{SPOR}$ detected in the PG pellet when different input quantities of protein were used. Note that saturation was not attainted even with 36 μg of protein. Symbols ■ and ◆ represent data points from different assays.

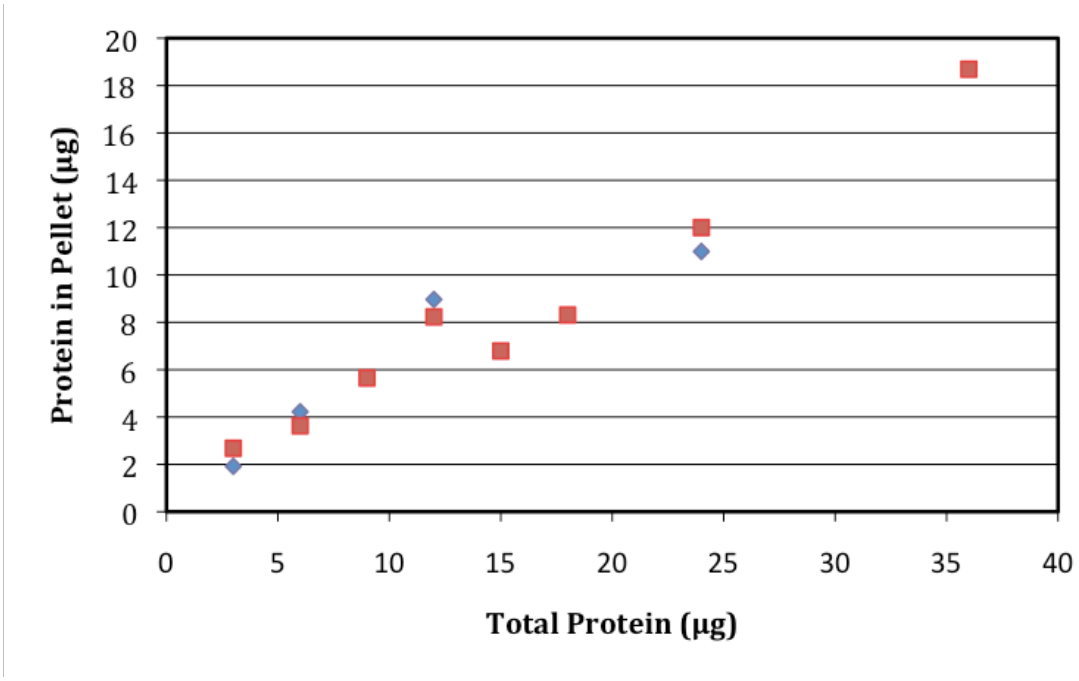
Protein in Pellet (µg)
20
18
16
14
12
10
8
6
4
2
0
0
5
10
15
20
25
30
35
40
Total Protein (µg)

Figure 3.3. PG binding assay with His_6-$DamX^{SPOR}$ and PG from different organisms. As described previously, purified protein was mixed with purified sacculi from *E. coli*, *B. subtilis*, *B. sphaericus*, or *S. aureus* and assayed for binding. Samples of the supernatant, the wash fluid, and the final pellet were analyzed by SDS-PAGE and Coomassie staining to determine what fraction of the input protein was in the final pellet. Bars indicate the averages and standard deviations of results from three independent experiments.

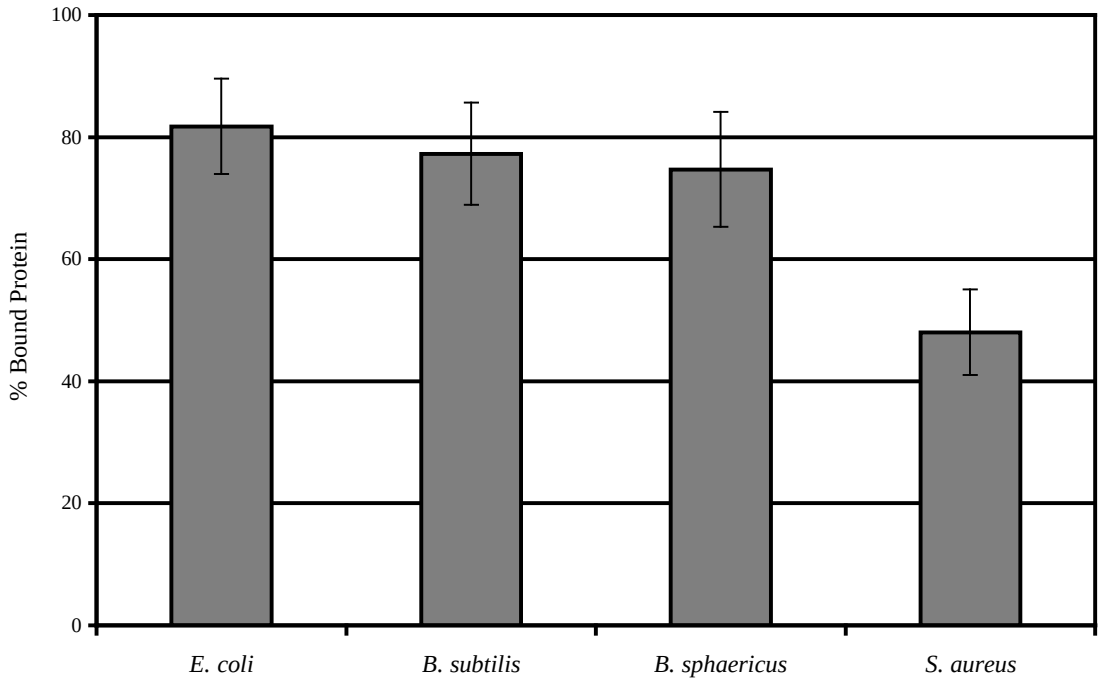
100
80
60
40
20
0
% Bound Protein
E. coli
B. subtilis
B. sphaericus
S. aureus

Figure 3.4. Many SPOR domains bind PG. Purified proteins were mixed with purified *E. coli* sacculi and subjected to ultracentrifugation to pellet the sacculi, which were washed and centrifuged again. Samples of the supernatant, the wash fluid, and the final pellet were analyzed by SDS-PAGE and Coomassie staining to determine what fraction of the input protein was in the final pellet. Bars indicate the averages and standard deviations of results from three independent experiments. MBP, maltose binding protein.

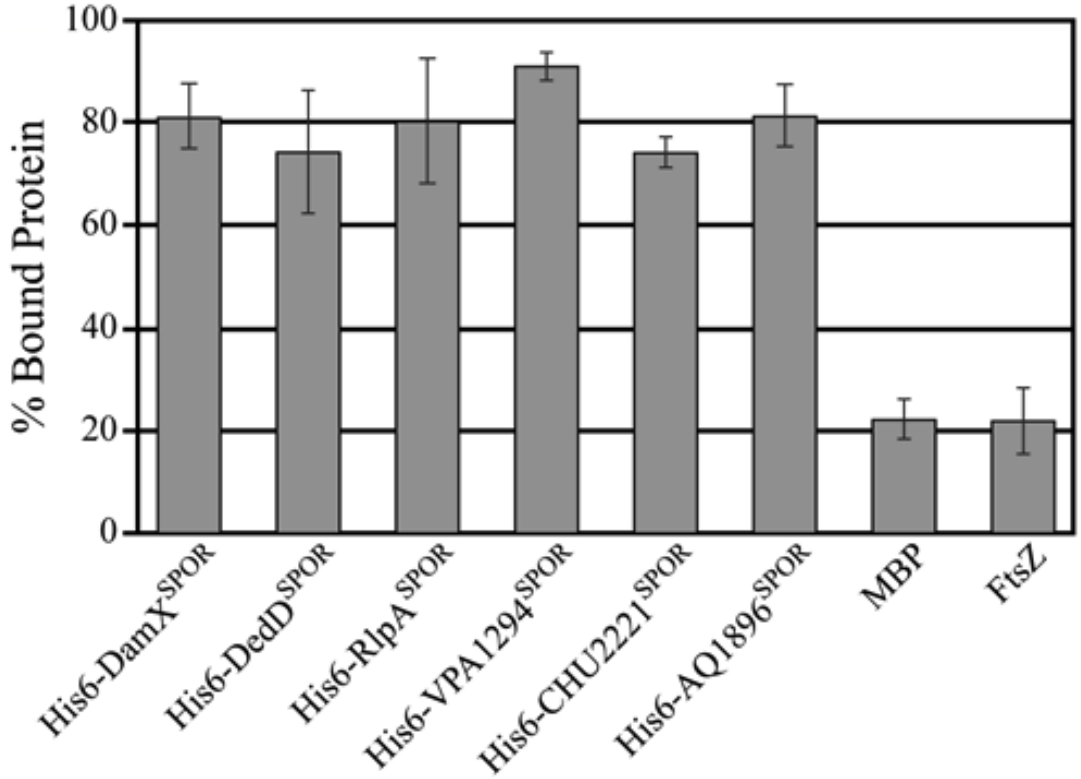
% Bound Protein
100
80
60
40
20
0
His6-DamX SPOR
His6-DedD SPOR
His6-RlpA SPOR
His6-VPA1294 SPOR
His6-CHU2221 SPOR
His6-AQ1896 SPOR
MBP
FtsZ

CHAPTER 4: IDENTIFICATION OF THE PG BINDING SITE IN THE SPOR DOMAIN FROM DAMX: A BACTERIAL CELL DIVISION PROTEIN

Introduction

SPOR domains (Pfam 05036) are about 70 amino acids long and are peptidoglycan binding domains present in over 2000 bacterial proteins in the sequence database (Finn et al., 2008). Several proteins containing SPOR domains are involved in cell division and many isolated SPOR domains can localize to the division septum in *E. coli* (Gerding et al., 2009; Moll & Thanbichler, 2009; Arends et al., 2010). This even includes some SPOR domains taken from very distantly related organisms, such as *Cytophaga hutchinsonii* and *Aquifex aeolicus* (Deckert et al., 1998; Xie et al., 2007; Arends et al., 2010). This is quite remarkable considering that in pairwise alignments any of these domains share less than 20% identity with each other (Table A1.1). Such observations beg the question of how these domains are recognizing the site of division.

The canonical method of division site recognition involves a highly ordered pathway of recruitment, thought to be mediated thorugh direct protein - protein interactions (Goehring et al., 2006; D'Ulisse et al., 2007; Gamba et al., 2009). While there is a possibility SPOR domains localize through these means, it seems highly unlikely. Given how evolutionarily divergent organisms such as *A. aeolicus* are and the fact that division proteins from closely related organisms, expressed *in trans* in *E. coli*, often fail to localize (Osawa & Erickson, 2006), we would not predict the necessary interactions to be preserved.

However, SPOR domains can bind peptidoglycan (PG) sacculi *in vitro* in a pull down assay, as we described in Chapter 3 (Ursinus et al., 2004; Gerding et al., 2009; Moll & Thanbichler, 2009; Arends et al., 2010). This raises the intriguing possibility that SPOR domains are discerning the midcell by binding preferentially to septal PG. The

division site is a place of active PG degradation and synthesis; there are amidases and transpeptidases at the division site remodeling the cell well (Weiss et al., 1999; Heidrich et al., 2002; Bernhardt & de Boer, 2003).

Nevertheless, studies of PG composition have yet to uncover convincing evidence of a septal-specific form of PG (Romeis et al., 1991; Obermann & Holtje, 1994; de Pedro et al., 1997; Ishidate et al., 1998). Despite this, we hypothesize that septal PG differs from PG found elsewhere around the cell and suggest that SPOR domains could serve as a biomarker for isolating and characterizing septal PG. Pursuing this line of investigation might provide novel insights into PG synthesis during division.

A complete understanding of the SPOR:PG interaction will require identification of the residues within the domain that constitute the PG binding site. Two SPOR domain structures have been published already, one from the *E. coli* cell division protein FtsN, the other form the *Bacillus subtilis* sporulation protein CwlC {Yang, 2004 #72}{Mishima, 2005 #31}. These domains adopt a similar fold despite being <20% identical at the amino acid level. Each domain comprises a βαββαβ secondary structure that assembles into a four-stranded antiparallel β-sheet buttressed by two α-helices. This fold places SPOR domains into a very large super family known as the RNP-fold, for ribonucleoprotein fold, so called because the first examples were RNA-binding domains from eukaryotic proteins involved in processing of mRNAs (Nagai et al., 1990; Oubridge et al., 1994; Allain et al., 1997; Varani & Nagai, 1998). In the meantime, RNP folds have been identified in a wide range of proteins and shown to bind an array of ligands, including proteins and carbohydrates. For example, the *E. coli* cell division protein ZipA uses an RNP fold to bind the C-terminus of FtsZ (Mosyak et al., 2000).

In those cases where the RNP:ligand interactions have been studied in detail, the ligand docks to the β-sheet (Allain et al., 1997; Varani & Nagai, 1998; Mosyak et al., 2000), suggesting the β-sheet of SPOR domains is likely to be the site where PG binds. Nevertheless, the report on FtsN's SPOR domain, which noted the similarity to the RNP

fold, did not comment on how the domain might bind PG (Yang et al., 2004). Conversely, the report on CwlC did not note the similarity to the RNP fold, but nevertheless suggested how the protein binds PG. On the basis of symmetry considerations (PG has a repeating structure) and NMR chemical shifts elicited by PG fragments, the authors of the CwlC study suggested there are two binding sites, one at the tip of either lobe of the molecule (Mishima et al., 2005). If this inference was correct, CwlC would bind its ligand through a fundamentally different set of interactions than known for other RNP-fold domains.

Here we report the solution structure of the SPOR domain from DamX and use a combination of genetics and biochemistry to identify residues important for septal localization and binding to PG. Briefly, we show the structure of the SPOR domain from DamX also belongs to the RNP fold super family, adopting a similar overall architecture. Lesions in the β-sheet of DamX impair both septal localization and, to a lesser degree, binding to PG sacculi in a pull down assay. In contrast, lesions in the previously suggested binding sites near the tips of the lobes have no obvious effect on septal localization or interaction with PG. We conclude that the ligand binding site in SPOR domains is the β-sheet, as is the case in other RNP domains. It seems that PG binding is necessary for the ability to localize to the septal ring, as expected if SPOR domains bind preferentially to septal PG.

Materials and Methods

Media. *E. coli* strains were grown in Luria-Bertani (LB) medium containing 10 g tryptone, 5 g yeast extract, and 10 g NaCl per liter. Plates contained 15 g agar per liter. Ampicillin was used at 200 µg/ml and spectinomycin at 100 or 35 µg/ml for plasmids or chromosomal alleles, respectively.

Strains. Strains used in this study are listed in Table 4.1. The CRIM plasmid pDSW1143 (P_{204}::*gfp-damX*(Q351K)) was integrated into the chromosome of EC1924 as described (Haldimann & Wanner, 2001). The resulting strain was designated EC2223.

Plasmids. Plasmids used in this study are listed in Table 4.2. Plasmids were constructed by PCR using VENT DNA polymerase (New England Biolabs) and sequenced to verify their integrity. All primers are listed in Table 4.3 and were obtained from Integrated DNA Technologies (Coralville, IA).

(i) Plasmid for localization of Tat-targeted(^{TT}) GFP-tagged SPOR domain from DamX. pDSW997 [P_{204}::^{TT}*gfp-damX*(338-428)] was constructed using primers P1144 and P1137 with pDSW918 as the template. The 301-bp product was cut with BamHI and HindIII and ligated into the corresponding sites of pDSW962.

(ii) Plasmids harboring amino acid substitutions within the DamX SPOR domain. Amino acid substitutions were created using megapriming (Sarkar & Sommer, 1990). pDSW1027 [P_{204}::^{TT}*gfp-damX*^{SPOR}(Q351A)] was constructed using primers P1167, which encodes the amino acid change, and P1137 with pDSW918 as the template. The product was isolated using a PCR Cleanup Kit (Qiagen) and 5µl used as a primer, along with P1136, in a second PCR to produce a full length *damX* encoding the lesion. The 1,312-bp product was used as a template for a third round of PCR, where P1137 and P1144 were used to amplify only the SPOR domain. The resulting 301-bp product was cut with BamHI and HindIII and ligated into the corresponding sites of pDSW962.

All other amino acid substitutions were made in a similar way using the primers listed below (see Table 4.3 for primer sequences): P1168 (Q351N), P1169 (Q351E), P1170 (S354A), P1171 (S354T), P1172 (S354Y), P1173 (N357A), P1174 (N360A), P1175 (N360V), P1176 (S395A), P1177 (E398A), P1178 (E398V), P1386 (Q351K), P1387 (S354F), P1388 (S354K), P1389 (W364A), P1390 (W364L), P1391 (W386A), P1392 (W386L), P1393 (W416A), P1394 (W416L)

pDSW1039 [P_{204}::^{TT}*gfp-damX*^{SPOR}(N357A/S395A)] was constructed as above, with pDSW1033 as template and P1176 as the mutagenesis primer. pDSW1040 [P_{204}::^{TT}*gfp-damX*^{SPOR}(N360A/E398A)] was constructed as above, with pDSW1034 as template and P1177 as the mutagenesis primer.

(iii) Plasmids for overproduction of His_6-tagged SPOR domains. Plasmids for the overproduction of His_6-tagged SPOR domains were constructed as described above for the ^{TT}GFP-SPOR domain. The PCR products were ligated into pQE80L using BamHI and HindIII, as above. All constructs carry the vector-derived sequence MRGSHHHHHHGSNNN at the N terminus.

(iv) Plasmids that encode GFP fusions to full-length SPOR domain proteins. pDSW983 allows for integration of P_{204}::*gfp-damX* into the chromosome at the ϕ80 *att* site. It was constructed by digesting pDSW918 with SphI and ScaI. The 4,322-bp fragment that carried *lacI*^{q} and P_{204}::*gfp-damX* was ligated into pJC69 that had been cut with SphI and HincII. A similar construct (pDSW1143) was made by digesting pDSW1089 [P_{204}::^{TT}*gfp-damX*^{SPOR}(Q351K)] with SphI and ScaI and ligating into pJC69 that had been cut with SphI and HincII.

Purified proteins. MBP2* was purchased from New England Biolabs (Beverly, MA). FtsZ was overproduced and purified as described previously (RayChaudhuri & Park, 1992), except that Q-Sepharose Fast-Flow was substituted for DEAE-Sephacel. His_6-tagged SPOR domains were overproduced in and purified from *E. coli* BL21(λ DE3) transformants by cobalt affinity chromatography on Talon affinity resin according to instructions from the manufacturer (Clontech, Mountain View, CA). The purified proteins were dialyzed into storage buffer (50 mM Tris-HCl, 200 mM NaCl, 5% glycerol, pH 7.5), and aliquots were stored at –80°C until needed. A 0.5-liter culture yielded 4 mg purified protein as determined by ultra violet absorption at 280 nm with a Nanodrop Spectrophotometer. The purity was >95% as judged by SDS-PAGE.

For NMR experiments, His_6-tagged SPOR domains were overproduced as above in M9 minimal media supplemented with B vitamins (1µg/mL), ^{15}N ammonium chloride (at 1 g/L) and/or ^{13}C glucose (at 4 g/L) (Sigma Aldrich, St. Louis, MO) as needed. Purified proteins were dialyzed into NMR buffer (50 mM Potassium Phosphate, 50 mM KCl, pH 6.5). Samples were supplemented with deuterium oxide when appropriate at either 10% or 100%.

Purification and quantification of PG. Whole PG sacculi were isolated from 1 L cultures of EC251 after being boiled in SDS essentially as described previously (Glauner, 1988). To quantify muramic acid, samples of purified PG were suspended in 6 N HCl and hydrolyzed at 95°C for 4 h. Hydrolysates were subjected to amino sugar analysis (González-Castro, 1997) and quantified relative to purified standards processed in parallel. Quantification was done by David Popham (Virginia Tech).

PG binding assays. Our standard binding assay (Ursinus et al., 2004; Arends et al., 2010) was conducted in 25 mM potassium phosphate, pH 7.5, and 200 mM NaCl. A standard assay mixture contained 12 µg protein and 75 µg PG in a total volume of 100 µl. This is equivalent to ~1 nmol of His_6-$DamX^{SPOR}$ and ~75 nmol of NAM-NAG disaccharide units. As a control, assay mixtures that lacked PG were also prepared. Mixtures were incubated for 1 h on ice and then centrifuged at 4°C in a Beckman TLA-55 rotor at 50,000 rpm (average *g* force, 112,000 x *g*) for 45 min. The supernatant was recovered and saved for analysis. The PG pellet was washed by suspending it in 100 µl of cold binding buffer and centrifuging as described above. The wash supernatant was also saved. The PG pellet was again suspended in 100 µl of binding buffer. The supernatant from the initial binding step, the wash fluid, and the resuspended pellet were

analyzed by SDS-15% PAGE. Gels were stained with GelCode blue (Pierce, Rockford, IL) and scanned using a Typhoon 8610 imager with the following instrument settings: excitation laser, 532 nm; emission filter, 560 nm, long pass; photomultiplier, 600 V; and pixel size, 100 µm. ImageQuant software was used to quantify fluorescence signals. Because there was not much protein in the wash, in later versions of the assay we pooled the initial supernatant and wash fractions before loading the gels.

Protein localization. Live cells were used in all cases for studies of protein localization. (i) Strains expressing full-length SPOR proteins fused to GFP carried IPTG-inducible fusions stably integrated into the chromosome, so antibiotic selection was not necessary. Cultures grown overnight in LB medium were diluted 1:200 into LB medium containing 10 µM IPTG and grown for 4 h at 30°C to an OD_{600} of ~0.5, at which point they were spotted onto thin agarose pads for microscopy (Tarry et al., 2009). (ii) Strains expressing fusions of GFP to isolated SPOR domains were grown similarly except that ampicillin was included to maintain plasmids, IPTG was omitted because basal expression proved sufficient, and overnight cultures were diluted 1:100 and grown to an OD_{600} of ~0.5 before microscopy.

General microscopy methods. Our microscope, camera, and software have been described previously, as has the immobilization of live cells on agarose pads (Mercer & Weiss, 2002; Arends et al., 2009; Tarry et al., 2009; Arends et al., 2010).

Western blotting. For Western blotting, typically 1 ml of culture at an OD_{600} of ~0.5 was centrifuged and the resulting cell pellet was taken up into ~0.5 ml of sodium dodecyl sulfate-polyacrylamide gel electrophoresis (SDS-PAGE) loading buffer. Samples were boiled, and 10-µl aliquots were subjected to SDS-10% PAGE.

Proteins were then transferred onto nitrocellulose and detected by standard methods. Rabbit anti-GFP antibodies were obtained from C. Ellermeier and used at a dilution of 1:10,000. The secondary antibody was horseradish peroxidase-conjugated goat anti-rabbit antibody (1:8,000; Pierce, Rockford, IL), which in turn was detected with SuperSignal Pico West chemiluminescent substrate (Pierce, Rockford, IL). Blots were visualized with an LAS-1000 luminescent imager from Fuji (Stamford, CT).

NMR Spectroscopy. All NMR spectra were collected at 25° C on a 4 channel Varian UnityInova NMR spectrometer operating at 600 MHz and equipped with a triple resonance PFG probe. ^{1}H-^{15}N HSQC spectra were collected on wild type and mutant proteins at ~500 μM, and it generally took less than 2 hours to obtain excellent spectra. All spectra were processed and overlays generated using the tools available in NMRPipe (Delaglio et al., 1995).

My contributions to the NMR work. The NMR investigations were a collaborative effort involving Dr. Andrew Fowler and I. This paragraph spells-out my contributions to that collaboration. (a) For NMR experiments related to determining the structure of the SPOR domain from DamX, I expressed and purified all ^{5}N and/or ^{13}C labeled protein that was used. In addition, to determine the quality of these protein preparations prior to handing them off to Dr. Fowler, in many cases I setup and ran ^{15}N HSQC spectra (e.g., Figure 4.1). One step in the process of determining the structure required obtaining spectra from aligned samples. This was accomplished with liquid bi-cells using 5% PEG(C12E5):hexanol that I prepared for Dr. Fowler. (b) Figure A.3 shows NMR chemical shifts elicited by adding purified muropeptides ^{15}N labeled DamX SPOR domain. I performed essentially all of the work to generate this figure, including protein purification, setting up sample tubes, collecting spectra and preparing the overlays shown in Fig. A.3. (c) I also preformed essentially of the work that went into Figure 4.9, which

shows that DamX SPOR domains with amino acid substitutions are properly folded. Specifically, I purified the proteins, set up the samples, collected the NMR spectra and prepared the overlays.

Results

Structure of the DamX SPOR domain. A pilot experiment was done to assess the feasibility of using NMR to determine the solution structure of DamX's SPOR domain. ^{15}N labeled His_6-$DamX^{SPOR}$ was generated as described in Materials and Methods and used to collect initial 1-D and 2-D NMR spectrum. The ^{1}H-^{15}N HSQC spectrum looked very promising, as signals were strong and well dispersed. From this point, I generated ^{13}C and/or ^{15}N labeled protein that was used by Dr. Andrew Fowler at the University of Iowa NMR Core Facility to complete the structure determination.

An example HSQC spectrum for the DamX SPOR domain was generated with tools available in NMRPipe (Delaglio et al., 1995) and is shown in Figure 4.1. Note that the resonance peaks are well dispersed. In this spectrum resonance peaks for backbone and side chain nitrogen atoms have been assigned to their respective amino acids. Except for the His-tag amino acid resonances, which cannot be unambiguously assigned, only one amide signal could not be assigned. This is for residue 381, an asparagine, which lies in a short loop between the second and third ß-strands. Only missing one assignment is excellent and, based on the overall high quality of the spectrum, it is likely this resonance is degenerate with another amide signal. The following summary of results is based on the data obtained from Dr. Fowler (personal communication).

The final ensemble of structures for the DamX SPOR domain was generated by taking the 25 lowest energy structures from an ensemble of 250 calculated structures. Several of the N-terminal residues have been omitted in the figures shown in this chapter as this region is significantly more flexible than the rest of the protein as characterized by

NMR relaxation (data not shown), has almost no long range distance restraints to the rest of the molecule and is essentially completely disordered in the structure calculations.

Figure 4.2 shows a cartoon representation of the molecule in both a side on and bottom up orientation. The domain is composed primarily of ß-strands and α-helices with short loops as connectors. The primary sequence of the DamX SPOR domain shows symmetrical homology with itself, whereby the first ~35 a.a. are similar to the second half of the domain. This repeating nature of the primary amino acid sequence also translates into a repeating secondary and tertiary structure for the protein. The DamX SPOR domain exhibits a βαββαβα secondary structure and falls into the common RNP (ribonucleoprotein) fold family (Birney et al., 1993; Varani & Nagai, 1998). This family is characterized by having two helices flanking a single four-stranded antiparallel beta sheet. DamX has an additional α-helix at its C-terminus. This is a feature found in some, but not all, members of this fold family. Interestingly, this helix is not present in the other two SPOR domains for which structures have been solved, CwlC and FtsN (Yang et al., 2004; Mishima et al., 2005). Overlays of the structures in Figures 4.3 and 4.4 illustrate this. It is possible the extra helix is a defining characteristic of DamX type SPOR domains.

Site-directed mutagenesis. To identify regions of DamX's SPOR domain that are important for septal localization and binding to PG, we targeted eight surface-exposed amino acids for mutagenesis. These are indicated in the amino acid sequence in Figure 4.5A and mapped onto the structure of the domain in Figure 4.6. In most cases, multiple substitutions were made at each site (Table 4.4). These residues were selected for a variety of reasons.

Gln 351 and Ser 354 were chosen because they are the most highly conserved residues in an alignment of 130 SPOR domains (Table A1.1). That said, it is interesting to note that SPOR domain sequences are quite degenerate: Gln 351 aligns with a Gln in

75% of the sequences, while Ser 354 aligns with a Ser in only 33% of the sequences (and with an Ala in an additional 47% of the sequences). Both Gln 351 and Ser 354 fall in ß1. The fact that the most highly conserved surface-exposed residues map to the ß-sheet is consistent with this being the site where PG binds to the protein.

Trp 364, Trp 385 and Trp 416, which map to α1, ß3 and ß4, respectively, were chosen because they exhibited NMR chemical shifts when the SPOR domain was incubated with a mixture of muropeptides obtained by digesting *B. subtilis* PG to completion with mutanolysin (Figure A1.3). We hasten to add, however, that we do know whether muropeptides are authentic ligands.

Finally, four amino acids were targeted because they correspond to residues suggested to interact with PG in CwlC: Asn 357, Asn 360, Ser 395 and Glu 398. The first two residues fall near the start of α1 and the last two near the start of α2. In terms of the three dimensional structure of the domain, these amino acids protrude into solution from the left and right lobes of the molecule as depicted in Figure 4.6.

Septal Localization. The mutant SPOR domains were fused to Tat-targeted GFP (^{TT}GFP) to direct their export to the periplasm via the Tat system and produced from plasmids in a wild type *E. coli* background. Septal localization was assayed by visualizing live cells by fluorescence microscopy (Figure 4.7, Table 4.4). Western blotting was used to verify that the wild type and each mutant SPOR domain were produced at similar levels (not shown). Interestingly, even proteins that showed dim GFP fluorescence showed wild type levels of steady state protein abundance.

Wild type and mutants with lesions near the start of α1 and α2 exhibited a strong band of fluorescence across the middle of most cells, indicting that lesions introduced at Asn 357, Asn 360, Ser 395 or Glu 398 had little or no deleterious effect on septal localization. Even a double mutant protein (N360A/E398A) localized as efficiently as wild type. This argues against the possibility we overlooked defects in the singly mutant

proteins because one intact PG binding site is sufficient for recruitment to the septum. Substitutions at Trp 385 were also well tolerated, indicating that this side-chain is also not important for targeting to the division site.

Remarkably, most lesions in Gln 351, Ser 354, and Trp 416 nearly abolished septal localization. These mutant proteins generally appeared as fluorescent halos illuminating the outline of most of the cells; for examples, see Figure 4.7A and B. Only in rare cells (< 6%, Table 4.4) did we observe septal localization. These bands were always faint and only present in the deepest constrictions, consistent with weak localization (Figure 4.7C). The uniform peripheral staining observed in most cells could arise because the mutant proteins diffuse freely in the periplasm or because they now associate with PG in a relatively non-specific manner. We noted three exceptions to the pattern of staining described here. The S354A mutant protein retained the ability to localize to the septal ring; in this context it is worth noting that an alignment of 130 SPOR domains revealed Ala occurs more frequently than Ser (47% vs. 33%) at this position (Table A1.1). The other anomalous proteins were the S354F and S354Y mutants. Cells expressing these proteins appeared dark, so we suspect these lesions interfered with folding and/or export.

During the course of these studies, we observed an interesting polar localization pattern that appeared to depend on the age of the agarose pads used to immobilize cells for microscopy. When cells expressing wild-type GFP-DamX^{SPOR} were spotted onto agarose pads that had been made 10 minutes before use and imaged quickly (within 2 minutes of placement on the slide), about 60% of the cells exhibited polar GFP signal (Figure 4.7D). Some of these cells had only polar GFP, while others had both polar and septal GFP. However, if the cells were allowed to sit on the pad for 5 minutes or longer before imaging, the frequency of polar localization was reduced to <2% of the population. If the same cultures were spotted onto agarose pads that had been allowed to sit at room temperature for 2 hours before use, polar localization was not observed. This

was true even when cells were imaged less than 2 minutes after spotting them onto the pad.

The underlying physiological basis of the transient polar localization phenomenon is a matter of speculation, but we presume it is somehow related to osmotic imbalances. Cells transferred from broth to a fresh agarose pad may undergo an osmotic shock that affects the size of the periplasmic space or the curvature of the cell wall in ways that cause GFP-DamX^{SPOR} to accumulate at the poles. Over a period of a few minutes those cells might restore proper osmotic balance, which in turn favors septal localization. By this logic, older agarose pads are presumably drier and do not provoke the same osmotic shock that fresh pads do. Preliminary experiments with a mutant GFP-DamX^{SPOR} domain (W416L) that does not localize to septa and does not bind PG in the pull-down assay indicate it too localizes transiently to the poles when cells are placed on fresh (but not on old) agarose pads (not show). This observation argues that PG binding is not relevant to polar localization. However, the definitive test of this notion will be to examine periplasmic GFP that is not fused to any other protein.

PG binding. We used a pull-down assay with whole cell sacculi to test one localizing mutant and six non-localizing mutants for their ability to bind PG (Figure 4.8). To establish the range of the assay, we used the wild type SPOR domain and two proteins that do not bind PG in a physiologically meaningful way, FtsZ and maltose binding protein (MBP). In all cases we verified that sedimentation of the protein depended upon the inclusion of PG in the reaction mixture.

Whereas 80% of the wild type SPOR domain co-sedimented with PG, only 20% of FtsZ or MBP did so. [The relatively high background (20% of the non-binding protein in the pellet) reflects the propensity of many proteins to interact non-specifically with PG.] The localization proficient SPOR domain mutant, N360A/E398A, bound PG about as well as wild type, but the localization defective proteins were all impaired in their

ability to bind PG. In some cases the defect was rather mild (S354K, S354T, and Q351E) but in others (Q351K, W416A, and W416L) binding was reduced to the background level observed for FtsZ and MBP. We infer that, within the limits of this assay, the three most severe lesions have essentially abolished specific affinity for PG. Nevertheless, it is remarkable that several proteins with severe localization defects retained significant affinity for PG. For example, the S354T substitution nearly abolishes septal localization (Figure 4.7A, Table 4.4) but has only a modest effect on PG binding (Figure 4.8). We hypothesize that the lesion reduces its specific binding to septal PG but not general PG binding affinity. Results from the binding assays in Chapter 3, using PG from filamentous cells, support the notion that the pull down assay is largely measuring a general affinity for PG.

^{15}N HSQC experiments of mutant DamX SPOR domains. In order to determine if the mutant proteins being used in the PG binding assays were stable and well folded we performed HSQC 2D NMR experiments. We collected ^{15}N-HSQC spectra for several mutant proteins that showed interesting phenotypes in the PG binding assay and localization experiments. These included Q351A, Q351N, Q351K, S354T, W416A, and W416L. The HSQC spectra all exhibited well dispersed signals and overall resonance patterns consistent with that of the wild type reference protein (Figures 4.9A-F). The few shifted peaks in each spectrum generally cluster near where the mutation was made, as expected.

Testing the role of DamX's SPOR domain *in vivo*. FtsN's SPOR domain is dispensable in the sense that a truncated *ftsN* allele deleted of the SPOR domain supports division almost as well as does full-length FtsN (Ursinus et al., 2004; Gerding et al., 2009). This surprising result suggested that DamX's SPOR domain might also be dispensable. Because deleting the entire SPOR domain might have unintended

deleterious effects on the folding or stability of the rest of the protein, we chose instead to work with an amino acid substitution, Q351K, that greatly diminishes septal localization (Fig. 4.7A) and reduces affinity for PG by about a factor of 2 in the pull-down assay (Fig. 4.8).

To test functionality, we produced the mutant protein (and control proteins) in a *damX dedD* double mutant. To understand why we chose this strain background, the reader needs to know that a *damX* null mutant has no division defect, a *dedD* null mutant has a mild division defect, but a *damX dedD* double mutant is very filamentous (Gerding et al., 2009; Arends et al, 2010). Moreover, production of a wild type GFP-DamX fusion protein largely corrects the division defect in the *damX dedD* double mutant (Arends et al., 2010).

Consistent with our previous report (Arends et al., 2010), a *damX dedD* double mutant was ~14 μm long during exponential growth in LB (Figure 4.1A). Both the *gfp-damX* and *gfp-damX*(Q351) alleles largely corrected that defect, with average cell lengths of 4.8 μm and 6.3 μm. Western blotting with anti-GFP antibody verified that both fusions were produced at similar levels (Figure 4.1C). Fluorescence microscopy revealed that the wild type GFP-DamX protein localized efficiently to the septum, with ~75% of the cells exhibiting a band of fluorescence at the division site. In contrast, the GFP-DamX(Q351K) protein localized poorly—cells were dim, only ~15% exhibited septal fluorescence and examples of polar localization were readily apparent (Figure 4.10B). In toto, these data suggest that the ability of the SPOR domain to bind PG and target DamX to the midcell might not be very important for DamX function in cell division (see discussion). Conversely, DamX probably has an important function that is distinct from its SPOR domain.

Discussion

The SPOR Domain of DamX Exhibits an RNP Fold. We used NMR to determine the solution structure of the SPOR domain (residues 338-428) of *E. coli* DamX. In terms of secondary structure, the domain contains four ß-strands and three α-helices, which are arranged as follows: ßαßßαßα. The four ß strands comprise an antiparallel ß-sheet on one face of the molecule, arbitrarily shown as the bottom face in Fig. 4.2A. It can also be seen from Fig. 4.2A that the ß-sheet is curved, which creates a cleft that we propose is the binding site for PG (see below). Helices α1 and α2 pack along the top of the ß-sheet; α2 is discontinuous owing to the presence of a proline reside (P397). The C-terminal helix, α3, is very short and occupies the cleft; in other words, α3 packs against the opposite face of the ß-sheet as do α1 and α2.

As noted in the Introduction, two SPOR domain structures have been published already. These are from the *B. subtilis* cell wall hydrolase CwlC and the *E. coli* cell division protein FtsN (Yang et al., 2004; Mishima et al., 2005). Overall, the three structures are quite similar, as can be seen from the overlays in Figs. 4.2 and 4.4, even though these three domains have less than 20% amino acid identity in pair-wise comparisons. Most notably, all three SPOR domains contain a ßαßßαß secondary structure that folds into a four-stranded antiparallel ß-sheet flanked on one side by two α-helices. This basic fold is known as an RNP-fold (Nagai et al., 1990; Varani & Nagai, 1998).

The overlays in Figs. 4.3 and 4.4 reveal three noteworthy differences among the SPOR domains.

(i) In DamX α2 is interrupted by a proline, resulting in a shape kink in that feature. This proline is not present in CwlC or FtsN, so α2 is longer in those proteins, and the loop connecting α2 with ß4 is longer. We do not have any reason at present to

think the kink (or lack of a kink) in α2 has any biological significance. SPOR domain alignments (Figs. 4.5, 4.12 and Table A1.1) indicate that most SPOR domains lack a proline in α2, so we presume α2 is usually extended rather than kinked. However, the proline is conserved among DamX's and is present in a few other SPOR domains, such as the SPOR domain from VPA1294 of *V. parahaemolyticus*.

(ii) Another striking difference among SPOR domains is the degree of curvature of the ß-sheet: CwlC and DamX have a curved ß-sheet that forms a cleft, whereas the ß-sheet of FtsN is rather flat. These different conformations might represent "closed" and "open" states sampled by all three domains. For the three SPOR domains to make homologous interactions with PG, they must adopt a similar overall shape when bound to their ligand. In this context it is worth noting that the structure of the eukaryotic U1A protein, which is the founding member of the RNP fold family, has been solved with and without ligand (Oubridge et al., 1994; Avis et al., 1996; Allain et al., 1997; Varani et al., 2000). Free U1A has a curved ß-sheet that forms a cleft reminiscent of DamX and CwlC but a flat ß-sheet similar to FtsN when bound to RNA.

(iii) The third major difference is the extra helix, designated α4, located at DamX's C-terminus. Neither CwlC nor FtsN have an α4; both of those SPOR domains are shorter than the SPOR domain from DamX. Sequence alignments reveal the extra helix is found in the SPOR domains from DamX proteins but not in most SPOR domains (Figs. 4.5 and 4.12). Remarkably, α4 of DamX occupies the cleft that we think is the PG binding site, in which case it will have to move out of the way for DamX to dock to PG. Again, parallels to U1A can be drawn for this element as well. The U1A RNP domain also contains an extra helix that packs against the ß-sheet and occludes the RNA binding site until RNA is encountered, at which point the helix moves out of the way and mediates homodimerization of the protein (Oubridge et al., 1994; Avis et al., 1996; Allain et al., 1997; Varani et al., 2000). Clearly, it will be of interest to study the effect of deleting α4 of DamX.

The PG binding site in DamX's SPOR domain is the ß-sheet. SPOR domains are thought to bind septal PG (Gerding et al., 2009; Moll & Thanbichler, 2009; Arends et al., 2010). Here we offer important new information in support of this hypothesis—namely, residues in the ß-sheet of the SPOR domain from DamX are important for septal localization in vivo and binding to PG in vitro. Specifically, substitutions of the glutamine at 351 (Q351E, Q351K), the serine at position 354 (S354K, S354F, S354T), and the tryptophan at 416 (W416A, W416L) impaired both activities. These residues fall in ß1 (Q351, S354) or ß3 (W416). All three amino acids (Q351, S354, and W416) have solvent exposed side-chains that could plausibly interact with PG. Moreover, all of the mutant proteins were shown to be largely folded by HSQC NMR (Figure 4.9).

In one respect, these findings are not too surprising because other members of the RNP fold super family (to which DamX belongs) use their β-sheet for ligand binding. Well-studied examples include the RNA binding protein U1A (Oubridge et al., 1994; Allain et al., 1997; reviewed in Varani and Nagai, 1998) and the bacterial cell division protein ZipA, which uses an RNP fold domain to engage FtsZ (Mosyak et al., 2000). Moreover, when we used an alignment of 130 SPOR domains (Table A1.1) to map sequence conservation onto the SPOR domain of CwlC (Fig. 4.5B), the most highly conserved surface-exposed residues were found to reside in the cleft formed by the curved ß-sheet. The two most conserved amino acids correspond to Q351 of DamX, which is a Q in ~75% of the sequences, and S354 of DamX, which is either Ser or Ala in ~80% of the sequences.

In another respect, however, our findings were somewhat unanticipated because Mishima et al. (2005) suggested that the SPOR domain from CwlC contains two pseudo-symmetric PG binding sites located near the beginning of α1 and α2, respectively. These sites are over 20Å apart and are labeled "tip" in the ribbon diagram of $DamX^{SPOR}$ in Fig. 4.2A. We introduced several lesions into these putative binding sites in the SPOR domain of DamX and found that the mutant proteins localized efficiently to the septal

ring and the one mutant protein that was tested bound to PG (Figure 4.7A, 4.8). Note that this mutant set included a protein with two substitutions (N360A, E398A), one at each tip, arguing against the possibility that single lesions had no effect because the protein retained one good PG binding site.

In retrospect, the evidence in favor of the binding sites suggested for CwlC is not very compelling. Mishima et al. (2005) did an alignment of five SPOR domains and noted an Asn residue that was universally conserved at each tip. However, this conservation appears to have been fortuitous—in a more extensive alignment these Asn residues are not well conserved (Table A1.1); instead, the most striking conservation is in the ß-sheet. Moreover, in our hands, mutagenesis of the corresponding residues in DamX (N360, E398) had no effects. The second consideration behind Mishima et al.'s suggestion was that PG has a repeating structure, so a protein with two binding sites would be well-designed to cross-link adjacent sites. This argument is more of a polemic than evidence. Third, Mishima et al. observed NMR chemical shifts in tip residues when they incubated CwlC SPOR domain with PG fragments obtained by digesting sacculi with an amidase. This is potentially a strong argument for their suggestion, but with chemical shifts in NMR experiments it is often difficult to separate specific interactions from non-specific interactions. Moreover, a small conformational change in one part of a protein can propagate into a larger one at another location, from which misleading conclusions could be drawn. Furthermore, there is presently no way to know if the PG fragments were representative of the domain's authentic ligand. Finally, in the discussion it was claimed that amino acid substitutions in the proposed binding sites reduced binding to PG, but the manuscript "in preparation" that was supposed to document this finding has yet to appear as of March, 2010.

One interesting observation that resulted from characterization of our mutant set is that some amino acid substitutions had a more dramatic effect on septal localization than on PG binding. For example, the S354T and S354K mutant proteins retained only

~10% of the septal localization activity but ~75% of the PG binding activity of wild type (Table 4.4). Similarly, septal localization was essentially abolished by the Q351E substitution, but PG binding was still near 50% of wild type. The basis of these discrepancies is a matter of speculation, but we suggest that it reflects limitations of the PG binding assay, which uses whole PG sacculi and probably measures affinity of the protein for bulk PG rather than affinity for septal PG. SPOR domains might have a general affinity for all (or most) PG in addition to a higher affinity for some form of PG that is enriched in division septa; this situation would be analogous to site-specific DNA binding proteins, which have significant affinity for DNA in general in addition to a higher affinity for the sequences that constitute their specific binding sites (Halford SE, 2004).

We found that the SPOR domain from DamX binds equally well to whole sacculi isolated from dividing (wild-type) or non-dividing [*ftsZ*(Ts)] cells (Chapter 3). Moreover, the procedures for isolating sacculi are quite harsh. They involve several hours of boiling in SDS, numerous washes and digestions with protease, amylase and DNase (Glauner, 1988). It is certainly plausible that the septal PG recognized by SPOR domains is lost during such a work-up. For example, it has been suggested that SPOR domains bind preferentially to glycan strands that lack peptide side-chains (Ursinus et al., 2004; Gerding et al., 2009). Assuming that such structures exist in PG (they have never been documented), they would not have any covalent linkage to the rest of the sacculus and thus might easily be lost. Clearly developing a physiologically relevant binding assay based on septal PG is a high priority. If our concerns about the binding assay are well founded, we could speculate that the SPOR domain lesions, which abolish localization without dramatically affecting PG binding, are the most interesting found from our mutagenesis. These mutant proteins probably have lost their specificity for septal PG but retain a general PG binding activity. The more dramatic reduction seen in PG binding from other lesions could represent a loss of this general affinity as well.

Binding substrate for the SPOR domain of DamX. We favor the notion that the SPOR domains localize to the division septum because they are preferentially binding to PG at this site. As mentioned earlier in the discussion, the possibility of septal PG is somewhat controversial in the cell division field. Nevertheless, we believe there are likely differences in the PG at these sub cellular locations that the SPOR domains are able to discern. One possibility is SPOR domains are targeting a transient, low abundance species at the division site. Since it is known a great deal of PG processing occurs at the septum (de Pedro et al., 1997), there are many possibilities for these transient structures. For instance, multi layer PG, PG with reduced amounts of covalently attached Lpp, or glycan strands that have yet to be crosslinked could all be enriched at the division site.

Gerding *et al.* suggested that SPOR domains target a specific PG turnover intermediate, namely, glycan strands that lack peptide side chains (Gerding et al., 2009). Naked glycan strands would arise if amidases ran ahead of lytic transglycosylases during PG degradation. This suggestion was based on their finding that SPOR domains did not localize to septal regions in an *E. coli* strain devoid of amidases and on a report from Vollmer's group that the purified SPOR domain from FtsN binds to naked glycan strands generated by amidase treatment of isolated sacculi (Ursinus et al., 2004). In that study, FtsN's SPOR domain did not bind to muropeptides or to free peptides (Ursinus et al., 2004), although it should be noted that glycan strands that carried peptides were not tested. It is also worth noting that a subsequent paper from Vollmer's group reported binding of FtsN's SPOR domain to muropeptides (Muller et al., 2007). The basis for this contradiction was not discussed but may have to do with the fact that in the second study the muropeptides contained 1,6-anhydromuramic acid ends owing to the use of a different enzyme to degrade the sacculi. Finally, to our knowledge, disaccharides indicative of naked glycan strands have never been reported in analyses of the

muropeptide composition of PG, implying either that they do not exist or that the analytical methods are not adequate to detect them. Clearly, more work will be needed to test the hypothesis that SPOR domains bind preferentially to glycan strands that lack peptide side chains.

Physiological importance of the SPOR domain. The fact that so many bacterial proteins carry SPOR domains argues for their importance. Nevertheless, we found that the DamX(Q351K) protein complimented about as well as wild type DamX (Fig. 4.10), despite the fact that the mutant protein localized predominantly to the cell poles. Further studies, with more point mutants and deletions of the entire SPOR domain, will be needed before firm conclusions can be drawn, but overall these results are reminiscent of what has been reported for FtsN ΔSPOR proteins (Ursinus et al., 2004; Gerding et al., 2010). They lend themselves to two potential interpretations. One is that SPOR domains serve to tether the PG to the inner and outer membranes so that all three layers invaginate synchronously during septation. In this case, the lack of a phenotype after loss of a SPOR domain could reflect simple functional redundancy—there are still multiple SPOR domain proteins and thus multiple tethers in the cell. Alternatively, SPOR domains might serve to target their host proteins to the septum. In this view, the "business end" of a SPOR domain protein resides elsewhere and phenotypes resulting from crippling the SPOR domain might only become manifest at very low levels of protein production, when mass action is going to be ineffective at delivering sufficient protein to the septum. This model appears to apply to FtsN (Gerding et al., 2009).

Table 4.1. Strains used in this study

Strain	Relevant features	Source or reference
BL21(λ DE3)	*ompT gal dcm hsdS*$_B$(r_B^- m_B^-) l (P_{lacUV5}::T7 gene 1)	Novagen
EC251	K-12 wild type MG1655	Lab collection
EC1924	BW25113 *damX dedD<>kan*	Arends, et al., 2010
EC2177	BW25113 *damX dedD<>kan* ϕ80::pDSW983(P_{204}::*gfp-damX* Sp^r)	Arends, et al., 2010
EC2223	BW25113 *damX dedD<>kan* ϕ80::pDSW983(P_{204}::*gfp-damX* (Q351K) Sp^r)	This work

Table 4.2. Plasmids used in the study

Plasmid	Relevant features[a]	Source or reference
pDSW918	P_{204}::*gfp-damX lacI*^{q} *bla* pBR ori	Arends et al., 2010
pDSW962	^{TT}*gfp* fusion vector (P_{204}::^{ss}*torA-gfp lacI*^{q} *bla* pBR ori)	Tarry et al., 2009
pDSW983	P_{204}::*gfp-damX lacI*^{q} Sp^{r} (pJC69 derivative)	Arends et al., 2010
pDSW997	P_{204}::^{TT}*gfp-damX*(338-428)	Arends et al., 2010
pDSW1000	pQE80L-*damX*(338–428)	This work
pDSW1027	P_{204}::^{TT}*gfp*-damX^{SPOR} (Q351A) Amp^{R}	This work
pDSW1028	P_{204}::^{TT}*gfp*-damX^{SPOR} (Q351N) Amp^{R}	This work
pDSW1029	P_{204}::^{TT}*gfp*-damX^{SPOR} (Q351E) Amp^{R}	This work
pDSW1030	P_{204}::^{TT}*gfp*-damX^{SPOR} (S354A) Amp^{R}	This work
pDSW1031	P_{204}::^{TT}*gfp*-damX^{SPOR} (S354T) Amp^{R}	This work
pDSW1032	P_{204}::^{TT}*gfp*-damX^{SPOR} (S354Y) Amp^{R}	This work
pDSW1033	P_{204}::^{TT}*gfp*-damX^{SPOR} (N357A) Amp^{R}	This work
pDSW1034	P_{204}::^{TT}*gfp*-damX^{SPOR} (N360A) Amp^{R}	This work
pDSW1035	P_{204}::^{TT}*gfp*-damX^{SPOR} (N360V) Amp^{R}	This work
pDSW1036	P_{204}::^{TT}*gfp*-damX^{SPOR} (S395A) Amp^{R}	This work
pDSW1037	P_{204}::^{TT}*gfp*-damX^{SPOR} (E398A) Amp^{R}	This work
pDSW1038	P_{204}::^{TT}*gfp*-damX^{SPOR} (E398V) Amp^{R}	This work
pDSW1039	P_{204}::^{TT}*gfp*-damX^{SPOR} (N357A, S395A) Amp^{R}	This work
pDSW1040	P_{204}::^{TT}*gfp*-damX^{SPOR} (N360A, E398A) Amp^{R}	This work
pDSW1041	pQE80L-*damX*^{SPOR} (Q351A)	This work
pDSW1042	pQE80L-*damX*^{SPOR} (Q351N)	This work
pDSW1043	pQE80L-*damX*^{SPOR} (Q351E)	This work
pDSW1044	pQE80L-*damX*^{SPOR} (S354A)	This work
pDSW1045	pQE80L-*damX*^{SPOR} (S354T)	This work
pDSW1046	pQE80L-*damX*^{SPOR} (S354Y)	This work
pDSW1047	pQE80L-*damX*^{SPOR} (N357A)	This work
pDSW1048	pQE80L-*damX*^{SPOR} (N360A)	This work
pDSW1049	pQE80L-*damX*^{SPOR} (N360V)	This work
pDSW1050	pQE80L-*damX*^{SPOR} (S395A)	This work
pDSW1051	pQE80L-*damX*^{SPOR} (E398A)	This work
pDSW1052	pQE80L-*damX*^{SPOR} (E398V)	This work
pDSW1053	pQE80L-*damX*^{SPOR} (N357A, S395A)	This work
pDSW1054	pQE80L-*damX*^{SPOR} (N360A, E398A)	This work

[a] ^{ss}*torA*, TorA signal sequence construct.

Table 4.2. continued

Plasmid	Relevant features	Source or reference
pDSW1084	pQE80L-*damX*^{SPOR} (S354K)	This work
pDSW1085	pQE80L-*damX*^{SPOR} (S354F)	This work
pDSW1086	pQE80L-*damX*^{SPOR} (Q351K)	This work
pDSW1087	P_{204}::^{TT}*gfp-damX*^{SPOR} (S354K)	This work
pDSW1088	P_{204}::^{TT}*gfp-damX*^{SPOR} (S354F)	This work
pDSW1089	P_{204}::^{TT}*gfp-damX*^{SPOR} (Q351K)	This work
pDSW1135	P_{204}::^{TT}*gfp-damX*^{SPOR} (W364A)	This work
pDSW1136	P_{204}::^{TT}*gfp-damX*^{SPOR} (W364L)	This work
pDSW1137	P_{204}::^{TT}*gfp-damX*^{SPOR} (W386A)	This work
pDSW1138	P_{204}::^{TT}*gfp-damX*^{SPOR} (W386L)	This work
pDSW1139	P_{204}::^{TT}*gfp-damX*^{SPOR} (W416A)	This work
pDSW1140	P_{204}::^{TT}*gfp-damX*^{SPOR} (W416L)	This work
pDSW1141	pQE80L-damX^{SPOR} (W416L)	This work
pDSW1142	pQE80L-damX^{SPOR} (W416A)	This work
pJC69	oriR6Kg *attP* ϕ80 Sp^{r} (CRIM vector)	Chen and Beckwith, 2001
pQE80L	Carries T5 promoter and *lac* operators; *lacI*^{q} ColE1 ori Amp^{r}	Qiagen

Table 4.3. Primers used in the study

Primer	Sequence[a]
P1136	CAGCAATTGAACAACAACATGGATGAATTCAAACCAGAAGAC
P1137	CTGAAGCTTACTTCAGATCGGCCTGTACCT
P1144	GCCGGATTCAACAACAACGGTTCGTTGAAATCGGCA
P1167	AGCCATTACACTCTGGCGCTGAGCAGTTCCTCT
P1168	AGCCATTACACTCTGAACCTGAGCAGTTCCTCT
P1169	AGCCATTACACTCTGGAGCTGAGCAGTTCCTCT
P1170	ACTCTGCAGCTGAGCGCTTCCTCTAACTACGAC
P1171	ACTCTGCAGCTGAGCACTTCCTCTAACTACGAC
P1172	ACTCTGCAGCTGAGCTATTCCTCTAACTACGAC
P1173	CTGAGCAGTTCCTCTGCCTACGACAACCTGAAC
P1174	TCCTCTAACTACGACGCCCTGAACGGTTGGGCG
P1175	TCCTCTAACTACGACGTCCTGAACGGTTGGGCG
P1176	TCTGGCGTGTACGCTGCGAAAGAAGAGGCGAAA
P1177	TACGCTTCGAAAGAAGTGGCGAAAAAAGCGGTA
P1178	TACGCTTCGAAAGAAGCGGCGAAAAAAGCGGTA
P1386	TTACACTCTGAAGCTGAGCAGTTCC
P1387	GCAGCTGAGCTTCTCCTCTAACTAC
P1388	GCAGCTGAGCAAGTCCTCTAACTAC
P1389	CCTGAACGGTGCGGCGAAGAA
P1390	CCTGAACGGTCTTGCGAAGAA
P1391	TAATGGTCAGCCGGCGTATGTC
P1392	TAATGGTCAGCCGCTTTATGTC
P1393	CCAAAAACCCGGCGGCGAAACC
P1394	CCAAAAACCCGCTTGCGAAACC

[a] DNA sequence is given in the 5’ to 3’ direction for all primers. Restriction sites underlined.

Table 4.4. Summary of GFP-DamX Localization and PG Binding

Lesion:	% of cells with ring(s)[a]	GFP signal[b]	PG Binding[c]
WT	77	+++	81
Q351A	1	+++	N.D.
Q351E	1	+++	42
Q351K	5	+++	20
Q351N	2	+++	N.D.
S354A	70	+++	N.D.
S354F	0	-	55
S354K	3	+++	56
S354T	6	+++	63
S354Y	0	+	N.D.
N357A	65	+++	N.D.
N360A	72	+++	N.D.
N360V	74	+++	N.D.
S395A	68	+++	N.D.
E398A	93	+++	N.D.
E398V	55	+++	N.D.
N357A/S395A	0	+	N.D.
N360A/E398A	81	+++	72
W364A	0	-	N.D.
W364L	0	+	N.D.
W385A	82	+++	N.D.
W385L	70[d]	+++	N.D.
W416A	0	+++	13
W416L	1	+++	13

[a]Plasmids carrying a *gfp* fusion to either the WT *damX* SPOR domain or a mutant allele were transformed in EC251 to test for septal localization. Over 150 cells were scored for each construct.

[b] Protein production as judged by GFP signal in the localization experiments. A score of (+) or (-) suggest the protein was not well produced.

[c] PG binding using purified His_6-SPOR domains and isolated PG sacculi. Values shown represent averages from at least three experiments. N.D. = Not Determined

[d] At first ~60% of cells exhibited polar localization, but within a minute the protein redistributed to the midcell.

Figure 4.1. Assigned ^{1}H-^{15}N HSQC spectrum of the SPOR domain from DamX. Residue numbers count from the beginning of DamX (not the beginning of the SPOR domain).

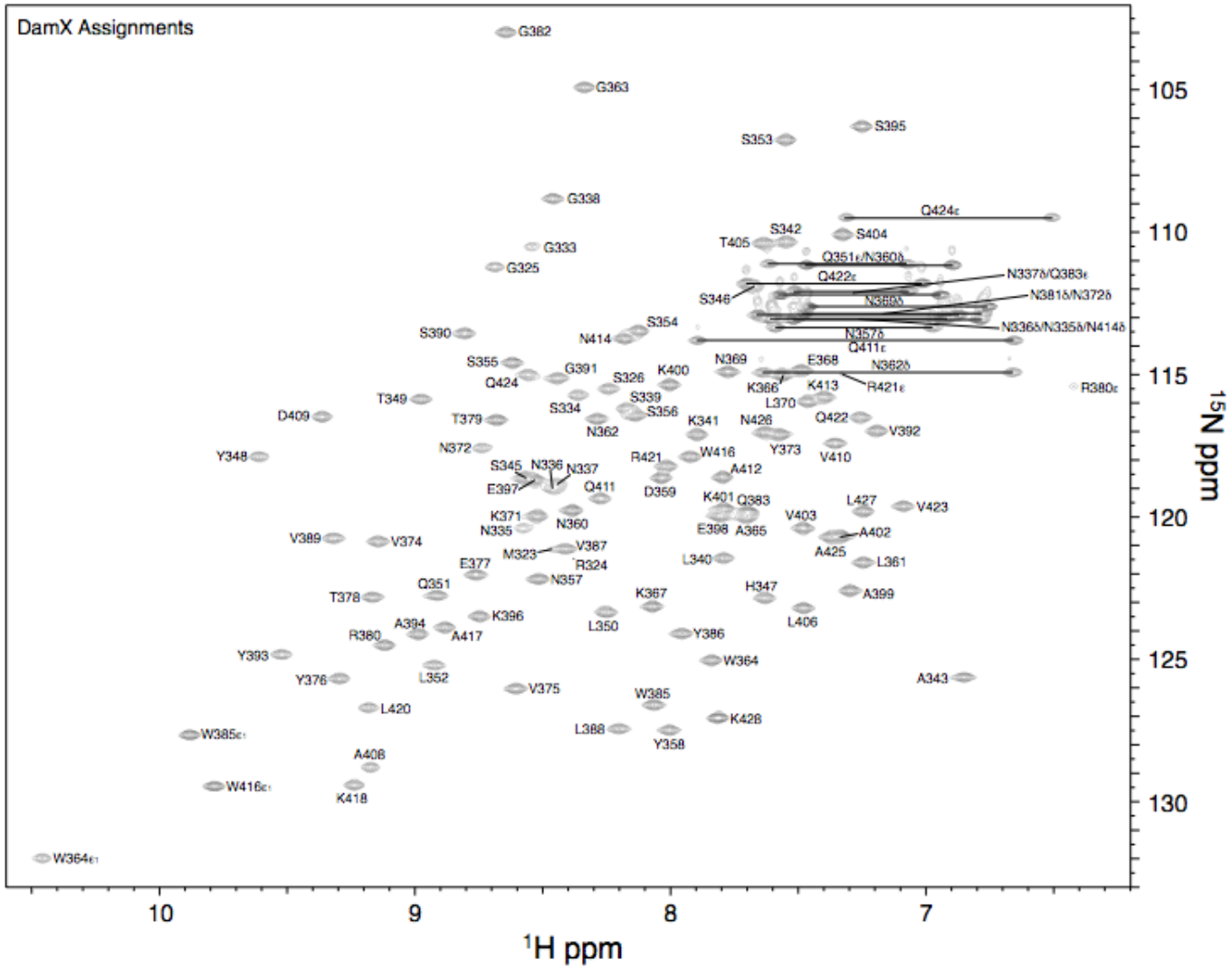
DamX Assignments
G382
G363
S395
S353
G338
Q424ε
S342
S404
T405
G333
Q351ε/N360δ
G325
Q422ε
N337δ/Q383ε
S346
N381δ/N372δ
N366δ
S354
N336δ/N335δ/N414δ
S390
N414
N357δ
Q411ε
S355
G391
N369
E368
N362δ
Q424
S326
K400
K366
K413
R421ε
R380ε
T349
S339
L370
S334
S356
D409
T379
K341
N426
Q422
V392
N362
N372
Y348
R421
W416
Y373
V410
S345
N336
N337
A412
E397
Q411
D359
K401
Q383
L427
V423
K371
N360
V403
N335
E398
A365
A402
V389
V374
V387
A425
M323
L340
L361
E377
R324
Q351
N357
H347
T378
K367
A399
K396
L406
A394
L350
R380
A417
Y386
Y393
W364
L352
A343
Y376
V375
W385
L420
K428
W385ε1
L388
Y358
A408
W416ε1
K418
W364ε1
105
110
115
120
125
130
15N ppm
10
9
8
7
1H ppm

Figure 4.2. Ribbon cartoon of $DamX^{SPOR}$. Cartoon is the average of the 25 lowest energy structures. Helices are colored cyan, ß-strands magenta, loops grey. A. Side on. B. Bottom up view.

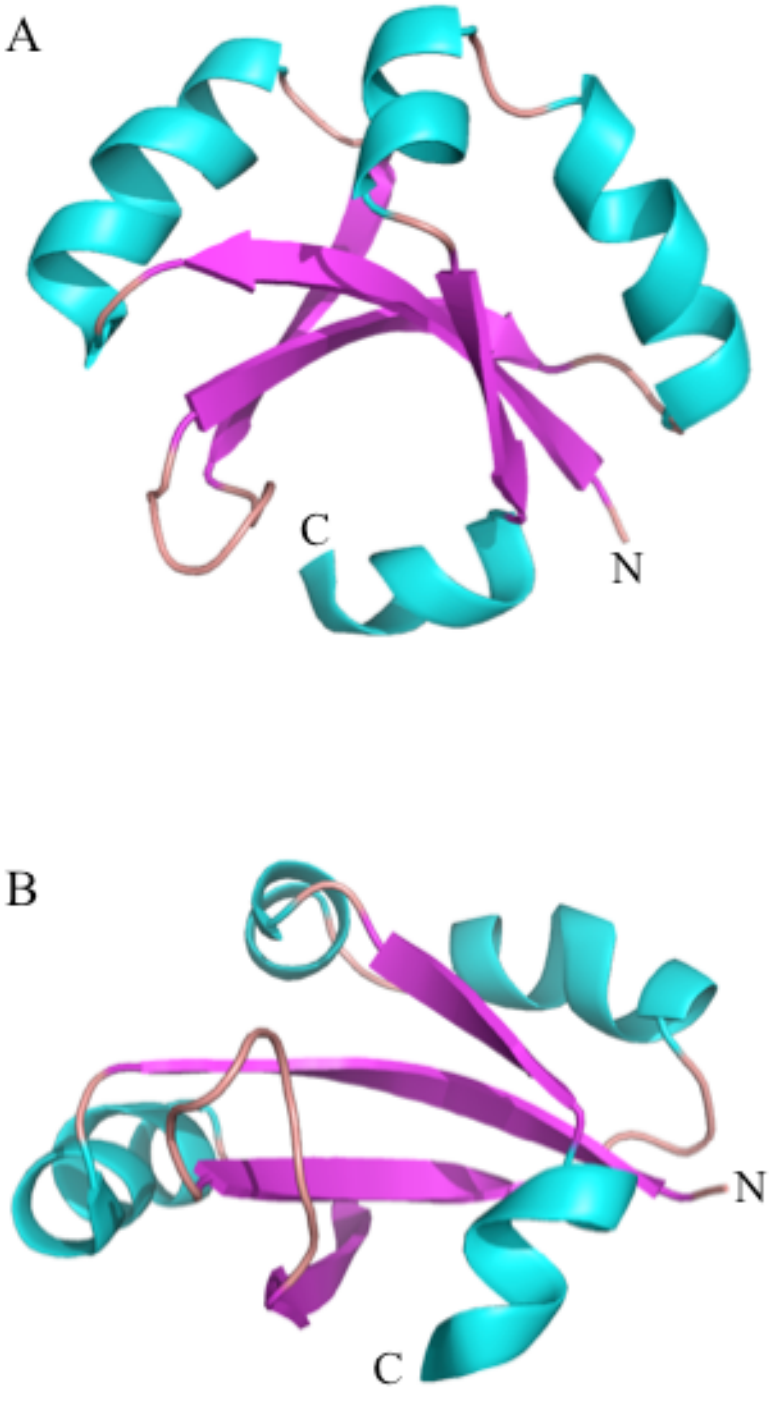
A
C
N
B
N
C

Figure 4.3. Structural comparison with CwlC . Overlay of the 3-D structures of $DamX^{SPOR}$, determined in this study, with a homologous SPOR domain from the *Bacillus subtilis* protein CwlC (Mishima et al., 2005). DamX is colored in green and CwlC in orange. Despite having extremely low primary sequence homology to each other, the overlays show the two domains have very similar structures.

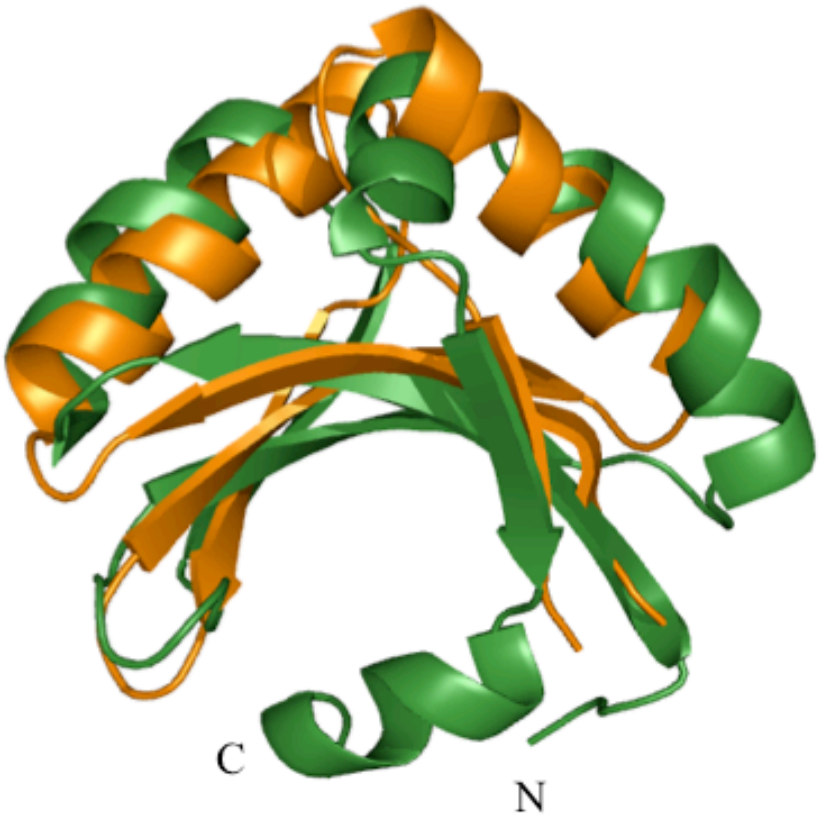
C
N

Figure 4.4. Structural comparison with FtsN. Overlay of the 3-D structures of $DamX^{SPOR}$, determined in this study, with a homologous SPOR domain from the *E. coli* protein FtsN (Yang et al., 2004). DamX is colored in green and FtsN in orange. N-terminus and C-terminus of $FtsN^{SPOR}$ are indicated as N' and C'. Overlays show the two domains have very similar structures, while having extremely low primary sequence homology. However, the ß-sheet face from FtsN is not as explicitly defined and adopts a flatter confirmation. Like CwlC, FtsN also lacks the C-terminal helix present in DamX.

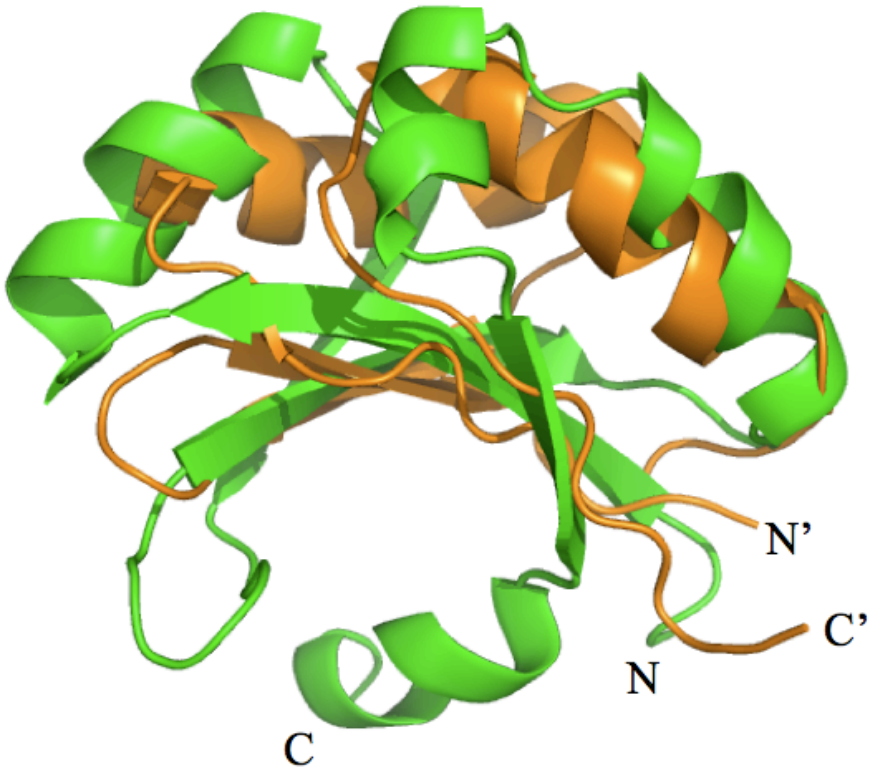
N'
C'
N
C

Figure 4.5. Topology of the SPOR domain. A. Multiple sequence alignment of SPOR domains that localize to the division septum in *E. coli*. Sequences were aligned manually to the position-specific scoring matrix (PSSM) from http://www.ncbi.nlm.nih.gov/Class/Structure/pssm/pssm_viewer.cgi with the SPOR domain (Pfam accession no. 05036) as the PSSM identifier (PSSM ID). Asterisk indicates residues that were targeted for site directed mutagenesis in this study. Numbers to the left refer to the first positions of the SPOR domains in the indicated proteins. The last residue shown for each homolog represents the final amino acid of that protein's sequence. Residues that comprise alpha helices and beta strands on the SPOR domain from DamX are indicated with bars. B. Homology mapping of SPOR domains. Consurf (Landau et al., 2005), was used to generate a color coded homology model of the SPOR domain, which is shown projected onto the CwlC SPOR domain structure (Mishima et al., 2005). Residues in blue are the most conserved while those in red are the least conserved. Conservation was assessed using an alignment of 130 SPOR domain sequences (Table A1.1). Residues corresponding to Q351 and S354 of DamX are indicated with arrows in the cleft.

A

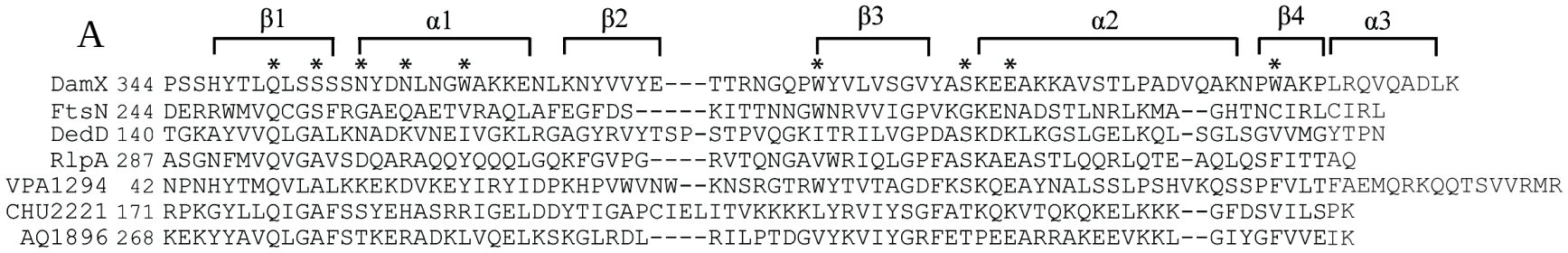
β1
α1
β2
β3
α2
β4
α3
DamX 344 PSSHYTLQLSSSSNYDNLNGWAKKENLKNYVVYE---TTRNGQPWYVLVSGVYASKEEAKKAVSTLPADVQAKNPWAKPLRQVQADLK
FtsN 244 DERRWMVQCGSFRGAEQAETVRAQLAFEGFDS-----KITTNNGWNRVVIGPVKGKENADSTLNRLKMA--GHTNCIRLCIRL
DedD 140 TGKAYVVQLGALKNADKVNEIVGKLRGAGYRVYTSP-STPVQGKITRILVGPDASKDKLKGSLGELKQL-SGLSGVVMGYTPN
RlpA 287 ASGNFMVQVGAVSDQARAQQYQQQLGQKFGVPG----RVTQNGAVWRIQLGPFASKAEASTLQQRLQTE-AQLQSFITTAQ
VPA1294 42 NPNHYTMQVLALKKEKDVKEYIRYIDPKHPVWVNW--KNSRGTRWYTVTAGDFKSKQEAYNALSSLPSHVKQSSPFVLTFAEMQRKQQTSVVRMR
CHU2221 171 RPKGYLLQIGAFSSYEHASRRIGELDDYTIGAPCIELITVKKKKLYRVIYSGFATKQKVTQKQKELKKK--GFDSVILSPK
AQ1896 268 KEKYYAVQLGAFSTKERADKLVQELKSKGLRDL----RILPTDGVYKVIYGRFETPEEARRAKEEVKKL--GIYGFVVEIK

B

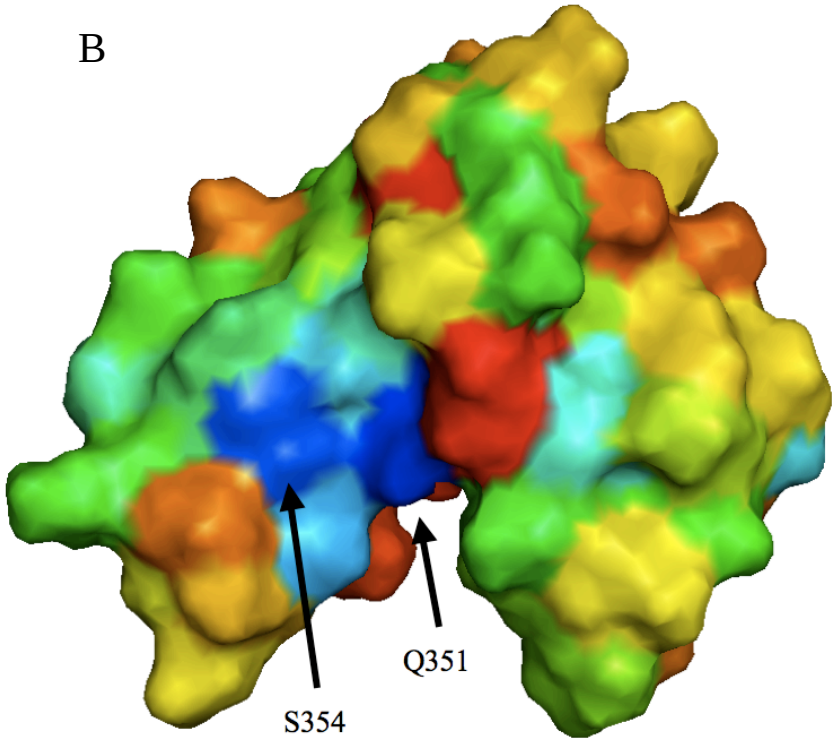
Q351
S354

Figure 4.6. Amino acids in the DamX SPOR domain targeted for mutagenesis. Three-dimensional ribbon diagrams of the DamX SPOR domain from *E. coli* showing the residues (shaded yellow) that were targeted for site directed mutagenesis.

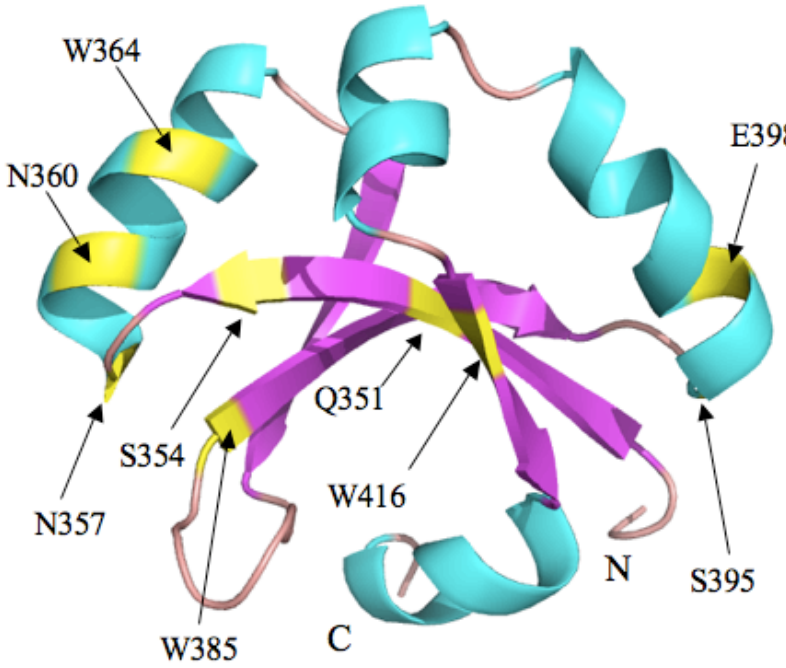
W364
N360
E398
S354
Q351
N357
W416
N
S395
W385
C

Side

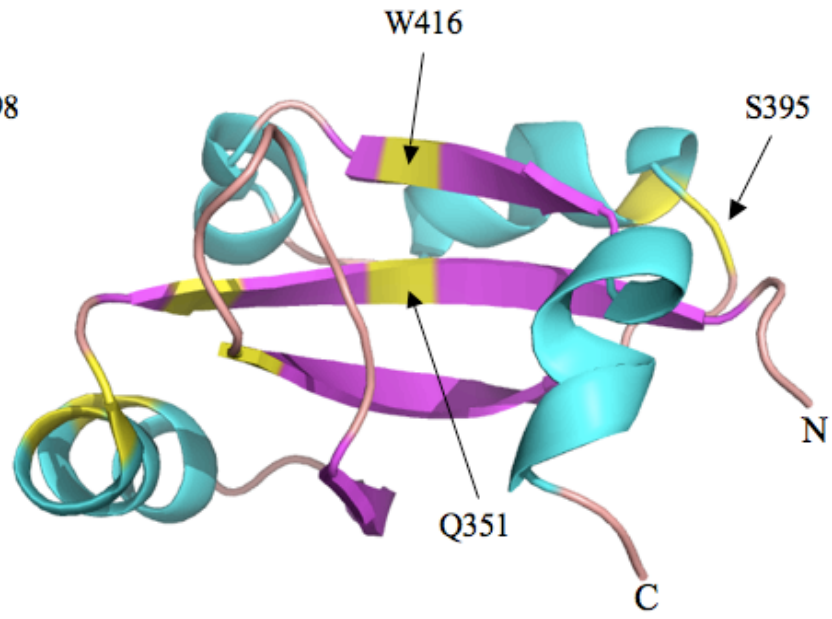
W416
S395
N
Q351
C

Bottom

Figure 4.7. Localization of GFP-DamX SPOR domains carrying amino acid substitutions. A and B. Wild type *E. coli* (EC251) cells were transformed with pDSW962-based plasmids carrying a *gfp* fusion to either wild type *damX*^{spor} or a mutant allele. Overnight cultures of these transformants were subcultured 1:200 and allowed to grow to an OD_{600} of ~0.5, at which time they were spotted onto slides containing agarose pads and photographed with fluorescence microscopy. C. Micrographs illustrating rare instances of septal localization of the Q351, Q251E, S354A, and S354T mutant proteins. Wild type is shown for comparison. Note that the mutant septal bands are faint and only observed in deep constrictions. D. Effect of agarose pad age on localization of GFP-DamX^{SPOR} in live cells. Top: Frequency distribution of polar and septal localization patterns. Bottom: Micrographs showing examples of cells photographed within 2 minutes of being spotted onto new (left) or old (right) agarose pads. Note the many examples of polar localization in cells on the new pad, whereas only septal localization is seen in cells on the old pad.

A

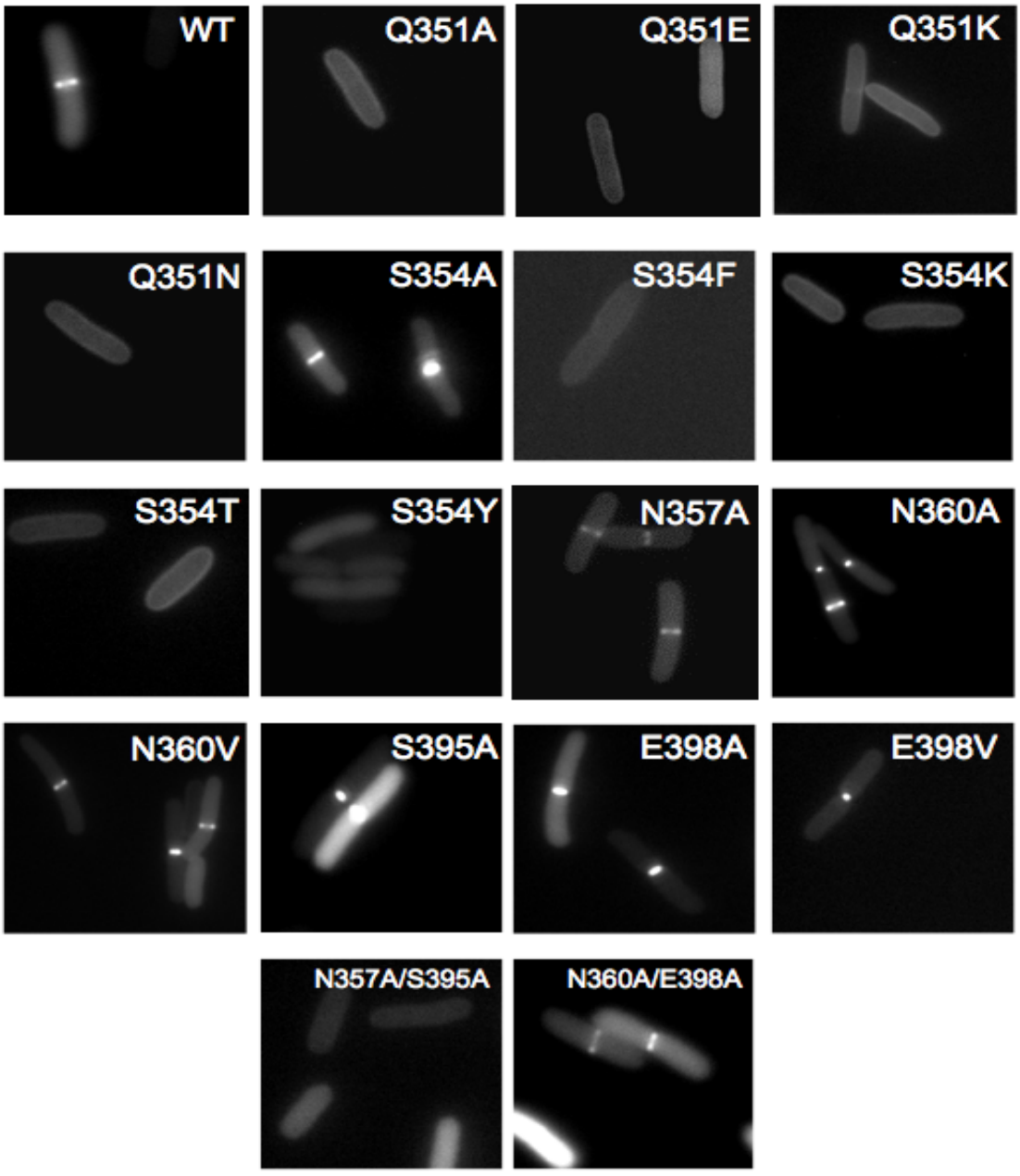
WT
Q351A
Q351E
Q351K
Q351N
S354A
S354F
S354K
S354T
S354Y
N357A
N360A
N360V
S395A
E398A
E398V
N357A/S395A
N360A/E398A

B

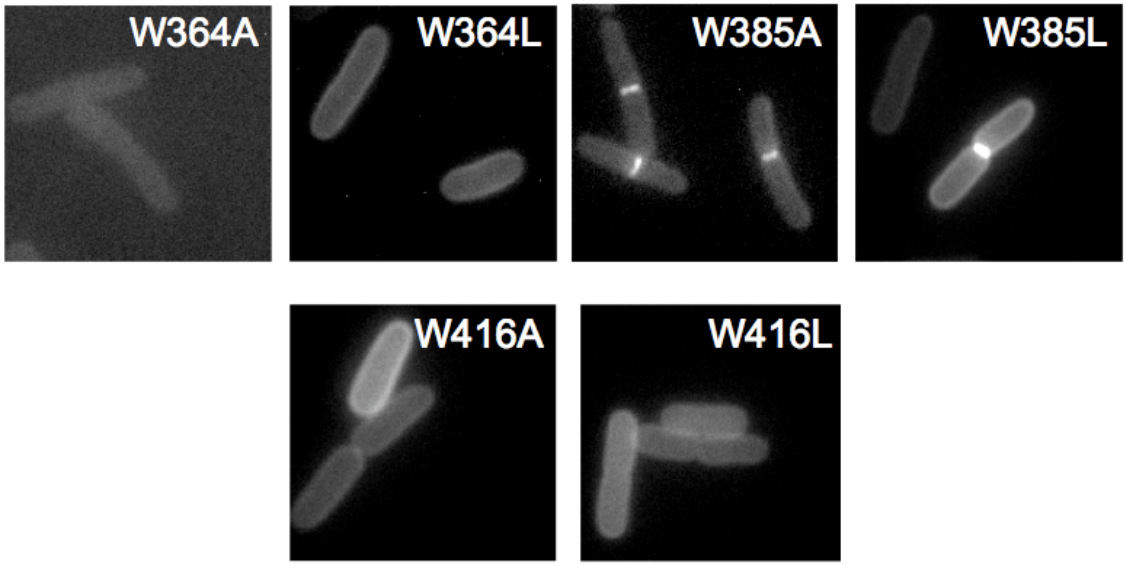

Figure 4.7 continued

C.

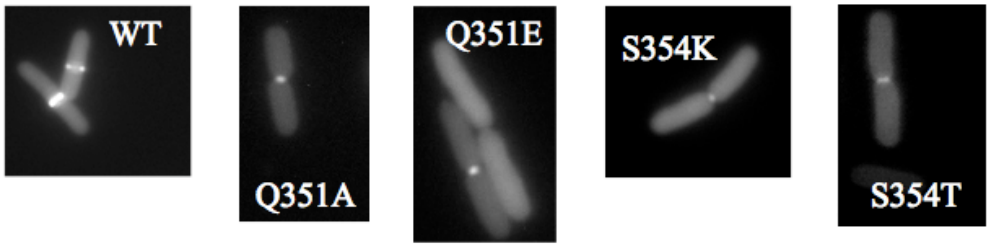

Figure 4.7 continued

D.

Effect of Agarose Pad Age on Localization GFP-DamX^{SPOR}

	New Pad[a]		Old Pad[b]
Localization[c]	**Time[d]**		
	< 2'	**> 5'**	**< 2'**
None	20%	30%	36%
Septal Only	17%	68%	64%
Septal and Polar	34%	< 1%	< 0.5%
Polar Only	29%	< 2%	< 0.5%

[a] New pads were allowed to polymerize on the glass slide for 10 minutes prior to use.

[b] Old pads were allowed to polymerize and remain at room temperature for 2 hours prior to use.

[c] Localization is reported as percent of cells showing the indicated pattern of GFP signal. Cells from two experiments were scored and the data pooled to generate these values. Please see panel below for examples of polar localization.

[d] Time (in minutes) after spotting cells onto the agarose pad.

Examples of Localization Patterns

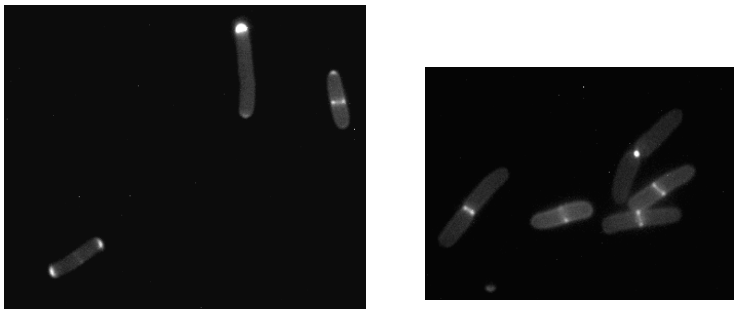

New Pad Old Pad

Figure 4.7 continued

Figure 4.8. PG binding assay with DamX^{SPOR} carrying amino acid substitutions. Purified proteins were mixed with purified *E. coli* sacculi and subjected to ultracentrifugation to pellet the sacculi, which were washed and centrifuged again. Samples of the supernatant, the wash fluid, and the final pellet were analyzed by SDS-PAGE and Coomassie staining to determine what fraction of the input protein was in the final pellet. Bars indicate the averages and standard deviations from three independent experiments. MBP, maltose binding protein, and FtsZ are controls for nonspecific binding (FtsZ and MBP data reproduced from Figure 3.3). These data show that mutations at residues in the "cleft" of the SPOR domain impair PG binding.

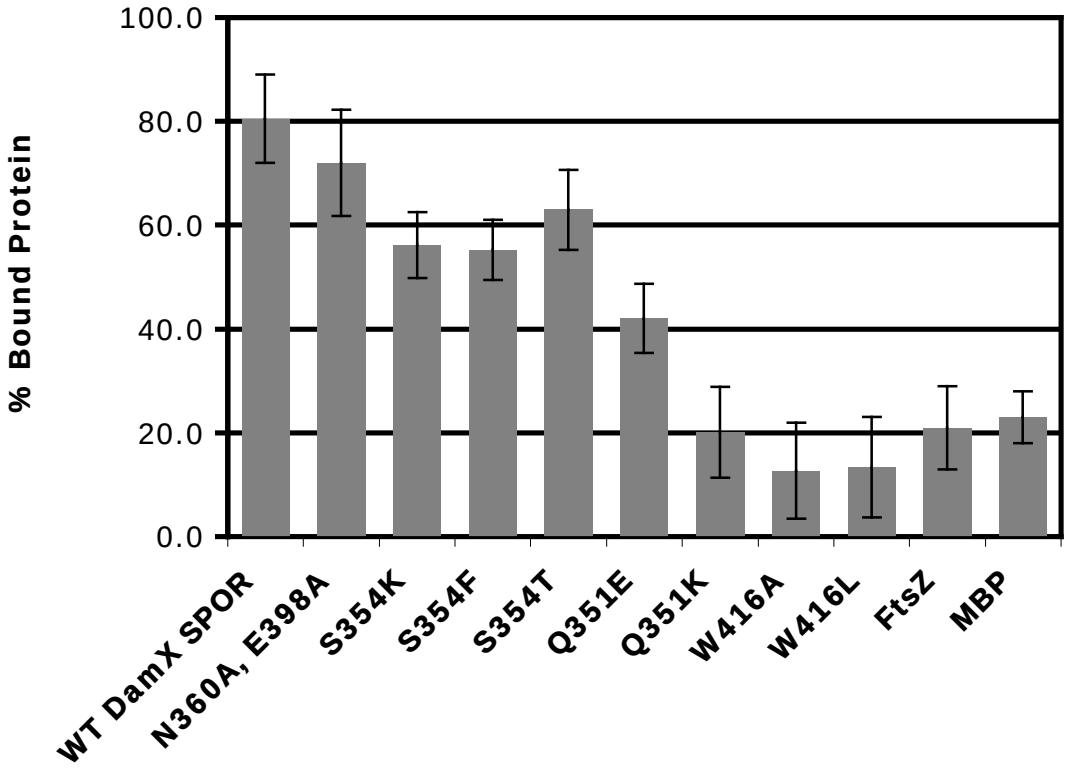
% Bound Protein
100.0
80.0
60.0
40.0
20.0
0.0
WT DamX SPOR
N360A, E398A
S354K
S354F
S354T
Q351E
Q351K
W416A
W416L
FtsZ
MBP

Figure 4.9. Comparison ^{1}H-^{15}N HSQC spectra. A. Overlay ^{1}H-^{15}N HSQC spectra of the SPOR domain from wild type DamX (Black) and the Q351A mutant protein (Red). Differences between the mutant and wild type are mostly localized near the site of the mutation, as would be expected. B-F. Similar mutant vs. wild-type HSQC overlays for the DamX SPOR domains containing the following amino acid substitutions: Q351K, Q351N, S354T, W416A, and W416L. There is some mild signal degradation present in the Q351K spectrum, indicating the protein is slightly less stable than the others, but the majority of the protein is still well folded.

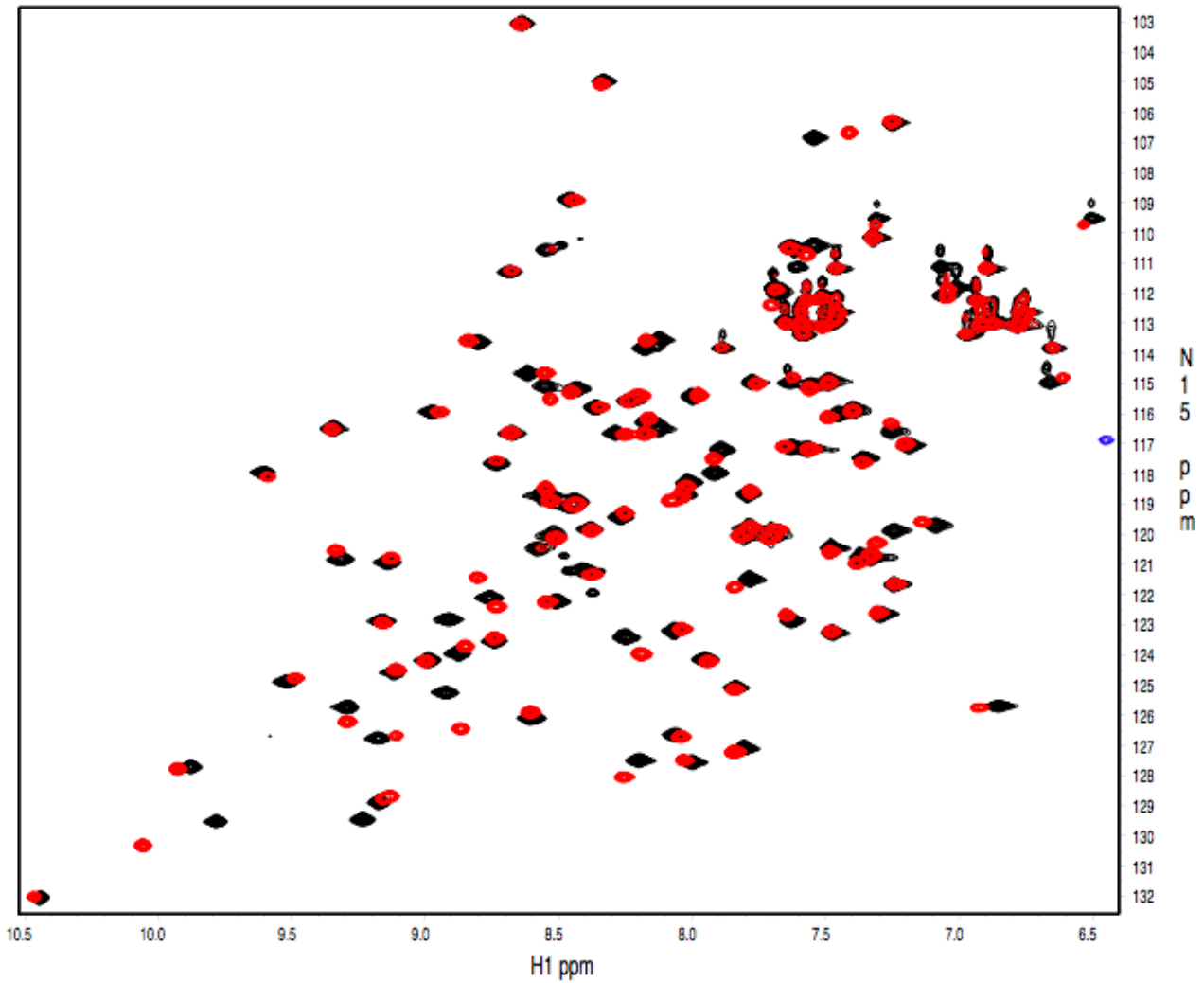
103
104
105
106
107
108
109
110
111
112
113
114
115
116
117
118
119
120
121
122
123
124
125
126
127
128
129
130
131
132
N
1
5
p
p
m
10.5
10.0
9.5
9.0
8.5
8.0
7.5
7.0
6.5
H1 ppm

A

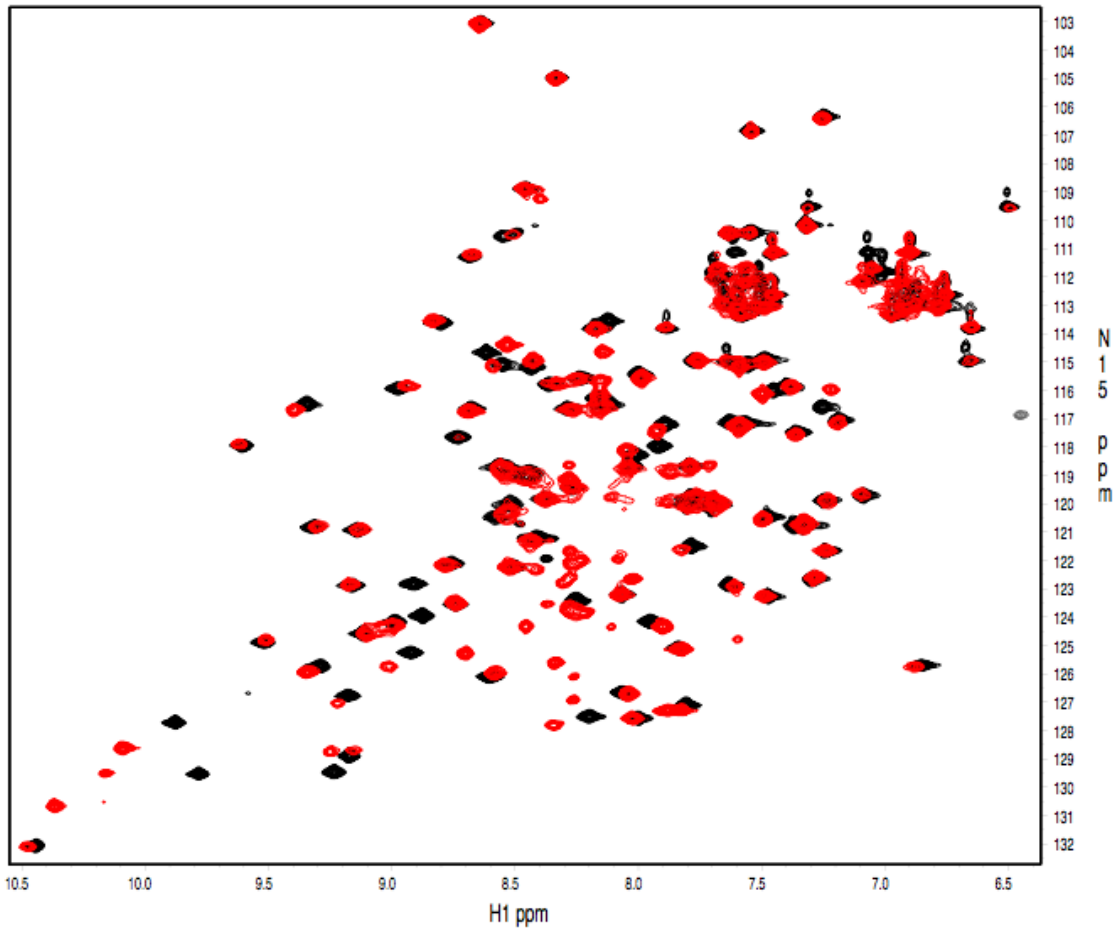

B

Figure 4.9 continued

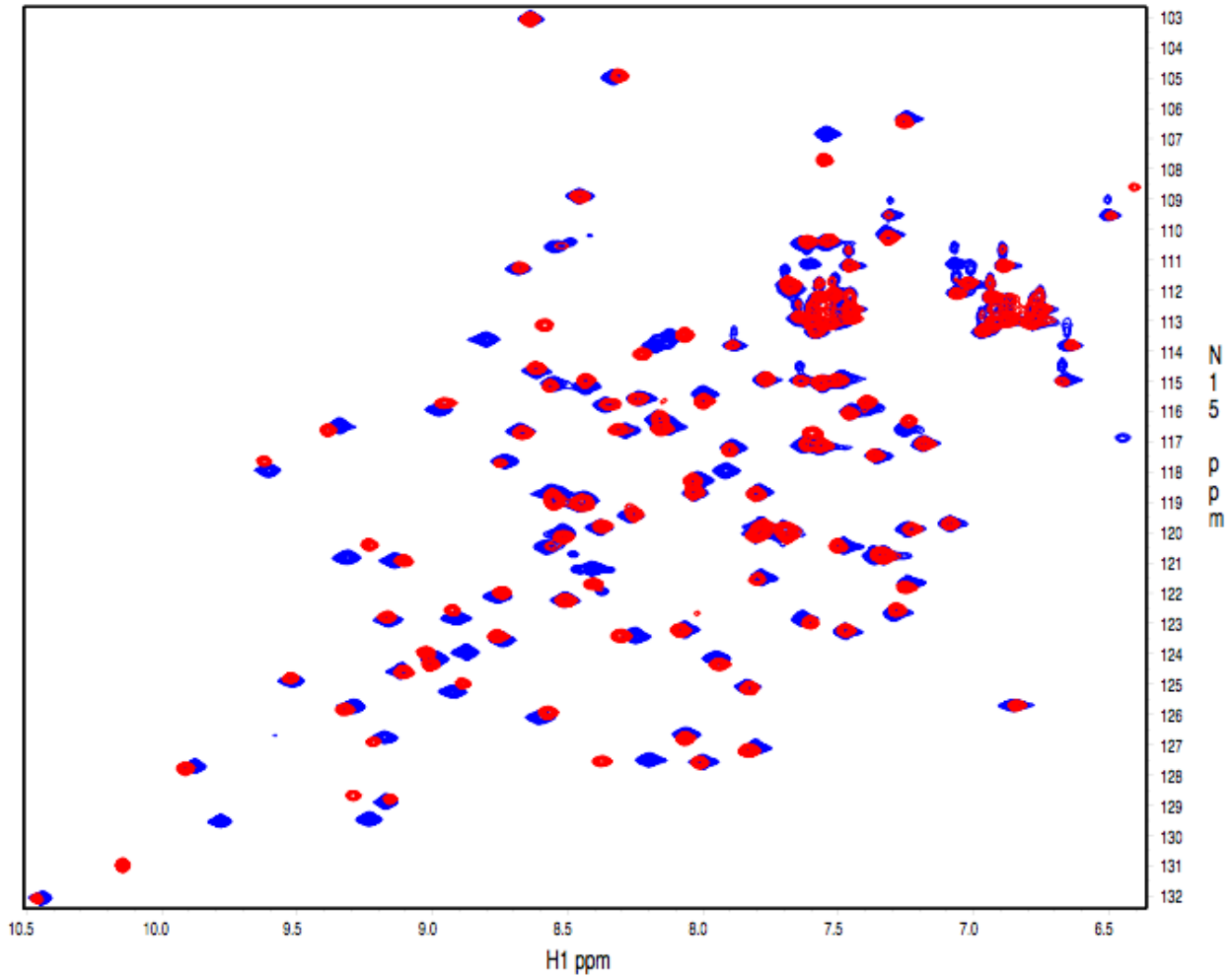

C

Figure 4.9 continued

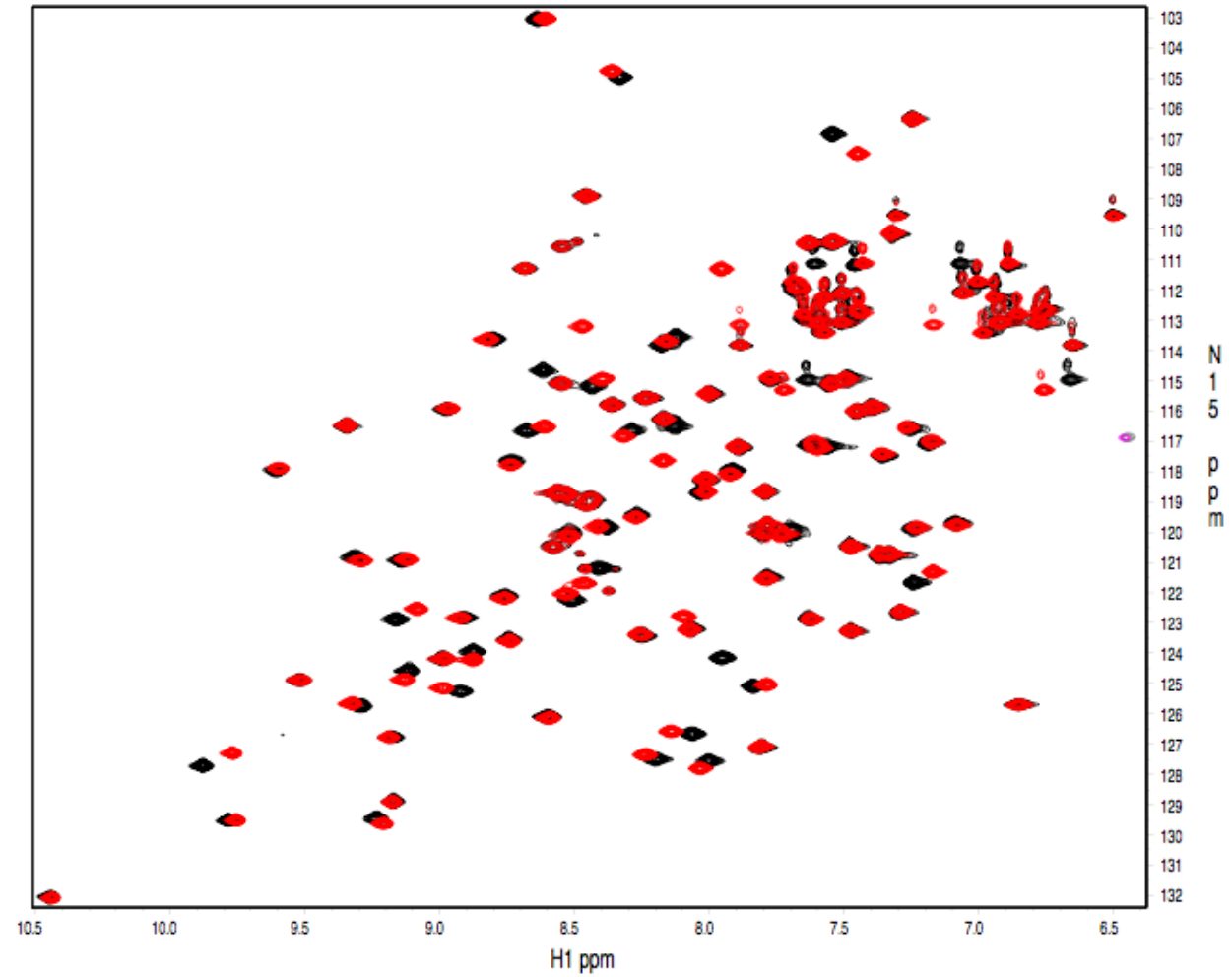

D

Figure 4.9 continued

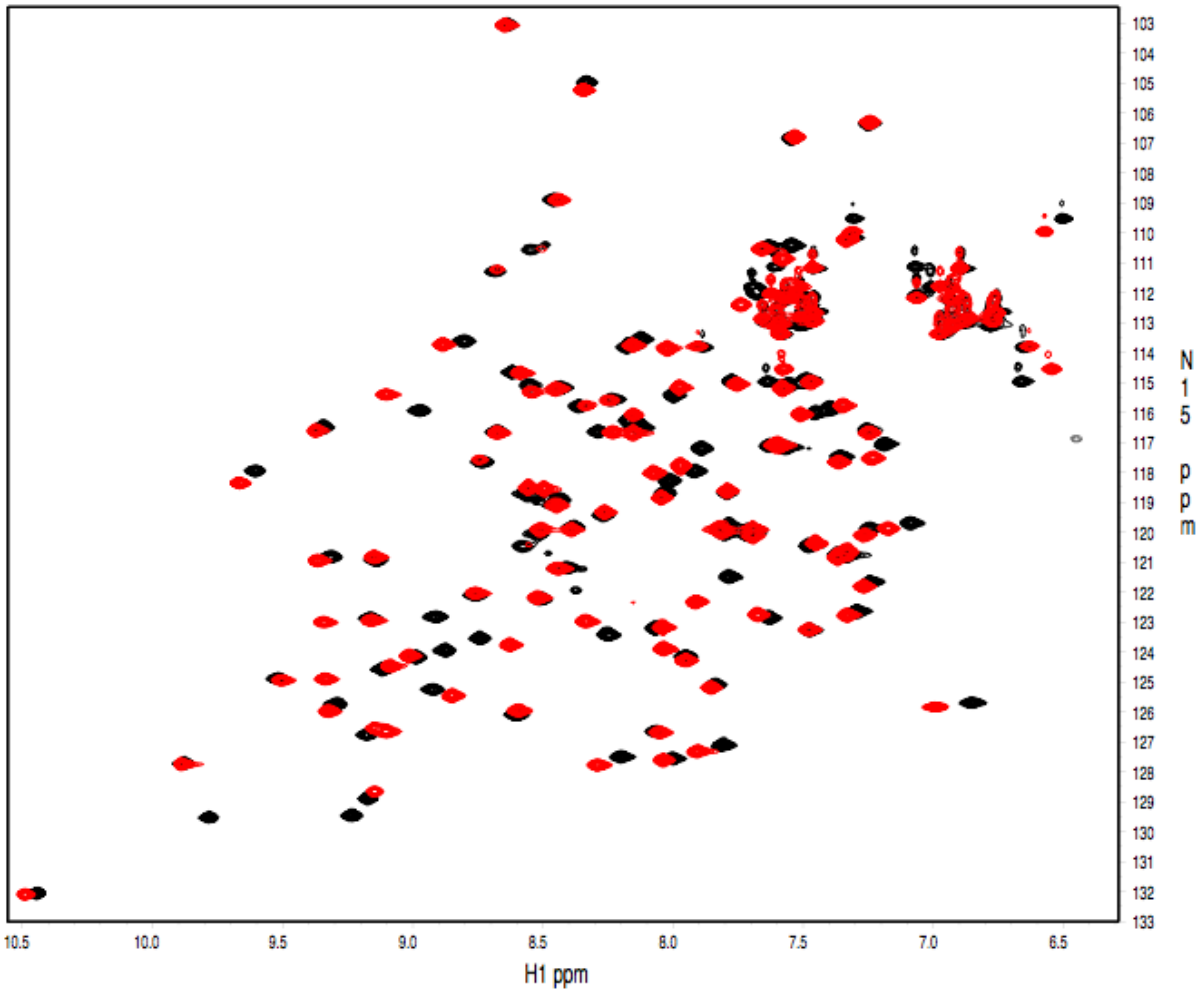

E

Figure 4.9 continued

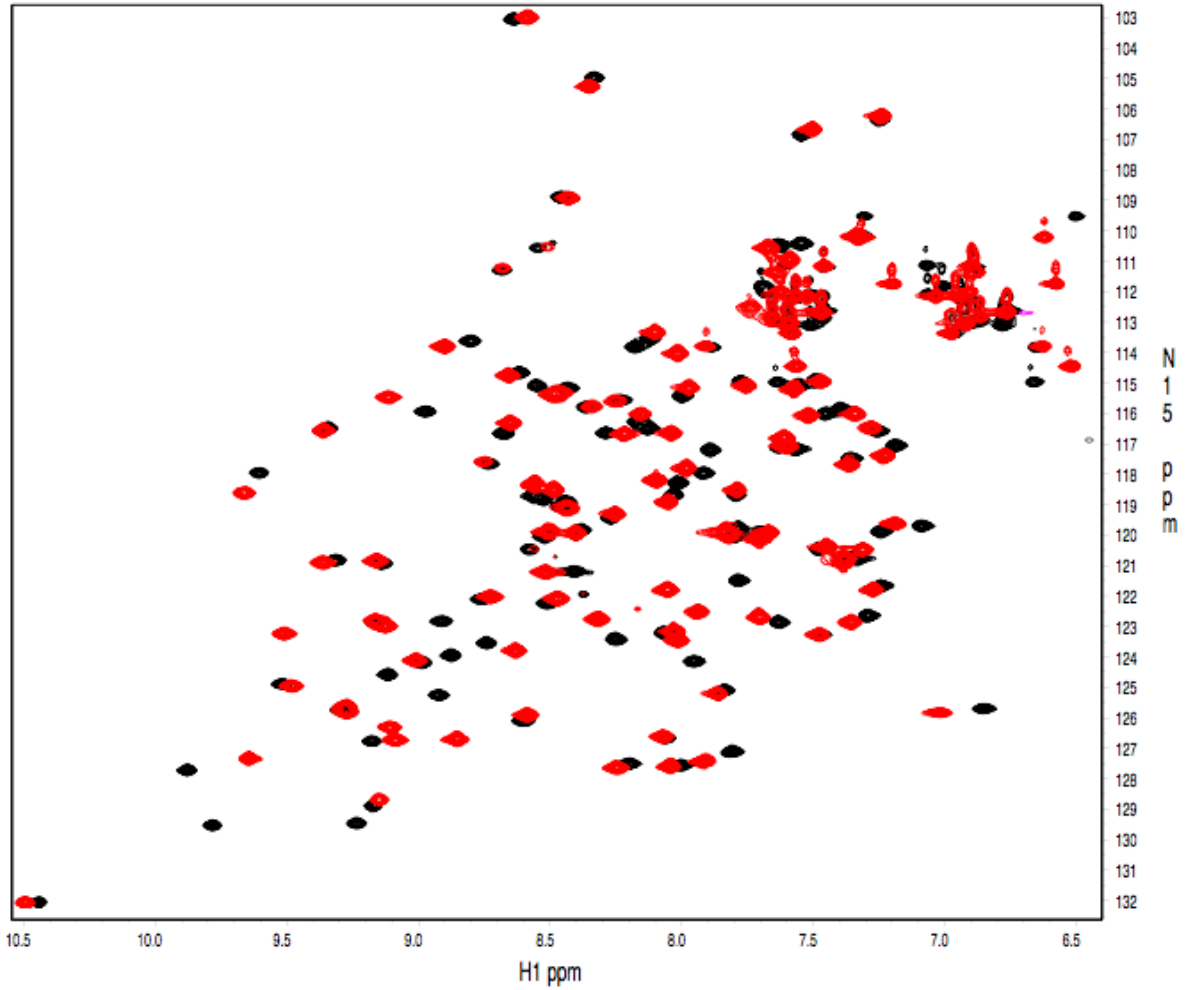

F

Figure 4.9 continued

Figure 4.10. Affect of a SPOR domain lesion on complimentaton. A. Division phenotypes of *damX dedD* null mutant and strains complemented with either wild-type *damX* or a copy of *damX* encoding the Q351K amino acid substitution. B. Fluorescence micrographs of strain EC2177 (Δ*damX dedD*<>*kan* P204::*gfp-damX*) and EC2223 (Δ*damX dedD*<>*kan* P204::*gfp-damX*(Q351K)) showing that GFP-DamX with a Q351K mutation fails to efficiently localize to the midcell. C. Analysis of steady state levels of GFP-DamX fusions in a *damx dedD* double mutant. Whole-cell extracts were subjected to SDS-PAGE, transferred onto nitrocellulose, and probed with anti-GFP. Molecular mass markers in kilodaltons are indicated to the left of the panel. Strains used for the western were as follows: (-), EC1924; GFP, EC251 P_{204}::*gfp*; WT DamX, EC2177(Δ*damX dedD*<>kan P_{204}::*gfp-damX*); Q351K DamX, EC2223(Δ*damX dedD*<>kan P_{204}::*gfp-damX*(Q351K)).

A.

Division phenotypes of mutants lacking *damX* and *dedD*[a]

Strain	Genotype	Average Length (SD)
EC251	Wild type	3.7 (1.1)
EC1924	Δ*damX dedD*<> *kan*	13.8 (13)
EC2177	Δ*damX dedD*<> *kan* P204::*gfp-damX*	4.8 (2.1)
EC2223	Δ*damX dedD*<> *kan* P204::*gfp-damX(Q351K)*	6.3 (2.0)

[a] Cells were grown grown for five to six doubles to an OD_{600} of ~0.5, placed on slides with agarose pads, and photographed with phase contrast and fluorescence microscopy.

B.

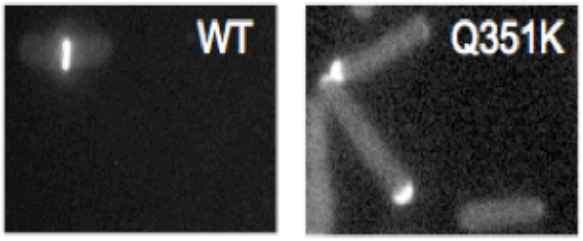

C.

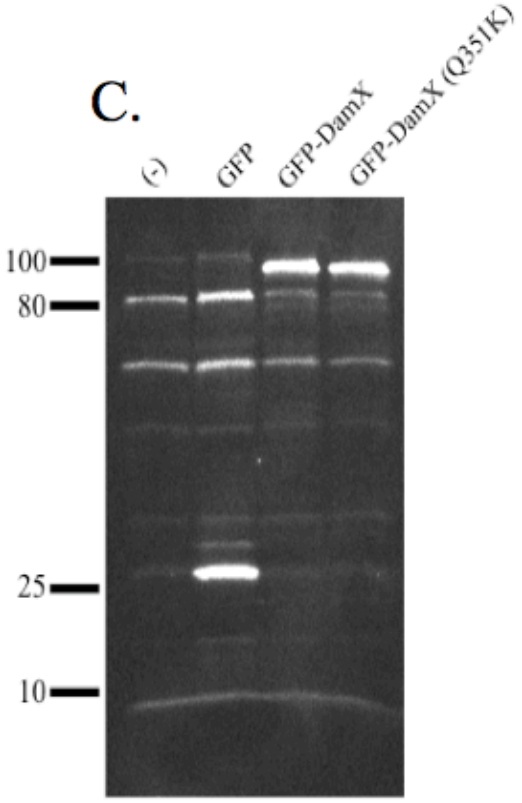

Figure 4.11. Location of DamX residues important for septal localization and PG binding. Substitutions at sites indicated in blue (Q351, S354, and W416) impaired localization of the protein to the division septum and PG binding. Side chains have been included on the bottom view to show proximity of the residues to each other in space.

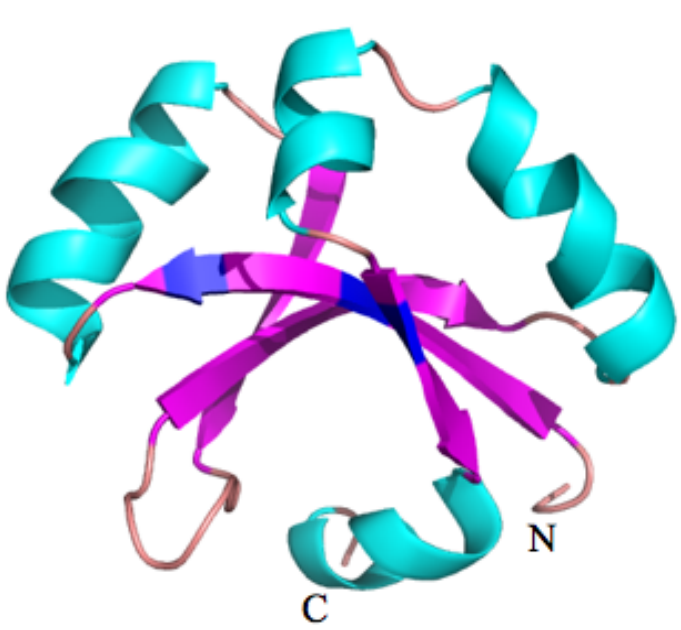

Side View

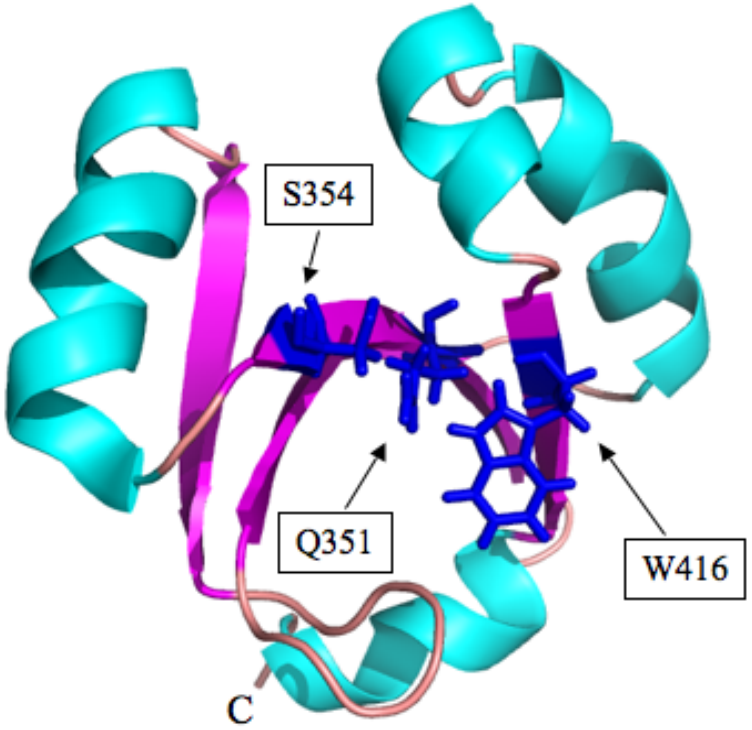

Bottom View

Figure 4.12. Multiple sequence alignment of DamX SPOR domains identified in several organisms. Residues that show 100% conservation within this subset are highlighted using the Zappo color scheme for chemistry type using Jalview {Waterhouse, 2009 #127}. We found authentic DamX homologs in *Vibrio parahaemolyticus*, *Pectobacterium wasabiae* WPP163, *Yersinia mollaretii*, and *Photorhabdus asymbiotica.* Interestingly, we could not identify a clear DamX homolog in any of the published genomes of *Pseudomonas* species, *Rhizobium leguminosarum*, *Agrobacterium tumefaciens,* or *Staphylococcus aureus* (which lacks any SPOR domain proteins).

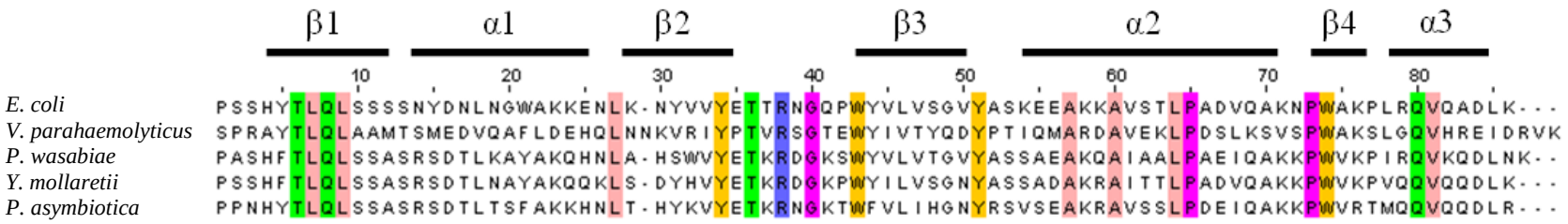
β1
α1
β2
β3
α2
β4
α3
10
20
30
40
50
60
70
80
E. coli PSSHYTLQLSSSSNYDNLNGWAKKENLK-NYVVYETTRNGQPWYVLVSGVYASKEEAKKAVSTLPADVQAKNPWAKPLRQVQADLK---
V. parahaemolyticus SPRAYTLQLAAMTSMEDVQAFLDEHQLNNKVRIYPTVRSGTEWYIVTYQDYPTIQMARDAVEKLPDSLKSVSPWAKSLGQVHREIDRVK
P. wasabiae PASHFTLQLSSASRSDTLKAYAKQHNLA-HSWVYETKRDGKSWYVLVTGVYASSAEAKQAIAALPAEIQAKKPWVKPIRQVKQDLNK--
Y. mollaretii PSSHFTLQLSSASRSDTLNAYAKQQKLS-DYHVYETKRDGKPWYILVSGNYASSADAKRAITTLPADVQAKKPWVKPVQQVQQDLK---
P. asymbiotica PPNHYTLQLSSASRSDTLTSFAKKHNLT-HYKVYETKRNGKTWFVLIHGNYRSVSEAKRAVSSLPDEIQAKKPWVRTMQQVQQDLR---

APPENDIX A: NMR OF DAMX

As discussed in Chapter 4, we solved the solution structure of the DamX SPOR domain using NMR in collaboration with Dr. Andrew Fowler. Within this appendix we have some useful figures and tables related to SPOR domains and structural features worth noting.

X-ray Crystallography Trials. Simultaneous to our work using NMR to solve the structure of $DamX^{SPOR}$, we were exploring the possibility of using X-ray crystallography for structure determination. We were successful at concentrating our protein to high levels without problems of insolubility. However, after conducting a few hundred crystallization trials we had no promising leads. By this time, our NMR work was proceeding nicely, so efforts were refocused on that front. There are a number of possible reasons our crystallization trails did not yield promising results. First, the DamX SPOR domain has proven to be very soluble. Concentrations approaching 100mg/ml were achieved without the protein becoming insoluble. This high degree of solubility could be working against crystal formation. Also the theoretical pI of the expression construct we were using is rather high at 9.8, as calculated using ExPASy software (Wilkins et al., 1999). Perhaps using crystallization trial conditions optimized for this pI would yield better results. Lastly, we now know the N-terminus of the protein is flexible and largely unordered in the NMR structure (Williams and Fowler, manuscript in preparation). The high degree of mobility could inhibit crystalization. If future work was undertaken on crystallography, removing some of these residues before the start of the actual SPOR domain sequence should be considered.

Large Scale SPOR Domain Alignment. Table A.1 shows the results from a large scale multiple sequence alignment of 130 SPOR domains from many different organisms. The SPOR domains in this alignment came from a tree seed set obtained from the Pfam database (Finn et al., 2008), edited to remove duplicate entries, and compiled using

ClustalW (Larkin et al., 2007). These data are the basis for the homology levels quoted throughout this thesis.

Table A.1 Alignment of SPOR domains from Pfam Database[a]

Protein[b]	Sequence
DamX	PSSHYTLQLSSSSNYDNLNGWAKKENLKNYVETTRNGQPWYVLVSGVYASKEEAKKAVSTLPAQAKNPWAKP
CwlC	SSGLYKVQIGAFKVKANADSLASNAEAKGFDSIVLLKDGLYKVQIGAFSSKDNADTLAARAKNAGFDAIVIL
FtsN	DERRWMVQCGSFRGAEQAETVRAQLAFEGFDSKITTNNGWNRVVIGPVKGKENADSTLNRLKMAGHTNCIRL
gi81679246	GNTFFYLQAGAYNLEKDAKIRQNELAKLVDQIKNLADKHLYLVQIGPIDDYPTARALKEKLSQTERQFNQIN
gi81682932	DAGGWLVKAATTHEESSARRVAAVLNHQGPPARAVKAGDGFEVLAGPFKDDKTAKTVAKRLKILELDAEVRP
gi81504437	KDGKFLLLIGAFASEDRARNWLSKLKGEKIPKKVPEKGDLALLRAGPFNDRASAEMAQKRAEQLGLTPKLVQ
gi81730187	LSISWSVQLASMSNRANADNLQKTLRTQGYNAYIRTADGVNRVFVGPLIERAEADRLRDQLDKQKLEGIVVR
gi81567205	LSGSFYVQIGAFSSQENARRLSARMQQRGFKFYYAELVSFWRVQVGPWSTLSEAERMRQQLRSEFPGDFVVA
gi81357402	VAERLYLQIGAFENPAEADNLKARLALAGIEAQLADGRTMHRVRIGPFAKPEDMNPVRTRLADAGFTGTVVK
gi81357002	TGESFVVQIGAFGEASKATALGAELKKRGFAAYTEKAGAVTRVRIGPFGSREEADKAAERLRLSGMSGVVVQ
gi81345417	APPT------ALKDRASADELAAELRRDGFEADYRGGTLGWRVRIGTFDSQTAATAERTRLRAGYSGSAVYT
gi75392987	KGGAFTLQLSAFQDKQEADRFAARLRDRGYAAEVAGKGTWYRVRMGSFASRDAATRYLSDFKRTSLDAFVAG
gi2495679	DSKKFGLQCGAFKNRAQAENLQGRLQMTGLNAQIQTNGEWNRVRVASFDTRELAVQAQSRAKT-VTDCVVIG
gi75434273	SAVGFAVQLGAFARAEDADALRDRVRAAGFSQVRTDKGALNRVRVGPVANRGDAEQLRAQVAAVGISGMVRP
gi75434273	AAGNYAVNFGAYATSADADAVIARLKQAQLPKTQINGRPAWRVRVGPYADQAQAARLQAKVRS-DVNAQVVT
gi81389665	PFQVHFVQVGAFRSEGAARNLVSELAGQQVVMTPRNAMGLVKVYVGPFMSGEEAGEVLDVMRETGVAPNAFT
gi81363843	PQGVYRVAVGAFANPENAARLRQALADQGYPARLEPAGSLTRVVVGPYATEAEARRVAEALR--DYAPQVYR
gi81729444	QAAGLFLQVGAFANPDAAELLRSKLSGMRAPSIARNQQTLYRVRMGPIDTPGEAQQLQNSVRSNLGQPSVVT
gi81425425	AGSGVYLQLGAFSQPANAESLVSRINGQDPAAVVEQANNLYRVRIGPYATREAALGAVQPVADTGILPSLSA
gi81363843	SPERVYLQVGAFQKRENALALAEKLRGLGF-SVVLSEDGLHRVRVGPVPVGQV-DEVKARLKALGLEALEVR
gi81551536	PAGPVYVQVGAFNNVEGAQRFVEQLRAQGFSSVNAPETGKVTVLLGPLTGSDLTEGRLD----AGLDHFRLR
gi81562210	ADRPWGVQLAGFNALASYARAMSRLSTVGERFRSRGTRPFYQVRIGA-ETRGEADDLCKQIRRAGQACLVLR
gi81368609	GQGHYYLQAGAFSSEALAKRLKEKLVHITPSVFIEHYKQHYIVRVGPFGNKSMADNLKTKLSNGIKGSFSVL
gi81681203	GVSAWLVQAGSFVEEANAKALVEKLRQNNLSVHGSTGKVTYRVRIGPEPDKARAEQVLRQLESAGIRGYLVP
gi81369043	TPKLWYISAGSFRDRNNAVALVKRLNGLGFTAFMSPYKDLLSVFVGPYEYRGHAGNGMERLKEAHVEGVLVT
gi81616251	AVGKFTVQVASYADEAEAQKMASDLKNKGYSPANIKGKQWFRVSVGQFATQKEAQAYRNLLSKAKVSSAIVQ
gi81425247	ANGNFVLQVASYTTQADAQARRGKLHQAGVTQASINGKQQYRLRVGPFPSREAAQAAQARLRTGYDNGFIAA
gi81655434	AHGKSVIQLAALSDPAKVDALRGKLAAIGVTKVETSKGEVTRVRVGPFSSQAEAQSALQKLARAGINGIIIN
gi81368289	NKGAYLVQVASFKARQDAEQMKGMLILKGFDPVTQAQGNWFRVVVGPYPNKALAQKAQMNLAKEHLNGMVRS
gi81393975	QASSFILQVRSYSDPDSADARRAEIILNGLSKTVENGKTWYRVISGPYDTQDAALAAQQTLQHSGIDSIVVK
gi75436951	DNTRYILQAGSFGASGDAESTKAKLAMMGLASADISGKTVYRVRMGPYGSASELAEAKQKLTGSGLSAIAIK

Table A.1 continued

Protein[b]	Sequence
gi81729205	AVTTFFLQAGSFRKQADAEKVRAQIILLGQTSGTVKDETWYRVLVGPFSNREQLTTAQKQLAGGGFSNLLLQ
gi81680655	PGGGYIVQAGSYRSRPDAEKMRAELAKLKVKRVKIENVEWFRVKIGPYENLAEADRLRTILKKNGIDSVVQK
gi81425531	ASGTYFLQAGAYRVLEDAEALRARIILLGLPRAEVNGVQVNRVRVGPFGRLDDMNRARSRLGENDIKSAVVR
gi81702118	EGGTYRVYAGSYFVAERAQREQARLASLGIKLRKSSVSVPTLVLTGMFETKDEALKAAAALKKAGLKPVLAG
gi81566898	DTFDYVYQVAAFKDEGPAKTMRGKLETAGLRTQKDKTVTWYRILVSFRGTPEDTRALRALLKQ-GIDKIIMR
gi81408132	APKGYTVQVGVFREQSRAESYKSNLGQEGEKTFLFTRDGLFVIQLGDFASRTEAESLKSKLKNDGIDCFIPK
gi133097	ASGNFMVQVGAVSDQARAQQYQQQLGQKGVPGRVTQNGAVWRIQLGPFASKAEASTLQQRLQTAQLQSFITT
gi75355351	ADKTYRVVLP---VSADAENQAAELSAKGFNIPFDGALSL-----GVGNSRENAQALQNRLADGFGGAHIVE
gi75346768	GGTIYRVQVGAFSVRANADQQQARLRADGYESIIVQSGSLFLVQAGAFSVRANADALANELRGRGYDAVVVS
gi585019	AAALYKVQIAAFRTKANADSLAAQAEAKGFDALVIYRDSLYKVQIGAFSSKENAEALVQQAKNAEFDTFIYQ
gi81785686	SGTFYRVITGSFKNRSNAEKRQQELKKAGFDADKHKGETFYRVVTGSFKDRSNAEKRQGDLKQNGFDSFIDI
gi81741386	SPNFFKVIAGSFKQRINAEERVDLLTDEDMEPVTISGQQWYRVQSGAFRDRDNANARINQLQDLGIEAFIIT
gi75542329	PNTNYKVRVEGYKNGKVVTKNEIVLK-----TLDIEDDKLYRVQVGAFKDKDNADKLRNELKNKGFNGFIKE
gi75355598	AEATHYLQMGAYADRRSAEGQRAKLAILGISGYQAGHKTLYRVQSGNMSADAV-KKMQDELKKHGVASLIRA
gi81629051	SPSHLFIQLGAFRERTHAENLKRELRAYIKKRSIYNQLPLYRVQIGPLSNINESNYLHDELKKLGFGEIITM
gi20139369	SGGKFSLQMGAFRNQIGAQTLADKLQAENPNVKVAFKDDLYKVLVQGFQSEEEARDFMKKYN----QNAVLT
gi81353822	EGGNFMVQIGAFKNPAGAQTIAARYKTYRTYIRTSSVDGLNRVFLTGFRSEDEARDFAAG---AFAGAFVVR
gi81790991	SGGGFTLQFGSFDSITNAEQMVAQLQYTP--ARVQQINGVYKVRLRTFTTQQEAAAFARTLP---IESIVVP
gi75540174	DNGKFYLQLAAFGSAHNAQSYLMQLKSEPSITHINQANGLHKIFVGPFHDLEAANRTANIITTGSPEPILVR
gi81701787	SRVGHAIQVGAFSDVKNAERLTARLQVRGIDFYFKRDNGLYAVRFGDFPSREAARREARRLVAGMIGSYFIA
gi81665250	KSPLYNVQVGSFNSVENAGRLVDSLNQKGLDAFLFKEAGMYKVRFGNYQSFEDA-----KIRAGLINEFFIV
gi81654052	DNPKY-LQLGSFNTLANAEALLQKTLDEDDKLGIVNQQGVYKVRLGPFSSDDAVRSAAENLH----VETVIT
gi81357629	VGRGVFLQLGTFSSAAKAEGLRARVRDEETLLELQEDGSRYRVQLGPFASADEARDEAGRLAALDIRPFVVT
gi81816571	KEKYYAVQLGAFSTKERADKLVQELKSKGLRLRILPTDGVYKVIYGRFETPEEARRAKEEVKKLGIYGFVVE
gi81368731	KQDIYAVQLASFTQIANAQALVNRLRSKGYKKSNSRNGIVYKVVVGHSPVKKDVIKLKTQLASMQLNGFVVN
gi586017	TYKTYAVQAGKFSNEKGAETLTEQLTEKGYSVSLSKDDGYTYVIAGLASEKEVSQQLGQLID----SDFEAW
gi81368738	LKRIYFLQLGAFSQKSNAQQLARKVQARQYPVIISHSGNAFSVRVGPVNTQELH-----QLSIQNSNLALIN
gi75434036	ALGDILLQVASFASRENANRALSQLASAGIADIVSGGRTLWRLRV---NARDHASEIAQRIAGGFGRPQIVA
gi14916893	NLRTYKFQVGAFRYRENAYKMAKIVRSKGFDAQVVKVGSLYRVYAVKAKNYWEAKREIKHFK----DAIFVR
gi75353706	AKSAWIIQLGVFRNADNAKNLALKLRKQGYQPKDPKPGDLVRVAVGPDVSKPDLEKLLPKLKETGLNGQLLK

Table A.1 continued

Protein[b]	Sequence
gi13432137	TGKAYVVQLGALKNADKVNEIVGKLRGAGYRPSTPVQGKITRILVGPDASKDKLKGSLGELKQSGLSGVVMG
gi81629121	TPTAWIIQVASFVNPDYAKHLLQQLRAKGFDQESHEGKVITRVFIGPEINRDKINKIQKELKQMRLNGVIKK
gi81411858	EGVLWRIQLGSFKREENALRLVIKLRKIGFEPAYEKTETTTRVVLGIRPHELEKVKRVLELN--SFNDYVLR
gi81597218	YKYTYIYQIASFRNMDETSWYVKKMKEDGLNPQFERVGNWIRMYIGPYDSKRAMAPDIIKLQRIGLNGGFPR
gi81342904	PNIEYYIQFVSLSDPINADNYIQKLLKYNIISATVDNKDIYRVRSGPYKTKSEAKADFKKIAGGEFKETYIL
gi81344753	PSVLFWVQAASLSSKLNAERARGVLAARHMKTKRTGAGLRHRVRVGPFTNRTEAVYWMKSIREAEFSGCYVF
gi81355188	TSERYWVQVASGENKANLLAVWQKLLTKYPLPWTSPWHKSHRLLAGPFSSDEQAQDFVNKLKKHGFSTIQFT
gi81393723	GDKNWMVQVALAANQANADAVVSKLRAKGYKVTTSQTSKGIRIMVGPSKDRDAADAARKKIVSNMKSAWVID
gi81390281	SHTSYKVQLGSVKSEAEAMEEGAKIKKKFPKVKYDDGKFYYLILAGEYSSLNQAQAVCKKLAH-NQQSCVLK
gi75348349	AGKKAAIQAG-YAEKERALSLQRKMKAAGIDEIMTDNGKVYRVKSSNYKNARDAERDLNKLRVHGIAGQVTN
gi75353334	SEIPYIMQCGAYKNRSQAEERKMNIAFQGITVRHAEGSSWYKVVLGPYKFKRDAEKDRHKLQRAKIEPCAIW
gi81567198	SGKAFYIDIRRFAYKSDALRLVRSLEKTGLARLEGTSNKAWMVAVGPFRNFHDAAGVRSTLQRKQPQSEIIL
gi75496921	GAGGYFIQIASQPSAELAQKSYANMAQKYASADIQGKGTYYRVRVQA-GSKEDALALCSRLKSAGGSCFVTQ
gi81647808	NSENYYVQLASQPTHALAKDSLKNMKSKFGFAVIPGKGTYYRVRVQA-QNRNEAINLCENIKNSGGSCFITR
gi81562422	TSGGYVVQVSSQRNEADAKASYRSLQSKFPSVDLGSKGTYYRAMVGPFSSAEQAQQVCGNLKSAGGQCVVQR
gi81766671	GQEYVMIQCGFYSNKENANNVKAQLEDDYI-AVSLSEAENYRVIV-HIGNEEEATKLSNELN--EKGVSNTK
gi81343853	KEAYYCIQVLSSRDLSSAERAYRKLADYPH-ARIEKIGDYYTVRVGLWENKSKAKEYLSQVKSVYPGAFLRT
gi81343922	SENYYCVQVASSEKLEDLIPLFEKFKNMDN-VRIEKIGGFYTLRIGFYLNKSDVLKILPEIKE-KYRDAFVR
gi81342990	KETDFYIQVGSYRKKDYADRAYRILKKAGLFVVVNSHGPFYTVFI---TNADDVQKNIELIKSAGYKDTLIR
gi81758777	KEDFFWIQCGILNPLADAKPLYKQITTD---VWMKPENKTYRCLIGPYQSFAQASKDLKQVKKGDYREAFIR
gi81354011	LASGIYVQIFSVSNLDQKSKELASVKQKGYDKTTVGGKEITKVLIGPFEKADIAAELAKIRKDIAKDAFSFT
gi81833698	LPKGLYVQVGSFSKFSPTSAFAQKIEQNRFAREVVNGNEIVRVLIGPYASRAEANNALRDAREIEPKAFIKQ
gi81665371	AEKGFYVQVGSFANKPSAD-FLKKISNYSYRAGTSNGQPTTKYLIGPYHSRTDAGRDLPKFTTSDPVHFEVK
gi81341229	IPKGYYLQIGSLN--APSKDFLQTLKTFP--YQIKKKDSLTHYFIGPYKTKEEALKQLEAIKSFKNKPVLVE
gi81641880	ERENFSVQIAALANKEKALALEKRFSRGGHRKARRDGKTLYLVQIFAGYSRVKAKGFKKLLAAGYPDAAVVT
gi81790748	QKGRYTVIVATFNTRKVVRQEIARLSEMGHRPVTSGGSRYYRLVIGDFETRKAALDSMKSMPKGLSSHSYIQ
gi81758140	NHPKYLIQVLSSKSAERARTLGQDLGQSLNVSFLESTDDTHRLMLGPFTDFTLTQQILDQVKLGHESAFIRK
gi81363041	SQSNYHIQLVASSDINRLSQLKRNLPPKFQEATTEKTDGLHKLMLGPVSEQKSY-DLLEQIRSGYPQAFRVK
gi81462932	SSGNHYIQLVASKDKQRLHKMAKDLEKKYQVTRVQPANNMFRLQLGPIGQAELADRLLIKVKQGYPAGYIVS
gi75354386	DPNQYHIQMVAVKNEQSADKIAKKLEAQNAPTNIIKSGNVYRVRLGPFIDRDRADKTLIEAKNQYTSAFIIQ

Table A.1 continued

Protein[b]	Sequence
gi81357239	APSAWWVRIPPEGGRDGADRKVTELRALGIRIVHEAGPNQFAVSLGLFKTEAKAQQHLAFLRTRVRGAGVTP
gi75437008	GVSTFRVMLPNVGDRAAAQALVKRIAAAGMGYYVIAQGEDNTVALGQYQSRERAERRQASLVGAGFPAQLVP
gi81656987	GSGRFWVYYPPLATQSETKTLSAELKDKGFDYIVSNDEFKGNLSLGLFGKEDAAKTLVARLKAAGYDKAVVK
gi81605959	AADFWTVNLGFYATQAAAQADAANLAAAGFATDLQGKVLGYWLSAGRYATQAEATAAAARIA--QATQNRYK
gi81382902	GLKDYSVVCGSFGLKANAEGLKDFLDKEGYNIAFNAETAMYRVIVNTFADRASAAQARDAFKADFQGAWLLY
gi81551536	LRSDYRVMLGTFGSEAALRSATAGVSALGYTVYAIDLGNQFVAQVGPFADEASGQQAAADIR----RAYARA
gi81441174	APQGWDVEVVQGANMGALSDMTARLIEKGIPSSVEYRDGKPVVLLGPFPTREEAQARRDEVMALGTDSVVIQ
gi81539995	ASESACLYLGGGGEEADARRLRQRLLGLDIEEARGEMSVDYWVYLPPLASREAALRQLKELQARNIDSYLIG
gi81349500	PVGTRLAQLGAYDSPEIARAEWDRLNGRGEYEASSGGRTFYRLRAAGFGDLAEARHFCSVLVAERADCIPVT
gi81351655	SGGTHEVQLGALDSEAAARKEWDSLRHQAPAKTTRGDHTFVRLRIGGFADLKSARAYCVKLH--AQSVACTP
gi81355186	PAGAGVIQLGAFGSEAKANEVWSHLTQRYSWSVKIGEKTFYRLRA---TAGSQANSFCSQLQAAGETCAHIG
gi81562577	PRTDFGVDLGAANTVEGLRGLWRKLSKTQKAIKENGNATQLRLIAGPIADAAAAAKVCAALGSDRACEASVY
gi81562206	AHSGWIIQVGALESEPEARKRLEAAREQASGVTTKGDRKLYRARFAGLERDEAE-AVCRKLKRSDISCFTIK
gi75496724	AASGWAIQIGSLPSEGQARDMLAKASATGRTTFNKGSATFYRARFVGFTSKQAAWDACASLKRNNFGCYAVA
gi75382542	ERSRWEVQIAATDSEAAARSLLANARSNGSYAVQSGSATLYRARFTGFEDQSSAVSACKELKAQSYACVVMT
gi75496791	GRSNWRIQLAATPSRAGASELQEKYAPVSRISPSPKGRKVYRVRFSGVRDSAAASKACAQLKRQQIACLAIQ
gi81351865	ATGNWAIQVGAFANAKQASIATSAAHSKGGVSVKGGRSHLYRARLTGLTHENAV-AACRRLSH-GSPCVVVP
gi81352309	SYGPWAVQVGAFGSIGQAKFAATMARQAAFTPTPSHGTTVWRARLTGISRVGAA-QACSTLSGQGMACMAVP
gi81535105	PKGEWGVQVGAFRSKSLANEQLKLVRGRITKGAVEGAGGMFRAQFG--MTNEAAREACSALKAKRMPCIVLK
gi81535201	STGPASVQIGALSSPALADKAWAEAVRLAPGTVDKNGTTLYRTSVTGFATREAAKAFCEAIAA-SGKSCFVK
gi81382477	KTFPYHIIIASVANTKDAEAMAGELKAKGYTAKVLTGDGKIRVSIMSCADREDANRQLLKLREAYKNAWMLA
gi81398185	DPARFTIQILAISQERDVRDYISEIKGQDPIWKRSRGQNWYAVIYGDFATKDEAKRVIDGLSFRQQGPFVRS
gi81725471	NPNHYTMQVLALKKEKDVKEYIRYIDPKHPVWKNSRGTRWYTVTAGDFKSKQEAYNALSSLPSKQSSPFVLT
gi75352799	NRYGYTLQILALSRKTDLSTYAAKLSGEQPVRKTVNNMPWYTILYGDYATPAEARAAIKQLPAQAYGPFVRS
gi81362388	NAGSYTLQISIISDPQLLRDFRNDYGITGNTQVYQRADQRYVVIFGSYPSIEQARAAATQLPAQQMEPWAKS
gi81615650	NSRHYALQLAALQSLSTAKKFVAEHKIQNIAETRRKGEAWFIVITGDYKDIVTARRAELLLPDQAVQPWVKS
gi75353327	SSKRYILQLAALTNEEAVQEFLDDHKIEGSAQALRNGSIWYIVSYGDYESISSARGAVKTLPAQSLGPWAKS
gi81629684	VHAHYTIQLFASRTLAEATAFKNKHRLHD--LRIIHQNGWYKVLSGHYSTRQAATIALHRLPSQKLKPWVVR
gi81629362	SKASYTVQLMASVDLKAIKDFVKRHHLEGQTHASYRGHQWYVLLYGAYKSQGEAKAAIQQLPQQKLRPWVKS
gi81368963	NSKLFTIQLAASHKVEDINRFKNQNKWLAQAHFTNAKGSWYILTIGEYESRNQALLNIKKLPGAKLSPWIRS

Table A.1 continued

Protein[b]	Sequence
gi81741585	PYNHYIIQINSSSNLEEIKKYADKKQINPYWKTSKNGKPWYELIIGTFSSFKEAKKAIEKFPKKNNKPWIRQ
gi81417634	LIQGYRIQVYNGNSKREANRRAAQITQLHPECYLTYRAPFWRLLVGDFSSREEAEEAKQQLKK-SFPSYARE
gi81381264	KSSGYRVQAYAGNNTRQAKNEAHQVGTRVKEVYTSFNPPRWLCRVGDFRSIEEADAMMRKLKATGVFKEVSI
gi81464055	PMQGFTIQLASVAQLKSLRSTLAQIEGVQD-ISIAKYKRRWVILVGHYESSKLAHEAAAQLAKRIDSPWVRK
gi75355493	ENKDIFIDLKSFGTEHEAQAYLNQAAQNFAALSVEKRRYEYVVKMGPFASQERAAEAEAQAR-----GMVRA
gi81820091	ADEVVWVQIEQPNAQERAQTYAADLSDV---AGFSLGGGWYGIVLGPYLREDAEQVLRVRAERRIPGDSFIA
gi20139707	YTTVYKIRILNLDSKKQAEKLISKLGREDIRADITVNQDKFDIYFGPFSDKSQVNDVKAQLRKNYSKPLIVY
gi2495670	GTEFYCLKMLELTSRSQANKLITQLALANIQTEVNRSGNKYEIYIGPFDDKTKMAQVRTKLQKANNKPLIVY
gi729969	GQAYYTFTTAAISGEANAKTLLQQLKQSTGIINQKTTVESYNVQSAYFKGLSTVKDAISQIKKTGVSGSYQQ

[a] Multiple sequence alignment of 132 SPOR domains found in the Pfam Database (Finn et al., 2008). Alignment was produced using ClustalW (Larkin et al., 2007).

[b] Protein names for DamX, FtsN and CwlC are given for reference. For the other proteins, the Pfam accession number is listed.

Figure A.1. Conservation mapping of the SPOR domain from DamX. Ribbon diagram cartoons of $DamX^{SPOR}$ from side on (A) and bottom up (B) views, with residues colored coded based on sequence conservation. Colors move from grey (unconserved) to red (higher than 45% identity) Conservation was determined by using the ClustalW (Larkin et al., 2007) program and manually grouping residues into categories.

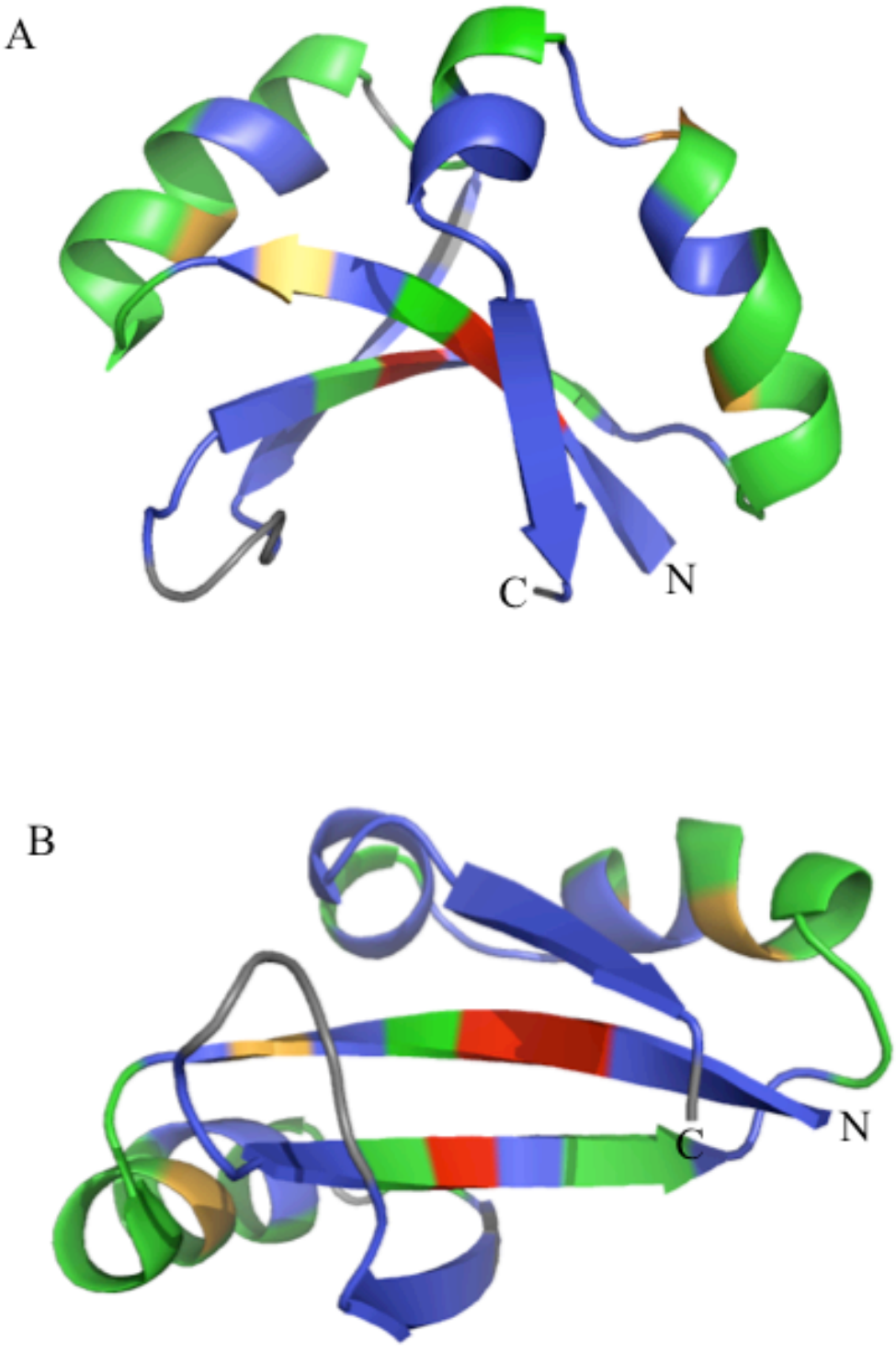
A
C
N
B
C
N

Figure A.2. Space filling models of the DamX SPOR domain. A. Projected surface structure of $DamX^{SPOR}$ looking at two alternate side on views. Residues are color coded by acid (red), base (blue), hydrophobic (yellow) as determined by Kyte-Doolittle hydropathy plot analysis (Kyte & Doolittle, 1982), and neutral (grey). B. Same as A, but with a top down and bottom up view of the protein domain. Bottom up view shows a swath of yellow hydrophobic resides across the putative PG binding cleft.

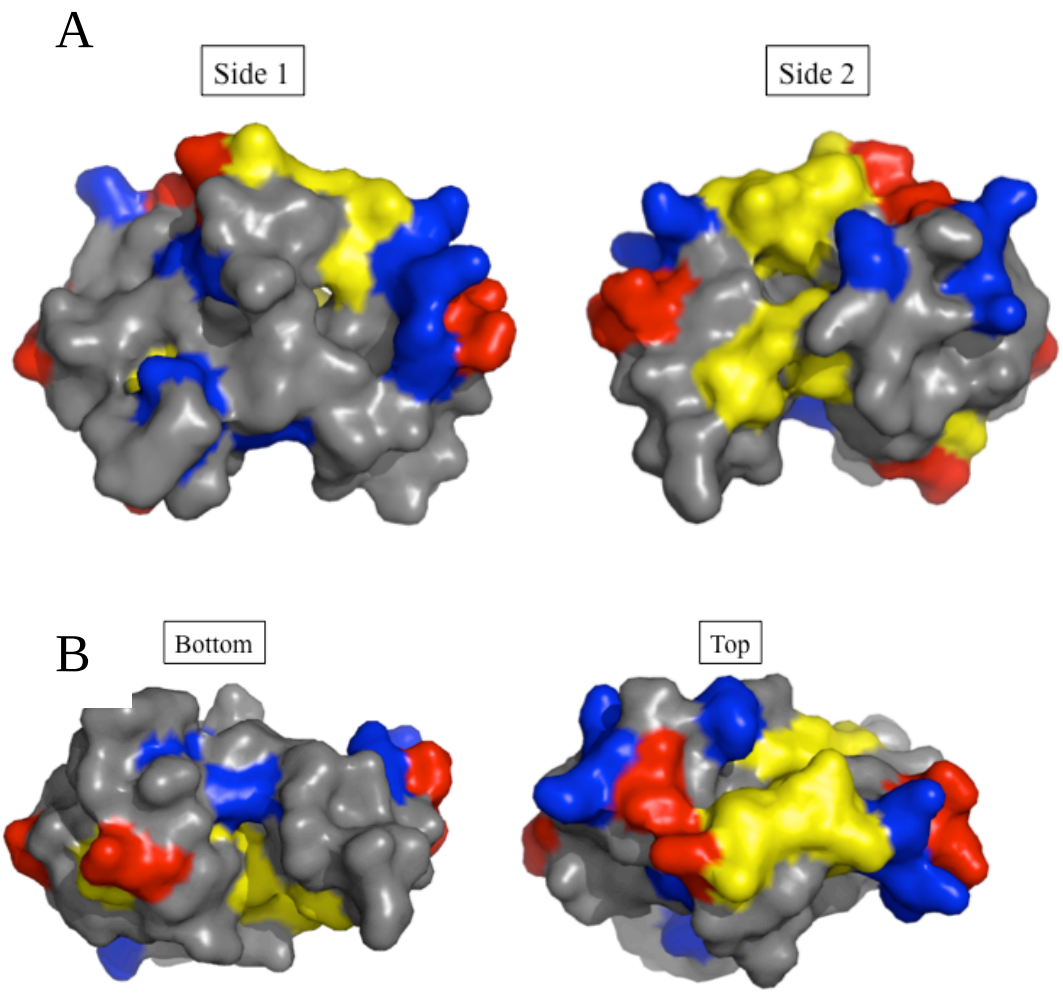
A
Side 1
Side 2
B
Bottom
Top

Figure A.3. Titration of $DamX^{SPOR}$ with PG fragments. Multiple, overlaid, ^{1}H-^{15}N HSQC spectrum of the SPOR domain from DamX in the presence of increasing amounts of PG fragments. Mutanolysin digested PG was obtained from David Popham and used in this study. This enzymatic digestion should yield free PG monomers with and without sidechains, as well as crosslinked PG monomers. Black contour shows the state of free protein. PG fragments were then used at 1x, 2x, and 4x, molar concentrations compared to the free protein (200 μM). Several residues show chemical shifts and some of these are indicated with arrows in the figure. D409 shows a very significant shift. It is located in the cleft, but its sidechain is buried in the structure and is not accessible. So, if it is playing a role in binding, this is mediated through its backbone atoms. All three of the tryptophan residues in the domains show some peak perturbations, although most are minor. Two of these peaks are highlighted in the spectrum. Please note these peaks correspond to the amino acid's side chain and not backbone nitrogen. Two of the tryptophan residues, W385 and W416, are located in the ß-sheet with their side chains extending into the cleft. Overlays created with tools available in NMRpipe (Delaglio et al., 1995).

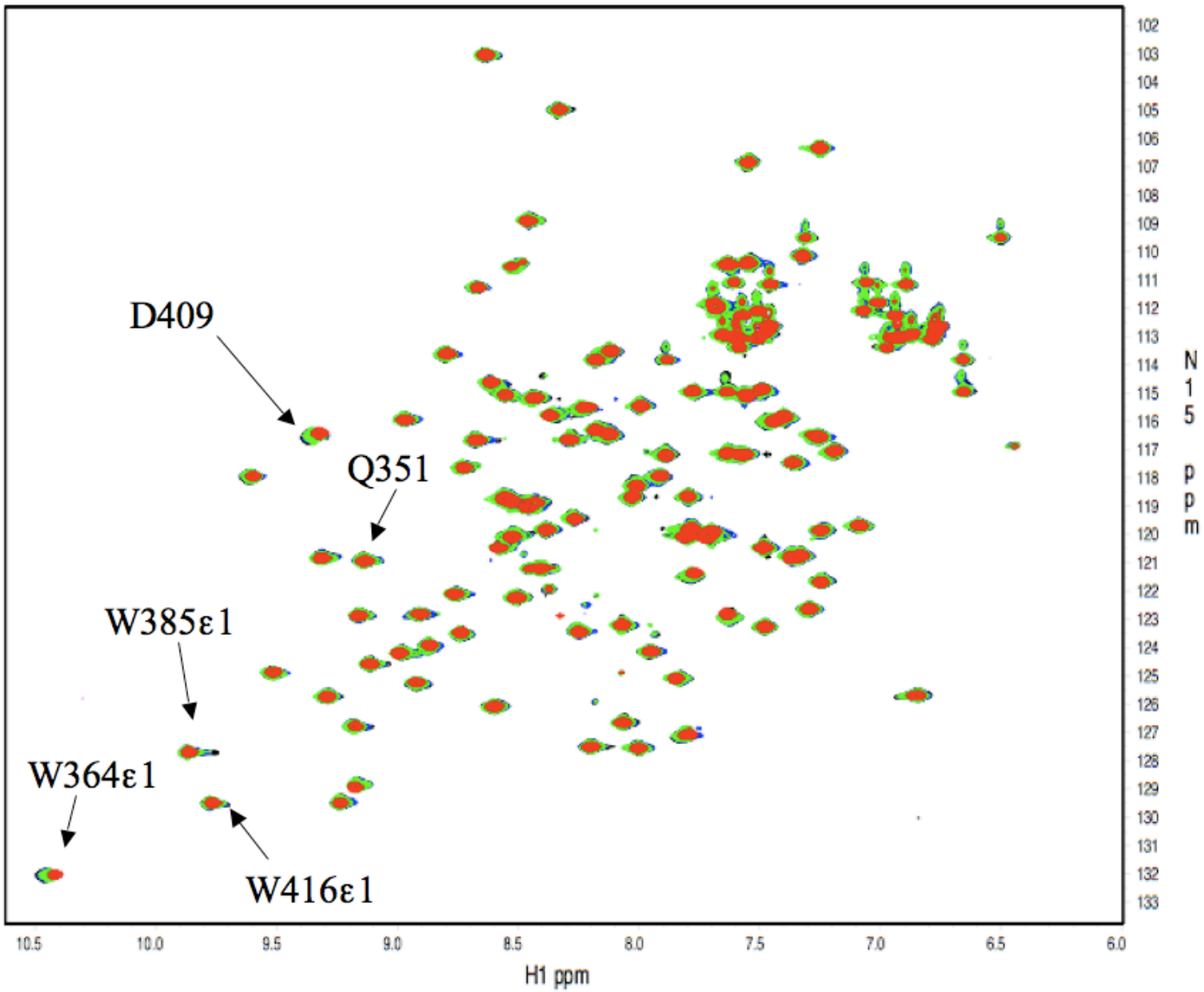
D409
Q351
W385ε1
W364ε1
W416ε1
10.5
10.0
9.5
9.0
8.5
8.0
7.5
7.0
6.5
6.0
H1 ppm
102
103
104
105
106
107
108
109
110
111
112
113
114
115
116
117
118
119
120
121
122
123
124
125
126
127
128
129
130
131
132
133
N15 ppm

APPENDIX B: TWO-HYBRID ANALYSIS OF SPOR DOMAIN PROTEINS

A number of bacterial two-hybrid assay systems have been created for studying potential protein-protein interaction partners (Karimova et al., 2000; Di Lallo et al., 2001; Strauch & Georgiou, 2007). Using the system based on the reconstitution of an adenylate cyclase pathway (bacterial adenylate cyclase two hybrid or BACTH system) a complex network of interactions has been observed for proteins involved with cell division in *E. coli* (Karimova et al., 2005). We wished to place the SPOR domain proteins, DamX, DedD, and RlpA, into this network. Doing so will bring us closer to an understanding of how the many division proteins work together to accomplish the complex process of septation. Also, identifying interaction partners can give us insight into the mechanism of how division proteins localize to the septal ring.

In order to place DamX and DedD into the cell division network, we used the BACTH system mentioned above. Full length *damX* and *dedD* were cloned into each of the test vectors used for this system (pUT18c and pKT25) and assayed for interactions against a set of cell division proteins, as described in Chapter 2 of this work.

We observed that DamX interacts strongly with itself, FtsQ, and FtsN (Figure B.1A). Weaker interactions were also detected with FtsZ, FtsA, FtsI, and possibly FtsL. These results hint at some interesting possibilities. For instance, in a recent publication, our laboratory has shown that DamX is a negative regulator of FtsQ function (Arends et al., 2010). The two-hybrid interaction suggests that DamX might be sequestering FtsQ. It is also intriguing that DamX interacted with FtsA and FtsZ. These proteins are cytoplasmic and are the earliest proteins to arrive at the division site. Indirect support for a DamX – FtsA and/or DamX – FtsZ interaction comes from localization studies showing that DamX is also an early recruit to the septum (Arends et al., 2010). An interaction of DamX with FtsZ would provide a direct link from the FtsZ Ring in the cytoplasm to the PG cell wall in the periplasm. This could be a method of transferring cytokinetic force

from the Z ring to the cell wall. If DamX were interacting with FtsA or FtsZ, it would be through its large cytoplasmic domain. An interesting follow up experiment would be to clone just the cytoplasmic domain of DamX into the two-hybrid vectors and test for interactions with FtsZ and FtsA. Also immunoprecipitation experiments could be done to look for FtsA/Z complexed with DamX.

Two hybrid analysis can yield false positives. In this case there are particular concerns for DamX – FtsQ, DamX – FtsN, and DamX – DamX. In published two-hybrid studies, numerous Fts proteins (~8) have been shown to interact with FtsQ (Karimova et al., 2005; Karimova et al., 2009), despite FtsQ being relatively small (276 a.a.). FtsN also has a SPOR domain. If these domains recognize the same site on PG, perhaps binding to that site would bring FtsN and DamX together in the absence of a direct protein - protein interaction. This is also a consideration with DamX's interaction with itself. It should be noted the interaction of DamX with FtsZ could only be tested in one plasmid configuration. This is because *ftsZ* is tolerated only in the low copy pKT25 plasmid.

A similar study was done with the full length DedD protein as well. For DedD the only observed interaction was with FtsQ (Figure B.1B). The same caveats, as discussed above, apply for the potential FtsQ – DedD interaction. Also, we did not see an interaction with DamX or FtsN. This is interesting since we believe the SPOR domains are recognizing the same site on PG. However, DedD is recruited to the septum at a later point than DamX (Arends et al., 2010), so perhaps they are not occupying the same site on PG, at least not the same time. This would also seem to argue that the DamX - FtsN interaction was direct and not simply driven by their binding to a similar PG site.

The third SPOR domain protein in *E. coli* that our lab has studied is RlpA. We would have liked to test it for interactions with other cell division proteins. However, that could not easily be accomplished with the system we are using, since RlpA is an

outer membrane lipoprotein. Attempts were made to link RlpA to an artificial inner membrane anchor. But, these constructs showed no interactions when assayed.

Figure B.1. Two-hybrid analysis of SPOR domain proteins. A. Findings from the bacterial two-hybrid assay of DamX interactions with itself and other division proteins. Transformants of DHM1 harboring derivatives of pUT18c and pKT25 were grown in LB medium containing ampicillin and kanamycin plus 0.5 mM IPTG to an OD_{600} of 0.6 to 0.8 and assayed for ß-galactosidase activity. Bars represent the means and standard deviations of results from at least three independent experiments. Black bars indicate results for the empty vector control harboring pUT18c and pKT25 (-/-), the positive control harboring pKT25-*zip* and pUT18-*zip* (zip/zip), and the homodimerization sample with pKT25-*damX* and pUT18c-*damX* (damX). Results for other samples are shown as pairs of gray and white bars reflecting the two potential genetic configurations, pKT25-*damX*/pUT18c-*fts* (gray) and pKT25-*fts*/pUT18c-*damX* (white). (-), empty vector control; nd, not determined (because the high-copy-number *ftsZ* plasmid is not stably maintained). B. Same as above, but using DedD instead. DedD only shows a positive interaction with FtsQ.

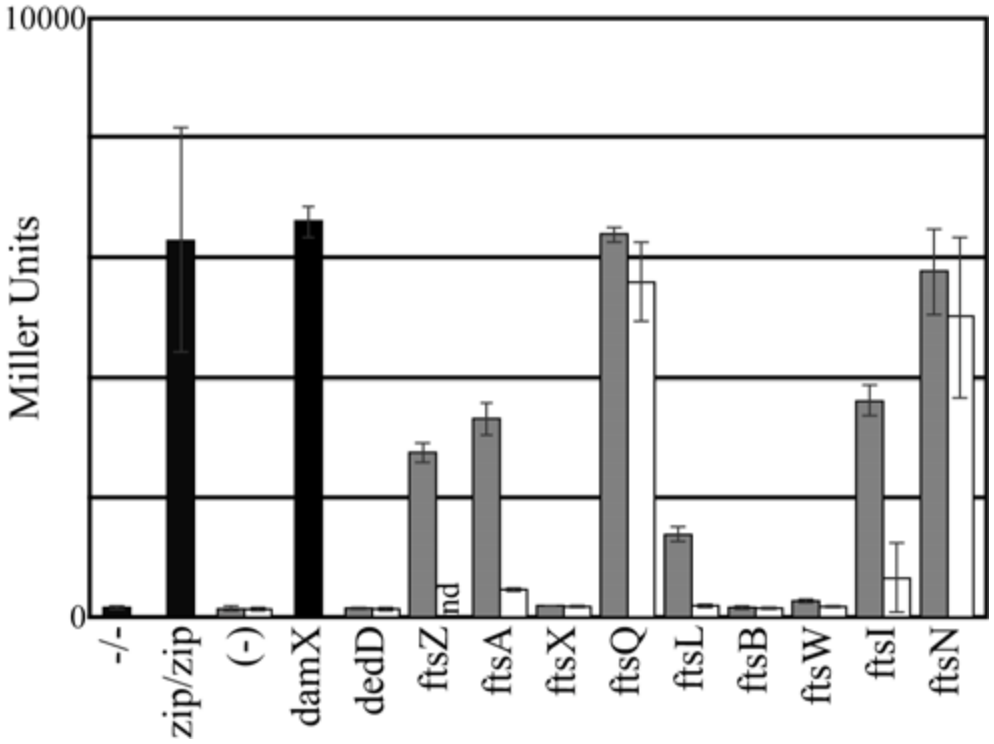
10000
Miller Units
0
-/-
zip/zip
(-)
damX
dedD
ftsZ
nd
ftsA
ftsX
ftsQ
ftsL
ftsB
ftsW
ftsI
ftsN

A

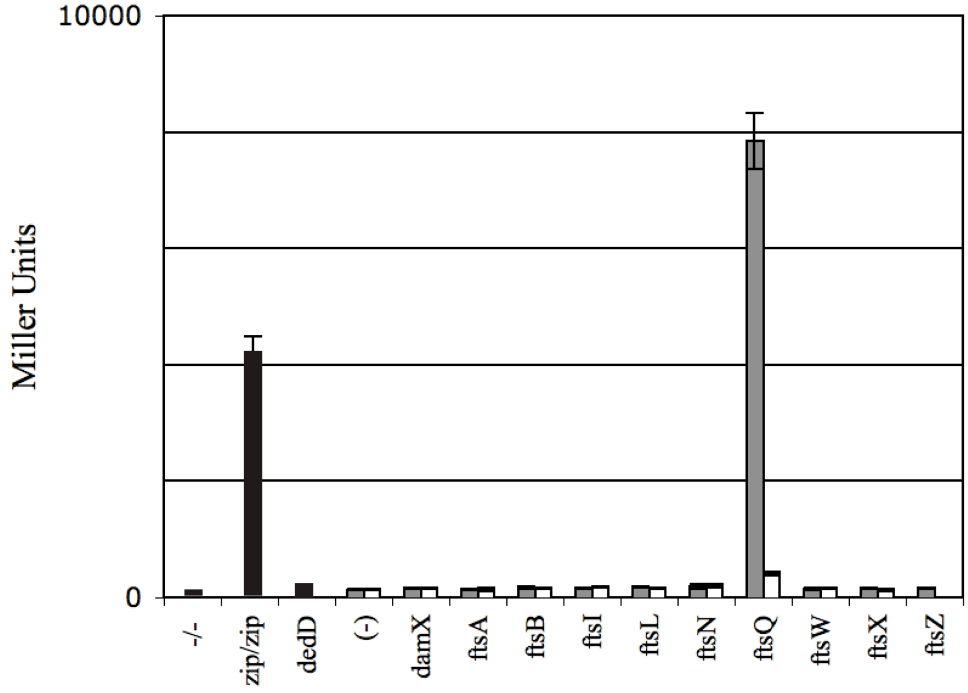
10000
Miller Units
0
-/-
zip/zip
dedD
(-)
damX
ftsA
ftsB
ftsI
ftsL
ftsN
ftsQ
ftsW
ftsX
ftsZ

B

REFERENCES

Aarsman, M. E., A. Piette, C. Fraipont, T. M. Vinkenvleugel, M. Nguyen-Disteche & T. den Blaauwen, (2005) Maturation of the *Escherichia coli* divisome occurs in two steps. *Mol Microbiol* **55**: 1631-1645.

Adam, M., C. Fraipont, N. Rhazi, M. Nguyen-Disteche, B. Lakaye, J. M. Frere, B. Devreese, J. Van Beeumen, Y. van Heijenoort, J. van Heijenoort & J. M. Ghuysen, (1997) The bimodular G57-V577 polypeptide chain of the class B penicillin-binding protein 3 of *Escherichia coli* catalyzes peptide bond formation from thiolesters and does not catalyze glycan chain polymerization from the lipid II intermediate. *J Bacteriol* **179**: 6005-6009.

Addinall, S. G., C. Cao & J. Lutkenhaus, (1997) FtsN, a late recruit to the septum in *Escherichia coli*. *Mol Microbiol* **25**: 303-309.

Allain, F. H., P. W. Howe, D. Neuhaus & G. Varani, (1997) Structural basis of the RNA-binding specificity of human U1A protein. *EMBO J* **16**: 5764-5772.

Arends, S. J., R. J. Kustusch & D. S. Weiss, (2009) ATP-binding site lesions in FtsE impair cell division. *J Bacteriol* **191**: 3772-3784.

Arends, S. J., K. Williams, R. J. Scott, S. Rolong, D. L. Popham & D. S. Weiss, (2010) Discovery and characterization of three new *Escherichia coli* septal ring proteins that contain a SPOR domain: DamX, DedD, and RlpA. *J Bacteriol* **192**: 242-255.

Arends, S. J., Williams, K., Ryan J. Kustusch, David S. Weiss, (2007) Cell Division. In: The periplasm. M. Ehrmann (ed). Washington, D.C.: ASM Press, pp. 173-197.

Atrih, A., G. Bacher, G. Allmaier, M. P. Williamson & S. J. Foster, (1999) Analysis of peptidoglycan structure from vegetative cells of *Bacillus subtilis* 168 and role of PBP 5 in peptidoglycan maturation. *J Bacteriol* **181**: 3956-3966.

Avis, J. M., F. H. Allain, P. W. Howe, G. Varani, K. Nagai & D. Neuhaus, (1996) Solution structure of the N-terminal RNP domain of U1A protein: the role of C-terminal residues in structure stability and RNA binding. *J Mol Biol* **257**: 398-411.

Bernhardt, T. G. & P. A. de Boer, (2003) The *Escherichia coli* amidase AmiC is a periplasmic septal ring component exported via the twin-arginine transport pathway. *Mol Microbiol* **48**: 1171-1182.

Birney, E., S. Kumar & A. R. Krainer, (1993) Analysis of the RNA-recognition motif and RS and RGG domains: conservation in metazoan pre-mRNA splicing factors. *Nucleic Acids Res* **21**: 5803-5816.

Blattner, F. R., G. Plunkett, 3rd, C. A. Bloch, N. T. Perna, V. Burland, M. Riley, J. Collado-Vides, J. D. Glasner, C. K. Rode, G. F. Mayhew, J. Gregor, N. W. Davis, H. A. Kirkpatrick, M. A. Goeden, D. J. Rose, B. Mau & Y. Shao, (1997) The complete genome sequence of Escherichia coli K-12. *Science* **277**: 1453-1462.

Bowler, L. D. & B. G. Spratt, (1989) Membrane topology of penicillin-binding protein 3 of *Escherichia coli*. *Mol Microbiol* **3**: 1277-1286.

Boyd, D., C. Manoil & J. Beckwith, (1987) Determinants of membrane protein topology. *Proc Natl Acad Sci U S A* **84**: 8525-8529.

Boyle, D. S., M. M. Khattar, S. G. Addinall, J. Lutkenhaus & W. D. Donachie, (1997) *ftsW* is an essential cell-division gene in *Escherichia coli*. *Mol Microbiol* **24**: 1263-1273.

Buddelmeijer, N. & J. Beckwith, (2002) Assembly of cell division proteins at the *E. coli* cell center. *Curr Opin Microbiol* **5**: 553-557.

Chen, J. C. & J. Beckwith, (2001) FtsQ, FtsL and FtsI require FtsK, but not FtsN, for co-localization with FtsZ during *Escherichia coli* cell division. *Mol Microbiol* **42**: 395-413.

D'Ulisse, V., M. Fagioli, P. Ghelardini & L. Paolozzi, (2007) Three functional subdomains of the *Escherichia coli* FtsQ protein are involved in its interaction with the other division proteins. *Microbiology* **153**: 124-138.

Dai, K., Y. Xu & J. Lutkenhaus, (1993) Cloning and characterization of *ftsN*, an essential cell division gene in *Escherichia coli* isolated as a multicopy suppressor of *ftsA*12(Ts). *J Bacteriol* **175**: 3790-3797.

Dai, K., Y. Xu & J. Lutkenhaus, (1996) Topological characterization of the essential *Escherichia coli* cell division protein FtsN. *J Bacteriol* **178**: 1328-1334.

Datta, P., A. Dasgupta, A. K. Singh, P. Mukherjee, M. Kundu & J. Basu, (2006) Interaction between FtsW and penicillin-binding protein 3 (PBP3) directs PBP3 to mid-cell, controls cell septation and mediates the formation of a trimeric complex involving FtsZ, FtsW and PBP3 in mycobacteria. *Mol Microbiol* **62**: 1655-1673.

de Pedro, M. A., J. C. Quintela, J. V. Holtje & H. Schwarz, (1997) Murein segregation in *Escherichia coli*. *J Bacteriol* **179**: 2823-2834.

Deckert, G., P. V. Warren, T. Gaasterland, W. G. Young, A. L. Lenox, D. E. Graham, R. Overbeek, M. A. Snead, M. Keller, M. Aujay, R. Huber, R. A. Feldman, J. M. Short, G. J. Olsen & R. V. Swanson, (1998) The complete genome of the hyperthermophilic bacterium *Aquifex aeolicus*. *Nature* **392**: 353-358.

Delaglio, F., S. Grzesiek, G. W. Vuister, G. Zhu, J. Pfeifer & A. Bax, (1995) NMRPipe: a multidimensional spectral processing system based on UNIX pipes. *J Biomol NMR* **6**: 277-293.

DeLano, W. L., (2002) The PyMOL Molecular Graphics System. In. Palo Alto: DeLano Scientific, pp.

Den Blaauwen, T., M. E. Aarsman, N. O. Vischer & N. Nanninga, (2003) Penicillin-binding protein PBP2 of *Escherichia coli* localizes preferentially in the lateral wall and at mid-cell in comparison with the old cell pole. *Mol Microbiol* **47**: 539-547.

Den Blaauwen, T., N. Buddelmeijer, M. E. Aarsman, C. M. Hameete & N. Nanninga, (1999) Timing of FtsZ assembly in *Escherichia coli*. *J Bacteriol* **181**: 5167-5175.

Derouaux, A., B. Wolf, C. Fraipont, E. Breukink, M. Nguyen-Disteche & M. Terrak, (2008) The monofunctional glycosyltransferase of *Escherichia coli* localizes to the cell division site and interacts with penicillin-binding protein 3, FtsW, and FtsN. *J Bacteriol* **190**: 1831-1834.

Di Berardino, M., A. Dijkstra, D. Stuber, W. Keck & M. Gubler, (1996) The monofunctional glycosyltransferase of *Escherichia coli* is a member of a new class of peptidoglycan-synthesising enzymes. *FEBS Lett* **392**: 184-188.

Di Lallo, G., L. Castagnoli, P. Ghelardini & L. Paolozzi, (2001) A two-hybrid system based on chimeric operator recognition for studying protein homo/heterodimerization in *Escherichia coli*. *Microbiology* **147**: 1651-1656.

Di Lallo, G., M. Fagioli, D. Barionovi, P. Ghelardini & L. Paolozzi, (2003) Use of a two-hybrid assay to study the assembly of a complex multicomponent protein machinery: bacterial septosome differentiation. *Microbiology* **149**: 3353-3359.

Draper, G. C., N. McLennan, K. Begg, M. Masters & W. D. Donachie, (1998) Only the N-terminal domain of FtsK functions in cell division. *J Bacteriol* **180**: 4621-4627.

Ehlert, K. & J. V. Holtje, (1996) Role of precursor translocation in coordination of murein and phospholipid synthesis in *Escherichia coli*. *J Bacteriol* **178**: 6766-6771.

Fay, A. & J. Dworkin, (2009) *Bacillus subtilis* homologs of MviN (MurJ), the putative *Escherichia coli* lipid II flippase, are not essential for growth. *J Bacteriol* **191**: 6020-6028.

Finn, R. D., J. Tate, J. Mistry, P. C. Coggill, S. J. Sammut, H. R. Hotz, G. Ceric, K. Forslund, S. R. Eddy, E. L. Sonnhammer & A. Bateman, (2008) The Pfam protein families database. *Nucleic Acids Res* **36**: D281-288.

Gamba, P., J. W. Veening, N. J. Saunders, L. W. Hamoen & R. A. Daniel, (2009) Two-step assembly dynamics of the *Bacillus subtilis* divisome. *J Bacteriol* **191**: 4186-4194.

Geissler, B. & W. Margolin, (2005) Evidence for functional overlap among multiple bacterial cell division proteins: compensating for the loss of FtsK. *Mol Microbiol* **58**: 596-612.

Gerard, P., T. Vernet & A. Zapun, (2002) Membrane topology of the Streptococcus pneumoniae FtsW division protein. *J Bacteriol* **184**: 1925-1931.

Gerding, M. A., B. Liu, F. O. Bendezu, C. A. Hale, T. G. Bernhardt & P. A. de Boer, (2009) Self-enhanced accumulation of FtsN at Division Sites and Roles for Other Proteins with a SPOR domain (DamX, DedD, and RlpA) in *Escherichia coli* cell constriction. *J Bacteriol* **191**: 7383-7401.

Ghigo, J. M., D. S. Weiss, J. C. Chen, J. C. Yarrow & J. Beckwith, (1999) Localization of FtsL to the *Escherichia coli* septal ring. *Mol Microbiol* **31**: 725-737.

Glauner, B., (1988) Separation and quantification of muropeptides with high-performance liquid chromatography. *Anal Biochem* **172**: 451-464.

Glauner, B., J. V. Holtje & U. Schwarz, (1988) The composition of the murein of *Escherichia coli*. *J Biol Chem* **263**: 10088-10095.

Goehring, N. W. & J. Beckwith, (2005) Diverse paths to midcell: assembly of the bacterial cell division machinery. *Curr Biol* **15**: R514-526.

Goehring, N. W., M. D. Gonzalez & J. Beckwith, (2006) Premature targeting of cell division proteins to midcell reveals hierarchies of protein interactions involved in divisome assembly. *Mol Microbiol* **61**: 33-45.

Goehring, N. W., C. Robichon & J. Beckwith, (2007) Role for the nonessential N terminus of FtsN in divisome assembly. *J Bacteriol* **189**: 646-649.

Goffin, C., C. Fraipont, J. Ayala, M. Terrak, M. Nguyen-Disteche & J. M. Ghuysen, (1996) The non-penicillin-binding module of the tripartite penicillin-binding protein 3 of *Escherichia coli* is required for folding and/or stability of the penicillin-binding module and the membrane-anchoring module confers cell septation activity on the folded structure. *J Bacteriol* **178**: 5402-5409.

Goffin, C. & J. M. Ghuysen, (1998) Multimodular penicillin-binding proteins: an enigmatic family of orthologs and paralogs. *Microbiol Mol Biol Rev* **62**: 1079-1093.

Gonzalez, M. D., E. A. Akbay, D. Boyd & J. Beckwith, (2010) Multiple Interaction Domains in FtsL, a Protein Component of the Widely Conserved Bacterial FtsLBQ Cell Division Complex. *J Bacteriol*.

González-Castro, M. J., J. López-Hernández, J. Simal-Lozano, and M. J. Oruña-Concha, (1997) Determination of amino acids in green beans by derivitization with phenylisothiocyanate and high-performance liquid chromatography with ultraviolet detection. *J. Chromatogr. Sci.*: 181-185.

Goodell, E. W., (1985) Recycling of murein by *Escherichia coli*. *J Bacteriol* **163**: 305-310.

Graumann, P. L., (2007) Cytoskeletal elements in bacteria. *Annu Rev Microbiol* **61**: 589-618.

Haldimann, A. & B. L. Wanner, (2001) Conditional-replication, integration, excision, and retrieval plasmid-host systems for gene structure-function studies of bacteria. *J Bacteriol* **183**: 6384-6393.

Hale, C. A. & P. A. de Boer, (1999) Recruitment of ZipA to the septal ring of *Escherichia coli* is dependent on FtsZ and independent of FtsA. *J Bacteriol* **181**: 167-176.

Halford SE, M. J., (2004) How do site-specific DNA-binding proteins find their targets? *Nucleic Acids Res.* **32**: 12.

Hantke, K. & V. Braun, (1973) [The structure of covalent binding of lipid to protein in the murein-lipoprotein of the outer membrane of *Escherichia coli* (author's transl)]. *Hoppe Seylers Z Physiol Chem* **354**: 813-815.

Heidrich, C., M. F. Templin, A. Ursinus, M. Merdanovic, J. Berger, H. Schwarz, M. A. de Pedro & J. V. Holtje, (2001) Involvement of N-acetylmuramyl-L-alanine amidases in cell separation and antibiotic-induced autolysis of *Escherichia coli*. *Mol Microbiol* **41**: 167-178.

Heidrich, C., A. Ursinus, J. Berger, H. Schwarz & J. V. Holtje, (2002) Effects of multiple deletions of murein hydrolases on viability, septum cleavage, and sensitivity to large toxic molecules in *Escherichia coli*. *J Bacteriol* **184**: 6093-6099.

Henriques, A. O., P. Glaser, P. J. Piggot & C. P. Moran, Jr., (1998) Control of cell shape and elongation by the *rodA* gene in *Bacillus subtilis*. *Mol Microbiol* **28**: 235-247.

Hirota, Y., A. Ryter & F. Jacob, (1968) Thermosensitive mutants of *E. coli* affected in the processes of DNA synthesis and cellular division. *Cold Spring Harb Symp Quant Biol* **33**: 677-693.

Holtje, J. V., (1998) Growth of the stress-bearing and shape-maintaining murein sacculus of *Escherichia coli*. *Microbiol Mol Biol Rev* **62**: 181-203.

Holtje, J. V., D. Mirelman, N. Sharon & U. Schwarz, (1975) Novel type of murein transglycosylase in Escherichia coli. *J Bacteriol* **124**: 1067-1076.

Hungerer, K. D. & D. J. Tipper, (1969) Cell wall polymers of *Bacillus sphaericus* 9602. I. Structure of the vegetative cell wall peptidoglycan. *Biochemistry* **8**: 3577-3587.

Ikeda, M., T. Sato, M. Wachi, H. K. Jung, F. Ishino, Y. Kobayashi & M. Matsuhashi, (1989) Structural similarity among *Escherichia coli* FtsW and RodA proteins and *Bacillus subtilis* SpoVE protein, which function in cell division, cell elongation, and spore formation, respectively. *J Bacteriol* **171**: 6375-6378.

Ishidate, K., A. Ursinus, J. V. Holtje & L. Rothfield, (1998) Analysis of the length distribution of murein glycan strands in *ftsZ* and *ftsI* mutants of *E. coli*. *FEMS Microbiol Lett* **168**: 71-75.

Ishino, F., W. Park, S. Tomioka, S. Tamaki, I. Takase, K. Kunugita, H. Matsuzawa, S. Asoh, T. Ohta, B. G. Spratt & et al., (1986) Peptidoglycan synthetic activities in membranes of *Escherichia coli* caused by overproduction of Penicillin-Binding Protein 2 and RodA protein. *J Biol Chem* **261**: 7024-7031.

Kadokura, H., H. Tian, T. Zander, J. C. Bardwell & J. Beckwith, (2004) Snapshots of DsbA in action: detection of proteins in the process of oxidative folding. *Science* **303**: 534-537.

Karimova, G., N. Dautin & D. Ladant, (2005) Interaction network among *Escherichia coli* membrane proteins involved in cell division as revealed by bacterial two-hybrid analysis. *J Bacteriol* **187**: 2233-2243.

Karimova, G., C. Robichon & D. Ladant, (2009) Characterization of YmgF, a 72-residue inner membrane protein that associates with the *Escherichia coli* cell division machinery. *J Bacteriol* **191**: 333-346.

Karimova, G., A. Ullmann & D. Ladant, (2000) A bacterial two-hybrid system that exploits a cAMP signaling cascade in *Escherichia coli*. *Methods Enzymol* **328**: 59-73.

Kraft, A. R., M. F. Templin & J. V. Holtje, (1998) Membrane-bound lytic endotransglycosylase in *Escherichia coli*. *J Bacteriol* **180**: 3441-3447.

Kuroda, A., Y. Asami & J. Sekiguchi, (1993) Molecular cloning of a sporulation-specific cell wall hydrolase gene of *Bacillus subtilis*. *J Bacteriol* **175**: 6260-6268.

Kyte, J. & R. F. Doolittle, (1982) A SIMPLE METHOD FOR DISPLAYING THE HYDROPATHIC CHARACTER OF A PROTEIN. *J. Mol. Biol.* **157**: 105-132.

Labischinski, H., E. W. Goodell, A. Goodell & M. L. Hochberg, (1991) Direct proof of a "more-than-single-layered" peptidoglycan architecture of *Escherichia coli* W7: a neutron small-angle scattering study. *J Bacteriol* **173**: 751-756.

Landau, M., I. Mayrose, Y. Rosenberg, F. Glaser, E. Martz, T. Pupko & N. Ben-Tal, (2005) ConSurf 2005: the projection of evolutionary conservation scores of residues on protein structures. *Nucleic Acids Res* **33**: W299-302.

Lara, B. & J. A. Ayala, (2002) Topological characterization of the essential *Escherichia coli* cell division protein FtsW. *FEMS Microbiol Lett* **216**: 23-32.

Lara, B., D. Mengin-Lecreulx, J. A. Ayala & J. van Heijenoort, (2005) Peptidoglycan precursor pools associated with MraY and FtsW deficiencies or antibiotic treatments. *FEMS Microbiol Lett* **250**: 195-200.

Larkin, M. A., G. Blackshields, N. P. Brown, R. Chenna, P. A. McGettigan, H. McWilliam, F. Valentin, I. M. Wallace, A. Wilm, R. Lopez, J. D. Thompson, T. J. Gibson & D. G. Higgins, (2007) Clustal W and Clustal X version 2.0. *Bioinformatics* **23**: 2947-2948.

Maggi, S., O. Massidda, G. Luzi, D. Fadda, L. Paolozzi & P. Ghelardini, (2008) Division protein interaction web: identification of a phylogenetically conserved common interactome between *Streptococcus pneumoniae* and *Escherichia coli*. *Microbiology* **154**: 3042-3052.

Margolin, W., (2000) Themes and variations in prokaryotic cell division. *FEMS Microbiol Rev* **24**: 531-548.

Marrec-Fairley, M., A. Piette, X. Gallet, R. Brasseur, H. Hara, C. Fraipont, J. M. Ghuysen & M. Nguyen-Disteche, (2000) Differential functionalities of amphiphilic peptide segments of the cell-septation penicillin-binding protein 3 of *Escherichia coli*. *Mol Microbiol* **37**: 1019-1031.

Meisel, U., J. V. Holtje & W. Vollmer, (2003) Overproduction of inactive variants of the murein synthase PBP1B causes lysis in *Escherichia coli*. *J Bacteriol* **185**: 5342-5348.

Mercer, K. L. & D. S. Weiss, (2002) The *Escherichia coli* cell division protein FtsW is required to recruit its cognate transpeptidase, FtsI (PBP3), to the division site. *J Bacteriol* **184**: 904-912.

Miller, J. H., (1972) *Experiments in molecular genetics,* p. xvi, 466 p. Cold Spring Harbor Laboratory, Cold Spring Harbor, N.Y.

Mishima, M., T. Shida, K. Yabuki, K. Kato, J. Sekiguchi & C. Kojima, (2005) Solution structure of the peptidoglycan binding domain of *Bacillus subtilis* cell wall lytic enzyme CwlC: characterization of the sporulation-related repeats by NMR. *Biochemistry* **44**: 10153-10163.

Moll, A. & M. Thanbichler, (2009) FtsN-like proteins are conserved components of the cell division machinery in proteobacteria. *Mol Microbiol* **72**: 1037-1053.

Monahan, L. G., A. Robinson & E. J. Harry, (2009) Lateral FtsZ association and the assembly of the cytokinetic Z ring in bacteria. *Mol Microbiol* **74**: 1004-1017.

Mosyak, L., Y. Zhang, E. Glasfeld, S. Haney, M. Stahl, J. Seehra & W. S. Somers, (2000) The bacterial cell-division protein ZipA and its interaction with an FtsZ fragment revealed by X-ray crystallography. *EMBO J* **19**: 3179-3191.

Muller, P., C. Ewers, U. Bertsche, M. Anstett, T. Kallis, E. Breukink, C. Fraipont, M. Terrak, M. Nguyen-Disteche & W. Vollmer, (2007) The essential cell division protein FtsN interacts with the murein (peptidoglycan) synthase PBP1B in *Escherichia coli*. *J Biol Chem* **282**: 36394-36402.

Nagai, K., C. Oubridge, T. H. Jessen, J. Li & P. R. Evans, (1990) Crystal structure of the RNA-binding domain of the U1 small nuclear ribonucleoprotein A. *Nature* **348**: 515-520.

Obermann, W. & J. V. Holtje, (1994) Alterations of murein structure and of penicillin-binding proteins in minicells from *Escherichia coli*. *Microbiology* **140 (Pt 1)**: 79-87.

Osawa, M., D. E. Anderson & H. P. Erickson, (2008) Reconstitution of contractile FtsZ rings in liposomes. *Science* **320**: 792-794.

Osawa, M. & H. P. Erickson, (2006) FtsZ from divergent foreign bacteria can function for cell division in *Escherichia coli*. *J Bacteriol* **188**: 7132-7140.

Oubridge, C., N. Ito, P. R. Evans, C. H. Teo & K. Nagai, (1994) Crystal structure at 1.92 A resolution of the RNA-binding domain of the U1A spliceosomal protein complexed with an RNA hairpin. *Nature* **372**: 432-438.

Pastoret, S., C. Fraipont, T. den Blaauwen, B. Wolf, M. E. Aarsman, A. Piette, A. Thomas, R. Brasseur & M. Nguyen-Disteche, (2004) Functional analysis of the cell division protein FtsW of *Escherichia coli*. *J Bacteriol* **186**: 8370-8379.

Prats, R. & M. A. de Pedro, (1989) Normal growth and division of *Escherichia coli* with a reduced amount of murein. *J Bacteriol* **171**: 3740-3745.

Priyadarshini, R., M. A. de Pedro & K. D. Young, (2007) Role of peptidoglycan amidases in the development and morphology of the division septum in *Escherichia coli*. *J Bacteriol* **189**: 5334-5347.

RayChaudhuri, D. & J. T. Park, (1992) *Escherichia coli* cell-division gene *ftsZ* encodes a novel GTP-binding protein. *Nature* **359**: 251-254.

Real, G., A. Fay, A. Eldar, S. M. Pinto, A. O. Henriques & J. Dworkin, (2008) Determinants for the subcellular localization and function of a nonessential SEDS protein. *J Bacteriol* **190**: 363-376.

Rogers, H. J., Perkins, H. R. and Ward, J. B., (1980) *Microbial Cell Walls and Membranes*. Chapman and Hall, London.

Romeis, T., U. Kohlrausch, K. Burgdorf & J. V. Holtje, (1991) Murein chemistry of cell division in *Escherichia coli*. *Res Microbiol* **142**: 325-332.

Ruiz, N., (2008) Bioinformatics identification of MurJ (MviN) as the peptidoglycan lipid II flippase in *Escherichia coli*. *Proc Natl Acad Sci U S A* **105**: 15553-15557.

Ruiz, N., (2009) *Streptococcus pyogenes* YtgP (Spy_0390) complements *Escherichia coli* strains depleted of the putative peptidoglycan flippase MurJ. *Antimicrob Agents Chemother* **53**: 3604-3605.

Sarkar, G. & S. S. Sommer, (1990) The "megaprimer" method of site-directed mutagenesis. *Biotechniques* **8**: 404-407.

Scheffers, D. J. & J. Errington, (2004) PBP1 is a component of the *Bacillus subtilis* cell division machinery. *J Bacteriol* **186**: 5153-5156.

Scheffers, D. J., L. J. Jones & J. Errington, (2004) Several distinct localization patterns for penicillin-binding proteins in *Bacillus subtilis*. *Mol Microbiol* **51**: 749-764.

Schleifer, K. H. & O. Kandler, (1972) Peptidoglycan types of bacterial cell walls and their taxonomic implications. *Bacteriol Rev* **36**: 407-477.

Schneider, B. L., W. Seufert, B. Steiner, Q. H. Yang, and A. B. Futcher, (1995) Use of polymerase chain reaction epitope tagging for protein tagging in Saccharomyces cerevisiae. *Yeast* **11**: 1265-1274.

Shah, I. M., M. H. Laaberki, D. L. Popham & J. Dworkin, (2008) A eukaryotic-like Ser/Thr kinase signals bacteria to exit dormancy in response to peptidoglycan fragments. *Cell* **135**: 486-496.

Shlomovitz, R. & N. S. Gov, (2009) Membrane-mediated interactions drive the condensation and coalescence of FtsZ rings. *Phys Biol* **6**: 046017.

Signoretto, C., F. Di Stefano & P. Canepari, (1996) Modified peptidoglycan chemical composition in shape-altered *Escherichia coli*. *Microbiology* **142 (Pt 8)**: 1919-1926.

Smith, T. J. & S. J. Foster, (1995) Characterization of the involvement of two compensatory autolysins in mother cell lysis during sporulation of *Bacillus subtilis* 168. *J Bacteriol* **177**: 3855-3862.

Spratt, B. G. & A. B. Pardee, (1975) Penicillin-binding proteins and cell shape in E. coli. *Nature* **254**: 516-517.

Strauch, E. M. & G. Georgiou, (2007) A bacterial two-hybrid system based on the twin-arginine transporter pathway of *E. coli*. *Protein Sci* **16**: 1001-1008.

Tarry, M., S. J. Arends, P. Roversi, E. Piette, F. Sargent, B. C. Berks, D. S. Weiss & S. M. Lea, (2009) The *Escherichia coli* cell division protein and model Tat substrate SufI (FtsP) localizes to the septal ring and has a multicopper oxidase-like structure. *J Mol Biol* **386**: 504-519.

Uehara T, P. K., Dinh T, Bernhardt TG, (2010) Daughter cell separation is controlled by cytokinetic ring-activated cell wall hydrolysis. *EMBO J*.

Ursinus, A., F. van den Ent, S. Brechtel, M. de Pedro, J. V. Holtje, J. Lowe & W. Vollmer, (2004) Murein (peptidoglycan) binding property of the essential cell division protein FtsN from *Escherichia coli*. *J Bacteriol* **186**: 6728-6737.

van Heijenoort, J., (2001) Formation of the glycan chains in the synthesis of bacterial peptidoglycan. *Glycobiology* **11**: 25R-36R.

Varani, G. & K. Nagai, (1998) RNA recognition by RNP proteins during RNA processing. *Annu Rev Biophys Biomol Struct* **27**: 407-445.

Varani, L., S. I. Gunderson, I. W. Mattaj, L. E. Kay, D. Neuhaus & G. Varani, (2000) The NMR structure of the 38 kDa U1A protein - PIE RNA complex reveals the basis of cooperativity in regulation of polyadenylation by human U1A protein. *Nat Struct Biol* **7**: 329-335.

Vasudevan, P., J. McElligott, C. Attkisson, M. Betteken & D. L. Popham, (2009) Homologues of the *Bacillus subtilis* SpoVB protein are involved in cell wall metabolism. *J Bacteriol* **191**: 6012-6019.

Vicente, M. & A. I. Rico, (2006) The order of the ring: assembly of *Escherichia coli* cell division components. *Mol Microbiol* **61**: 5-8.

Vollmer, W., (2007) Structure and biosynthesis of the murein sacculus. In: The periplasm. M. Ehrmann (ed). Washington, D.C.: ASM Press, pp. 198-213.

Vollmer, W. & U. Bertsche, (2008) Murein (peptidoglycan) structure, architecture and biosynthesis in *Escherichia coli*. *Biochim Biophys Acta* **1778**: 1714-1734.

Vollmer, W. & S. J. Seligman, (2010) Architecture of peptidoglycan: more data and more models. *Trends Microbiol* **18**: 59-66.

Weidel, W. & H. Pelzer, (1964) Bagshaped Macromolecules--a New Outlook on Bacterial Cell Walls. *Adv Enzymol Relat Areas Mol Biol* **26**: 193-232.

Weiss, D. S., J. C. Chen, J. M. Ghigo, D. Boyd & J. Beckwith, (1999) Localization of FtsI (PBP3) to the septal ring requires its membrane anchor, the Z ring, FtsA, FtsQ, and FtsL. *J Bacteriol* **181**: 508-520.

Wientjes, F. B. & N. Nanninga, (1989) Rate and topography of peptidoglycan synthesis during cell division in *Escherichia coli*: concept of a leading edge. *J Bacteriol* **171**: 3412-3419.

Wientjes, F. B. & N. Nanninga, (1991) On the role of the high molecular weight penicillin-binding proteins in the cell cycle of *Escherichia coli*. *Res Microbiol* **142**: 333-344.

Wientjes, F. B., C. L. Woldringh & N. Nanninga, (1991) Amount of peptidoglycan in cell walls of gram-negative bacteria. *J Bacteriol* **173**: 7684-7691.

Wilkins, M. R., E. Gasteiger, A. Bairoch, J. C. Sanchez, K. L. Williams, R. D. Appel & D. F. Hochstrasser, (1999) Protein identification and analysis tools in the ExPASy server. *Methods Mol Biol* **112**: 531-552.

Wissel, M. C. & D. S. Weiss, (2004) Genetic analysis of the cell division protein FtsI (PBP3): amino acid substitutions that impair septal localization of FtsI and recruitment of FtsN. *J Bacteriol* **186**: 490-502.

Wissel, M. C., J. L. Wendt, C. J. Mitchell & D. S. Weiss, (2005) The transmembrane helix of the *Escherichia coli* division protein FtsI localizes to the septal ring. *J Bacteriol* **187**: 320-328.

Xie, G., D. C. Bruce, J. F. Challacombe, O. Chertkov, J. C. Detter, P. Gilna, C. S. Han, S. Lucas, M. Misra, G. L. Myers, P. Richardson, R. Tapia, N. Thayer, L. S. Thompson, T. S. Brettin, B. Henrissat, D. B. Wilson & M. J. McBride, (2007) Genome sequence of the cellulolytic gliding bacterium *Cytophaga hutchinsonii*. *Appl Environ Microbiol* **73**: 3536-3546.

Yang, J. C., F. Van Den Ent, D. Neuhaus, J. Brevier & J. Lowe, (2004) Solution structure and domain architecture of the divisome protein FtsN. *Mol Microbiol* **52**: 651-660.